

Aus dem Institut für Immunologie im Biomedizinischen Centrum
der Ludwig-Maximilians-Universität München
Vorstand: Prof. Dr. rer. nat. Thomas Brocker



Dissertation
zum Erwerb des Doctor of Philosophy (Ph.D.)
an der Medizinischen Fakultät der
Ludwig-Maximilians-Universität zu München

***TGF β differentially specifies T follicular helper versus
Th17 cell fates of murine CD4⁺ T cells***

vorgelegt von

Yinshui Chang

aus

Wuhan, China

2023

Mit Genehmigung der Medizinischen Fakultät der
Ludwig-Maximilians-Universität zu München

Erster Gutachter: Herr Prof. Dr. Dirk Baumjohann
Zweiter Gutachter: Frau Prof. Dr. Anne Krug
Dritter Gutachter: Frau Prof. Dr. Barbara Schraml-Schotta
Vierter Gutachter: Herr Prof. Dr. Florian Greten

Dekan: **Prof. Dr. med. Thomas Gudermann**

Datum der Verteidigung:

10.07.2023

“Everything is theoretically impossible until it is done.” – Robert A. Heinlein

Table of contents

Table of contents	7
Summary	9
Zusammenfassung	11
List of figures	13
List of tables	13
List of abbreviations	14
1. Introduction	19
1.1 Innate immunity	19
1.2 Adaptive immunity	19
1.2.1 T cell-mediated immunity	20
1.2.2 T helper cell subsets	20
1.2.3 T cell differentiation.....	22
1.2.4 Multistep differentiation of Tfh cells <i>in vivo</i>	23
1.2.5 Differentiation of Tfh cells <i>in vitro</i>	24
1.2.6 Transcription factor networks regulating Tfh cell differentiation.....	26
1.2.7 Tfh cell plasticity	26
2. Aims of the thesis	29
3. Material and Methods	31
3.1 Resources tables	31
3.1.1 Mice	31
3.1.2 Viruses	31
3.1.3 Antibodies	32
3.1.4 Chemicals, consumables, and recombinant proteins	33
3.1.5 Commercial assays	34
3.1.6 Oligonucleotides	35
3.1.7 Deposited data.....	36
3.1.8 Instruments	37
3.1.9 Software and algorithms	37
3.2 Methods	38
3.2.1 Experimental animals	38
3.2.2 <i>In vitro</i> cell culture.....	38
3.2.3 <i>In vitro</i> tamoxifen treatment	38
3.2.4 <i>In vivo</i> Tfh cell differentiation	39
3.2.5 Flow cytometry.....	39
3.2.6 Transwell migration assay	40
3.2.7 B cell-T cell co-culture	40
3.2.8 Bulk RNA sequencing and GSEA.....	40
3.2.9 MS-based proteomics.....	41
3.2.10 Single-cell RNA-sequencing	42
3.2.11 CRISPR in naïve CD4 ⁺ T cells.....	43

3.2.12	LCMV infections.....	44
3.2.13	Statistical analysis	44
4.	Results.....	45
4.1	Validation of established T cell differentiation protocols	45
4.2	TGF β induces CXCR5 and Bcl6 protein expression in activated murine CD4 ⁺ T cells <i>in vitro</i>	46
4.3	TGF β -induced CXCR5 and Bcl6-expressing cells share transcriptional and proteomic features of <i>bona fide</i> Tfh cells.....	48
4.4	TGF β -induced CXCR5 ⁺ Bcl6 ⁺ Tfh cells are functional.....	50
4.5	TGF β signaling is required for CXCR5 and Bcl6 expression.....	52
4.6	<i>In vivo</i> relevance of TGF β signaling for Tfh cell differentiation.....	53
4.7	Differential IL-6 and Stat3 signaling requirements for the induction of CXCR5 and Bcl6.....	55
4.8	Cell density-mediated IL-2 production inhibits Tfh cell differentiation <i>in vitro</i>	56
4.9	TGF β -induced CXCR5-expressing cells are distinct from Th17 cells.....	59
4.10	Identification of Tfh cell fate deciders with an arrayed CRISPR/Cas9 screen	62
4.11	c-Maf functions as a switch factor determining Tfh versus Th17 cell fates.....	65
5.	Discussion.....	68
5.1	Improved <i>in vitro</i> culture recapitulates early <i>in vivo</i> differentiation of mouse Tfh cells	68
5.2	TGF β in human versus mouse Tfh cell differentiation	69
5.3	Cell density-mediated effects on Tfh cell differentiation	69
5.4	APC-based systems of Tfh cell differentiation	71
5.5	Limitations of <i>in vitro</i> culture systems	72
5.6	<i>In vivo</i> sources of TGF β	72
5.7	Adoptive transfer of Th17 cells and the development of ectopic lymphoid follicles	73
5.8	Role of Bcl6 and c-Maf in Tfh and Th17 differentiation.....	74
5.9	Summary and future directions.....	75
	References.....	76
	Acknowledgements	98
	Affidavit.....	99
	Confirmation of congruency.....	100
	List of publications	101

Summary

The generation of high-affinity antibodies is of most importance for the clearance of pathogens and the efficacy of vaccines. Potent antibody responses require interactions between B cells and T follicular helper (Tfh) cells, which are specialized in providing cognate help to B cells. However, despite Tfh cells being first described in the year 2000, no robust and reliable protocol is available for *in vitro* Tfh cell differentiation of murine CD4⁺ T cells.

In this thesis, we challenged the longstanding theory of the inhibitory effect of TGF β on murine Tfh cell differentiation, by identifying TGF β as a critical driver of murine Tfh cell differentiation *in vitro*. TGF β was required to initiate CXCR5 protein expression, the characteristic chemokine receptor expressed by Tfh cells, and to aid in its maintenance. By going against the common practice of including a TGF β -neutralizing antibody into murine Tfh cell cultures, we first established a robust and reproducible *in vitro* protocol to generate Tfh cells from naïve mouse CD4⁺ T cells with plate-bound anti-CD3 and anti-CD28 stimulation. The *in vitro* TGF β -induced CXCR5⁺ T cell population exhibited transcriptional and functional features of *in vivo*-generated Tfh cells. The TGF β signaling pathway was biologically relevant, as the disruption of this pathway by knockout of the TGF β receptor significantly reduced CXCR5 expression and also reduced the Tfh cell population in an *in vivo* immunization setting. An important optimization step of the Tfh cell culture was the reduction of cell density, which reduced paracrine IL-2 signaling, thereby strongly enhancing Tfh cell differentiation.

Tfh and Th17 cells show substantial plasticity between the two T helper subsets. Interestingly, we next discovered that in the *in vitro* model system a mixture of both Tfh-like and Th17-like cells were generated. To identify potential transcription factors that drive the divergence between Tfh and Th17 cells, we performed bulk RNA-seq analyses of sorted Tfh and Th17 cells. We next analyzed a selection of promising targets in an arrayed CRISPR/Cas9 screen and identified c-Maf as a transcription factor regulating Tfh versus Th17 cell fate as a molecular switch. Ablation of *Maf* strongly shifted the balance from Tfh towards Th17 cells. Finally, we confirmed in an acute LCMV setting that c-Maf also regulated Tfh versus Th17 differentiation *in vivo*.

Taken together, we established a robust and reproducible *in vitro* protocol to differentiate murine Tfh cells. This protocol provides a versatile platform for studying Tfh cell differentiation and plasticity in more detail. By using this culture, we identified c-Maf driving the divergent differentiation of Tfh and Th17 cells. We also debunked the longstanding concept of the inhibitory effect of TGF β on murine Tfh cells. Since TGF β can also induce human Tfh cells, our data indicate that human and mouse Tfh biology may actually be closer related than previously believed.

Zusammenfassung

Die Produktion von hochaffinen Antikörpern ist von großer Bedeutung sowohl für die Abwehr von Krankheitserregern als auch für die Wirksamkeit von Impfungen. Eine effektive Antikörperantwort erfordert das Zusammenspiel von B-Zellen und folliculären T-Helfer (Tfh)-Zellen, eine auf die Hilfe von B-Zellen spezialisierte Population von CD4⁺ T-Zellen. Obwohl Tfh-Zellen bereits im Jahre 2000 zuerst beschrieben wurden, fehlt bis heute ein robustes und reproduzierbares Protokoll für deren *in vitro* Differenzierung aus murinen CD4⁺ T-Zellen.

In der hier vorliegenden Arbeit wurde TGFβ als ein essentieller Faktor für die *in vitro* Tfh-Zell-Differenzierung identifiziert. TGFβ wurde nicht nur für die Initiierung sondern auch für die Aufrechterhaltung der Proteinexpression des für Tfh-Zellen charakteristischen Chemokinrezeptors CXCR5 benötigt. Zuerst wurde ein robustes und reproduzierbares Protokoll für die Tfh-Zell-Generierung aus naiven Maus-CD4⁺ T Zellen mit anti-CD3 und anti-CD28 Stimulation etabliert. Diese *in vitro*-generierte, TGFβ-induzierte CXCR5⁺ Zellpopulation wies transkriptionelle und funktionale Eigenschaften von *in vivo*-generierten Tfh-Zellen auf. Wir zeigten, dass der TGFβ Signalweg von biologischer Relevanz für die Tfh-Differenzierung *in vivo* ist. Ein Knockout des TGFβ Rezeptors in CD4⁺ T-Zellen verhinderte die Expression von CXCR5 und resultierte in einer signifikanten Reduktion der Tfh-Zellen in einem Protein-Immunisierungs-Szenario. Eine weitere Optimierung der *in vitro* Tfh-Zell-Differenzierung basierte auf der Reduktion der Zelldichte in der Zellkultur, wodurch die parakrine Signalweiterleitung von IL-2 reduziert und dadurch eine Verstärkung der Tfh-Zell-Differenzierung erreicht werden konnte.

Im weiteren Verlauf wurde das neuartige *in vitro*-Zellkulturprotokoll angewendet, um die Plastizität von Tfh- und Th17-Zellen zu untersuchen. So konnte gezeigt werden, dass in klassischen Th17-Zellkulturen sowohl Th17- als auch Tfh-Zellen induziert werden. Mittels RNA-Sequenzierung wurden potentielle Transkriptionsfaktoren identifiziert, die im weiteren Verlauf der Arbeiten funktional mittels CRISPR/Cas9 getestet wurden. c-Maf wurde dabei als ein molekularer Schalter für die Zell-Schicksalsentscheidung zwischen Tfh und Th17 identifiziert und sowohl *in vitro* als auch *in vivo* im akuten LCMV-Model validiert.

Zusammengefasst wurde in dieser Arbeit ein robustes und reproduzierbares Protokoll für die Tfh-Zell-Differenzierung aus naiven Maus-CD4⁺ T-Zellen entwickelt und validiert. Dieses Protokoll schafft eine vielseitige Plattform, die es erlaubt, die Tfh-Zell-Differenzierung und Plastizität in Zukunft noch viel detaillierter untersuchen zu können. Mit Hilfe dieser Zellkultur wurde c-Maf als ein treibender Faktor für die beobachtete Divergenz zwischen Tfh- und Th17-Zellen identifiziert. Darüber hinaus widerlegten wir das bisher gängige Konzept des hemmenden Effekts von TGFβ auf die Maus-Tfh-Zell-Differenzierung. Da TGFβ auch humane Tfh-Zellen induzieren kann, deuten unsere Daten darauf hin, dass die Unterschiede zwischen Mensch und Maus in Bezug auf die Tfh-Zell-Biologie womöglich kleiner sind als vorher angenommen.

List of figures

Figure 1: In vitro Th1, Th2, and Th17 differentiation of murine CD4 ⁺ T cells.....	45
Figure 2: CXCR5 and Bcl6 expression of <i>in vitro</i> differentiated cells.....	46
Figure 3: Validation of CXCR5 expression	47
Figure 4: TGFβ induces CXCR5 and Bcl6 expression in CD4 ⁺ T cells in Balb/c mice	47
Figure 5: TGFβ-induced CXCR5-expressing cells have transcriptomic features of Tfh cells.....	49
Figure 6: Proteomic analysis of CXCR5-expressing cells confirms features of Tfh cells.....	50
Figure 7: TGFβ-induced CXCR5 expressing cells migrates toward a CXCL13 gradient in a transwell migration assay.....	50
Figure 8: TGFβ-induced Tfh-like cells provide critical help to B cells in an <i>in vitro</i> T-B cell co-culture assay	51
Figure 9: Continuous TGFβ availability is required for the maintenance of CXCR5 expression.....	52
Figure 10: CD4 ⁺ T cells from <i>Tgbr2</i> knockout mice resemble the Tfh (anti-TGFβ) condition <i>in vitro</i>	53
Figure 11: TGFβ signaling is required for optimal Tfh cell differentiation <i>in vivo</i>	54
Figure 12: Induction of CXCR5 and Bcl6 protein expression requires Stat3 signaling	56
Figure 13: Increased cell density causes reduction in CXCR5 and Bcl6 protein expression <i>in vitro</i>	57
Figure 14: IL-2 reduces CXCR5 and Bcl6 expression in the <i>in vitro</i> Tfh culture.....	58
Figure 15: In a co-culture setting, <i>iTgfr2</i> ^{+/+} cells assume the phenotype of <i>iTgfr2</i> ^{Δ/Δ} cells	59
Figure 16: <i>In vitro</i> Tfh cell culture gives rise to distinct CXCR5 ⁺ and IL-17A ⁺ cell populations	60
Figure 17: <i>In vitro</i> -generated CXCR5 ⁺ and IL-17A ⁺ cells are transcriptomically distinct and resemble Tfh and Th17 cells.....	61
Figure 18: scRNA-sequencing confirms two distinct cell populations within Tfh (TGFβ) <i>in vitro</i> cell cultures	62
Figure 19: Efficient generation of CRISPR/Cas9-generated gene knockout CD4 ⁺ T cells .	63
Figure 20: TGFβ-induced CXCR5 expression is independent of Bcl6.....	63
Figure 21: Arrayed CRISPR/Cas9 screen to identify transcription factors driving Tfh versus Th17 cell differentiation	64
Figure 22: c-Maf expression is independent of Bcl6	65
Figure 23: Absence of c-Maf shifts the phenotype from Tfh towards Th17 in the Tfh (TGFβ) cell culture	66
Figure 24: T cell-specific absence of Maf results in reduced Tfh cell and concurrently increased Th17 cell frequencies <i>in vivo</i>	67
Figure 25: Intra- and inter-cellular signaling pathways in murine <i>in vitro</i> -cultured Tfh cells	75

List of tables

Table 1: The different T helper cell lineages	22
Table 2: List of published studies from January 2021 to October 2022 that included at least one murine <i>in vitro</i> Tfh cell differentiation condition using mixtures of cytokines and cytokine-blocking antibodies.	25

List of abbreviations

α	Alpha
β	Beta
Δ	Delta
γ	Gamma
μ	Micro
%	Percent
°C	Degree Celsius
3'	3 prime
5'	5 prime
AF	Alexa Fluor™
APC	Allophycocyanin
APC	Antigen-presenting cell
Ascl2	Achaete-scute homologue 2
Batf	Basic leucine zipper transcriptional factor ATF-like
Bcl6	B cell lymphoma 6
BCR	B cell receptor
Blimp-1	B lymphocyte-induced maturation protein-1
bp	Base pair
BM	Bone marrow
BV	Brilliant Violet™
Cas9	CRISPR-associated endonuclease 9
CCR	C-C chemokine receptor
CD	Cluster of differentiation
ChIP	Chromatin immunoprecipitation
CNS	central nervous system
CRISPR	Clustered regularly interspaced short palindromic repeat
CTL	Cytotoxic lymphocyte
CXCR	CXC chemokine receptor
CXCL	CXC chemokine ligand
cy	Cyanine
d	Day
DC	Dendritic cell
DB	DNA-binding domain
DD	Dimerization domain
DNA	Deoxyribonucleic acid
DMEM	Dulbecco's Modified Eagle Medium
DMSO	Dimethyl sulfoxide
DZ	Dark zone
e	Exponent of 10

EC50	Half-maximal effective concentration
EDTA	Ethylenediamine tetra-acetic acid
eF	eFluor™
ERT2	Estrogen receptor type 2
EtOH	Ethanol
FACS	Fluorescence-assisted cell sorting
FC	Fold change
FC	Flow cytometry
FCS	Fetal calf serum
FDC	Follicular dendritic cell
FITC	Fluorescein isothiocyanate
fl	Flanked by LoxP (flox)
Foxp3	Forkhead box protein 3
FSC	Forward scatter
g	Gram
GATA3	GATA binding protein 3
GC	Germinal center
gDNA	Genomic DNA
gMFI	Geometric mean fluorescence intensity
GP	Glycoprotein
h	Hour
H	Hinge region
HEPES	4-(2-hydroxyethyl)-1-piperazineethane sulfonic acid
HEV	High endothelial venule
hNGFR	Human nerve growth factor receptor
i	Induced
ICOS	Inducible T cell co-stimulator
IFN γ	Interferon gamma
Ig	Immunoglobulin
Ikzf	IKAROS family zinc finger
IL	Interleukin
iono	Ionomycin
i.p.	Intraperitoneal
IRF	Interferon regulatory factor
k	Kilo
kb	Kilo base pair
KO	Knockout
l	Liter
L	Ligand
LCMV	Lymphocytic choriomeningitis virus
LEF-1	Lymphoid enhancer binding factor-1

LN	Lymph node
log	Logarithm
LZ	Light zone
mAb	Monoclonal antibody
MHC	Major histocompatibility complex
m	Mili
Maf	Musculoaponeurotic fibrosarcoma oncogene homolog
mes	Mesenteric
min	Minutes
MOG	Myelin oligodendrocyte glycoprotein
miR	MicroRNA
mRNA	Messenger RNA
n	Nano
NKT	Natural killer T cell
NES	Normalized enrichment score
NP-OVA	Conjugate of 4-Hydroxy-3-nitrophenylacetyl and ovalbumin
OH-tamoxifen	Hydroxy-tamoxifen
p	Pobability (value)
padj	Multiple testing adjusted p-value
PAMP	Pathogen-associated molecular pattern
PBS	Phosphate-buffered saline
PC	Plasma cell
PCA	Principal component analysis
PD-1	Programmed cell death protein 1
PD-L1	Programmed cell death ligand 1
PE	Phycoerythrin
PerCP	Peridinin chlorophyll protein
PMA	Phorbol myristate acetate
PRR	Pattern recognition receptor
PSGL-1	P-selectin glycoprotein ligand-1
r	Receptor
RNA	Ribonucleic acid
Rorgt	Retinoic acid-related orphan receptor gamma
RPMI	Roswell Park Memorial Institute 1640 medium
RT	Room temperature
sc	Single-cell
s.c.	Subcutaneous
s.e.m.	Standard error of the mean
seq	Sequencing
sgRNA	Single-guide RNA
SHM	Somatic hypermutation

SLAM	Signaling lymphocytic activation molecule
SM	SMARTA
SMAD3	SMAD family member 3
SSC	Sideward scatter
STAT	Signal transducer and activator of transcription
TA	Transactivation domain
Tam	Tamoxifen
Tbet	T-box transcription factor
TCR	T cell receptor
TCF-1	T cell factor-1
TF	Transcription factor
Tg	Transgenic
Th cell	T helper cell
Tfh cell	T follicular helper cell
Tfr cell	T follicular regulatory cell
TLR	Toll-like receptors
TNF α	Tumor necrosis factor alpha
Treg	Regulatory T cells
U	Units
UTR	Untranslated region
qPCR	Quantitative polymerase chain reaction
wt	Wildtype

1. Introduction

Throughout the lifetime, we experience a plethora of pathogens, toxins, and environmental cues. In order to ensure health and survival, our body evolved a complex system to fend off the waves of harmful microorganisms including viruses, bacteria, fungi, and parasites, termed the immune system. The most primitive defense of the immune system consists of anatomical and chemical barriers, e.g. the skin epithelium (Kabashima et al., 2018), or host defense peptides, e.g. defensins (Xu & Lu, 2020). With time, the pathogens evolved to evade the simple barrier; hence, the immune system coevolved and created a more sophisticated host defense, namely the innate and the adaptive immune system (Charles A Janeway et al., 2001).

1.1 Innate immunity

Once a pathogen has penetrated the physical barriers, the innate immune response is rapidly activated (Kabashima et al., 2018). The innate immune system consists of effector cells, including macrophages, dendritic cells (DCs), neutrophils, natural killer (NK) cells and NK-like innate lymphoid cells (ILCs) (Gasteiger et al., 2017). They express a set of pattern recognition receptors (PRRs), including toll-like receptors (TLRs). Through these receptors, innate immune cells are capable of recognizing foreign molecules, termed pathogen-associated molecular patterns (PAMPs), including bacterial DNA, RNA, and components of the bacterial cell wall (Medzhitov & Janeway, 1997; Paludan et al., 2020). Upon pattern recognition, macrophages and granulocytes will eliminate the pathogen directly via phagocytosis (Aderem & Underhill, 1999; Gasteiger et al., 2017), and further induce inflammation via secretion of cytokines and chemokines, to hinder the spread of the pathogen and to facilitate the recruitment of immune cells (Medzhitov, 2010; Paludan et al., 2020). However, with a limited repertoire of PRRs, the innate immune system is only capable of recognizing a limited set of invariant PAMPs, shared by multiple pathogens. This renders the host vulnerable to reinfections. In order to recognize pathogen-specific antigenic structures, vertebrates thus evolved the adaptive immune system (Cooper & Alder, 2006).

1.2 Adaptive immunity

The adaptive immune response consists of two groups of lymphocytes, T cells and B cells (Sette & Crotty, 2021). In order to detect unique foreign antigens from a plethora of pathogens, these two cell populations evolved highly variable antigen-binding receptors, the B cell receptor (BCR) as well as the T cell receptor (TCR). In order to generate these receptors, the lymphocytes undergo somatic recombination, also termed V(D)J-rearrangement. During this process, RAG (recombination-activating gene) proteins rearrange the variable (V), diversity (D) and joining (J) receptor gene segments (Christie et al., 2022; Davis & Bjorkman, 1988; Grawunder et al., 1998). This random recombination occurs independently in individual lymphocytes, giving rise to a diverse and polymorphic receptor repertoire of potentially $1e13$ distinct TCRs in mice (Nikolich-Zugich et al., 2004). Since this recombination is random in nature, it will also yield receptors that

are specific for self-antigens (BURNET, 1962; Hogquist et al., 2005; Kisielow et al., 1988). In order to prevent autoimmunity, self-reactive lymphocytes have to be eliminated efficiently (Hogquist et al., 2005). This stringent selection process occurs during the maturation phase of the lymphocytes. B cells develop in the bone marrow (BM), where they undergo negative selection (Nemazee, 2017). T cell maturation occurs in the thymus, where they undergo sequential selection processes, namely positive selection, followed by negative selection through clonal deletion or clonal diversion (BURNET, 1962; Charles A Janeway et al., 2001; Klein et al., 2014).

T cell precursors migrate from the BM to the thymus, starting as double-negative thymocytes at the subcapsular region of the cortex. Here they proliferate and mature into double-positive thymocytes expressing both the CD4 and the CD8 co-receptors (Klein et al., 2014). Dependent on the TCR specificity toward either the major histocompatibility complex (MHC) I or II, the T cell precursors select the cognate co-receptor and lose expression of the other co-receptor, and differentiate into either single-positive CD8⁺ or CD4⁺ T cells (Klein et al., 2014). Thymocytes showing no affinities towards the MHC classes die by neglect. After migration into the medulla of the thymus, precursors exhibiting strong binding to the self-peptide:MHC complexes are eliminated by clonal deletion (Klein et al., 2014; Kyewski et al., 2002). Only after this stringent selection process, thymocytes are permitted to exit the thymus as naïve T cells (Klein et al., 2014).

1.2.1 T cell-mediated immunity

Conventional T lymphocytes can be classified into two major subtypes, namely CD8-positive cytotoxic T lymphocytes (CTLs) as well as CD4-positive T helper (Th) cells, based on the expressed co-receptor of the TCR.

Naïve CD8⁺ T cells are incapable of killing infected cells. However, upon recognition of their cognate peptide-MHC (pMHC) complex on licensed DCs, naïve CD8⁺ T cells begin to proliferate and differentiate into activated effector cells, acquiring the capacity to produce effector cytokines (Smith et al., 2004; Zhang & Bevan, 2011). After leaving the LN, CTLs then access the peripheral tissues through expression of tissue-specific homing receptors (Krummel et al., 2016). In peripheral tissues, CTLs arrive at the site of infection through random search or following signals by other leukocytes (Niño et al., 2020). Upon re-stimulation with the cognate pMHC, activated CD8⁺ CTLs are able to destroy the infected cells directly by exocytosis of granules containing perforin and granzymes, as well as by induction of apoptosis via the Fas pathway (Philip & Schietinger, 2021; Russell & Ley, 2002).

Contrary to CTLs, T helper cells mostly do not directly eliminate infected cells, but they assume a supportive role by coordinating, enhancing and maintaining the immune response mediated by other immune cells.

1.2.2 T helper cell subsets

To accommodate for the different types of invading pathogens, the immune system has to tailor its immune response to successfully eliminate the pathogen. In order to coordinate the different

immune responses, naïve CD4⁺ T cells are able to differentiate into a variety of distinct T helper cell subsets. The major T helper cell subsets include Th1, Th2, Th17, regulatory T (Treg), and T follicular helper (Tfh) cells (Saravia et al., 2019; Zhu, 2018) (Table 1).

Th1 cells mediate the type I immune response against intracellular infections with microorganisms, including viruses, protozoa and bacteria, by secreting interferon-gamma (IFN γ), interleukin-2 (IL-2), and the tumor necrosis factor alpha (TNF α) (Butcher & Zhu, 2021; Mosmann et al., 1986). The secreted IFN γ activates cytolytic activities of infected macrophages, IL-2 boosts the effector functions and proliferation of CTLs, and TNF α activates endothelial cells lining local blood vessels for better adhesion and entry of the immune cells into the site of infection.

The type II immune response is characterized by the generation of Th2 cells, which function is to fight extracellular parasites, especially helminths (Walker & McKenzie, 2017). Th2 cells secrete the cytokines IL-4, IL-5 and IL-13. Secretion of IL-5 recruits eosinophils to the site of infection, which in turn produces granule proteins, including major basic proteins, to kill the parasites directly (Acharya & Ackerman, 2014). IL-4 and IL-13 reprogram macrophages, enhancing tissue repair after resolution of the infection (Allen & Wynn, 2011).

Protection against extracellular bacteria and fungi is mediated by Th17 lymphocytes, termed as type III immunity. Th17 cells are named after the production of their signature cytokines IL-17A/F (Acosta-Rodriguez et al., 2007; Harrington et al., 2005; Park et al., 2005). IL-17A and IL-17F are quite similar in their biological activity, both initiating neutrophil trafficking, and activation (Aggarwal & Gurney, 2002; Hoshino et al., 1999).

After resolution of an acute infection, the ongoing inflammation and effector T cell activities have to be repressed in order to restore tissue homeostasis (Sakaguchi et al., 2020; Shevryev & Tereshchenko, 2020). During homeostasis and during an ongoing immune response, an overshooting immune reaction has to be prevented in order to avoid tissue damage. The main lymphocyte subpopulation with a suppressive role are Treg cells (Sakaguchi et al., 1985). Tregs are broadly categorized into thymic tTregs and peripheral pTregs, named after the site of their development (Sakaguchi et al., 2020). Treg cells have a variety of suppressive mechanism, ranging from expression of co-inhibitory molecules such as CTLA-4 (Sakaguchi et al., 2020; Wing et al., 2008), secretion of anti-inflammatory cytokines such as IL-10, or competition for IL-2, resulting in cytokine deprivation (Pandiyani et al., 2007; Sakaguchi et al., 2020).

Tfh cells connect the T cell-mediated adaptive immune response with humoral immunity through the formation and maintenance of germinal centers (GCs), hence promoting a long-lived and high-affinity antibody response (Baumjohann & Fazilleau, 2021; Crotty, 2019; Vinuesa et al., 2016). In the GC, Tfh cells closely interact with their cognate B cells and stimulate them to undergo affinity maturation, class-switching, as well as memory B cell and plasma cell differentiation.

Table 1: The main T helper cell subsets

	Cytokine requirements	Master regulators	Effector cytokines	Function
Th1	IL-12, IFN γ	Tbet	IFN γ	Cell-mediated immunity against intracellular parasites
Th2	IL-4	Gata3	IL-4, IL-5, IL-13	Humoral immunity against parasites
Th17	IL-6, IL-1 β , TGF β , IL-23	Rorgt	IL-17A, IL-17F	Host defense against extracellular pathogens
Treg	TGF β	FoxP3	IL-10	Immune suppression, Homeostasis
Tfh	IL-6, IL-21, TGF β (human)	Bcl6	IL-21	B cell help in humoral immunity

1.2.3 T cell differentiation

The variety of different cell fates for naïve CD4⁺ T cells is decided during priming by DCs. Here, the T cells receive a variety of different signals, the combination of various quality and quantity of signals finally decides the cell fate of a naïve T cell. The signals can be roughly categorized into three categories: TCR stimulation, co-stimulation and cytokine stimulation.

1.2.3.1 TCR stimulation and co-stimulation

As the purpose of the adaptive immune system is to mount a response against specific structures of a pathogen, precise control is required in the activation of T cells. CD4-positive and CD8-positive T cells are only activated when they recognize their cognate antigen. As APCs are presenting large quantities of both self and non-self antigens, chances appear rather low for a given T cell to find its cognate pMHC. Nevertheless, 0.03% occupation of the MHC with the cognate peptide is sufficient to activate a T cell (Demotz et al., 1990; Harding & Unanue, 1990). By serial triggering of multiple TCRs by a single cognate pMHC, a high TCR occupancy can be achieved (Valitutti et al., 1995). This activation threshold increases fivefold without additional signaling through co-stimulatory signals (Viola & Lanzavecchia, 1996). This is in line with the two-signal model of T cell activation, postulating that both antigenic signal and co-stimulatory signal are required for full activation of the T cell (Bretscher & Cohn, 1970). APCs can interact with a T cell through a variety of surface receptors, both stimulatory as well as inhibitory. Through the interaction of both co-stimulatory and co-inhibitory signals, T cell activation is fine-tuned (L. Chen & Flies, 2013). Difference in TCR signaling strength and interaction with the APC have profound effects on T cell differentiation (Rogers & Croft, 2000). Stronger TCR activation shifts the T cell fate from Th2 towards Th1 (Constant et al., 1995). The signaling lymphocytic activation molecule (SLAM) family molecules, for instance, promotes IL-4 production and decreases IFN γ production (Cannons et al., 2010, 2011).

1.2.3.2 Cytokine patterns

The main decider for cell fate commitment is the cytokine signal provided during the priming of a naïve T cell. IL-4 initiates Th2 cell fate commitment (Kaplan, Schindler, et al., 1996), whereas

IL-12 results in differentiation towards a Th1 cell fate (Kaplan, Sun, et al., 1996). pTreg commitment is facilitated by the presence of TGF β and IL-2 and favored by the lack of pro-inflammatory signaling (Bettelli et al., 2006; W. J. Chen et al., 2003).

Th17 cell differentiation is promoted by IL-6 (Bettelli et al., 2006; Zhou et al., 2007). In the absence of IL-6, IL-21 assumes many functions of IL-6 (Korn et al., 2007; R. Nurieva et al., 2007). For the final maturation of Th17 cells, IL-23 is required (McGeachy et al., 2009). However, for the initial differentiation, IL-23 is not relevant, as the receptor for IL-23 is only expressed after Th17 cells have completed their differentiation (Zhou et al., 2007). Th17 cells are a heterogeneous population. Context-dependent cytokine signal can result in either a pro- or anti-inflammatory phenotype. IL-6 in combination with TGF β results in an anti-inflammatory fate, while in combination with IL-1 β results in a pro-inflammatory fate (Chung et al., 2009; Veldhoen et al., 2006; Zielinski et al., 2012).

1.2.4 Multistep differentiation of Tfh cells *in vivo*

Tfh cell differentiation is characterized by a multistep differentiation process (Baumjohann & Fazilleau, 2021). Naïve CD4⁺ T cells are activated in the T cell zone of secondary lymphoid organs by DCs. While differentiating effector cells such as Th1 and Th2 leave the secondary lymphoid organs after activation and differentiation, other activated CD4-positive T cells, if committed to the Tfh cell fate, migrate toward the T-B cell border of the follicle, through their induction of CXCR5 expression and their concurrent downregulation of CCR7 expression (Hardtke et al., 2005; Haynes et al., 2007). Upon interaction with cognate B cells, these pre-Tfh cells migrate into the B cell follicle and mature into GC Tfh cells (Baumjohann & Fazilleau, 2021). In order to provide efficient help to B cells, Tfh cells express a plethora of co-stimulatory molecules, including inducible co-stimulator (ICOS), CD40 ligand (CD40L), and OX40, but also co-inhibitory molecules, namely programmed cell death protein 1 (PD-1) (Baumjohann & Fazilleau, 2021; Qi, 2016; Vinuesa et al., 2016). Further, to maintain a durable immunological synapse for sustained T-B cell interaction, homotypic interactions of SLAM is required, as well as the intracellular expression of the adaptor molecule SLAM-associated protein (SAP) in Tfh cells (Cannons et al., 2011; Qi et al., 2008). GC Tfh cells also produce IL-21 and IL-4 to support the B cells (Baumjohann & Fazilleau, 2021; Crotty, 2019; Qi, 2016; Vinuesa et al., 2016).

To initiate the cell fate commitment of activated CD4⁺ T cells to the Tfh cell phenotype, naïve CD4⁺ T cells are primed by DCs (Baumjohann et al., 2011; Goenka et al., 2011). More specifically, CD11b⁺ migratory type 2 cDCs (cDC2s) have been described as the primary DC subset responsible for Tfh cell differentiation (Krishnaswamy et al., 2017). While the initial step is independent of B cells (Baumjohann et al., 2011; Goenka et al., 2011), full commitment and maturation of Tfh cells requires continued interactions with B cells (Baumjohann et al., 2011, 2013; Deenick et al., 2010; Goenka et al., 2011).

Tfh cell commitment is favored by enhanced TCR signaling strength, both in quality and quantity. In a polyclonal T cell response, T cells with a higher affinity TCR preferentially developed into Tfh

cells (Fazilleau et al., 2009). In a protein immunization setting, increased antigen availability resulted in an increased Tfh cell response (Baumjohann et al., 2013). However, further increasing the protein dose above 200 µg showed an adverse effect on Tfh cell differentiation (Krishnamoorthy et al., 2017). Furthermore, it was shown that persistent weak TCR activation through TCR:self-peptide:MHC interactions inhibited Tfh cell development (Bartleson et al., 2020).

Tfh cell commitment requires a set of costimulatory molecules. Absence of CD28 results in a complete blockade in Tfh cell differentiation (Baumjohann & Ansel, 2015; Ferguson et al., 1996; Linterman et al., 2009, 2014). ICOS-deficiency causes a severe reduction in Tfh cells (Akiba et al., 2005; Bossaller et al., 2006). OX40^{-/-} mice have normal Tfh differentiation, indicated by a normal GC and antibody responses (Kopf et al., 1999). However, OX40 is required for the migration to the T-B border after priming (Fillatreau & Gray, 2003). Similarly, PD-1 is required to control tissue positioning of Tfh cells (Shi et al., 2018).

Tfh cell commitment *in vivo* is dependent on various cytokines, both positively and negatively regulating Tfh cell differentiation. IL-6 and IL-21 are important for initiating Tfh cell differentiation (Eto et al., 2011; R. I. Nurieva et al., 2008; Suto et al., 2008). IL-6 can be produced by various cell types, e.g. by DCs and B cells (Dodge et al., 2003; Karnowski et al., 2012). Upon IL-6 stimulation, IL-21 is mainly produced by T cells and NKT cells (Eddahri et al., 2009; Leonard & Wan, 2016). Similar to the cytokine requirements for Th17 cells, there are redundancies in the requirements for IL-6 and IL-21 (Eto et al., 2011; R. I. Nurieva et al., 2008, 2009). In an acute LCMV infection system, while a single knockout of either IL-6 or IL-21 did not strongly reduce Tfh cell commitment, the combined knockout exhibited a synergistic effect by further reducing Tfh cell numbers (Eto et al., 2011). Blocking of IL-7 in addition to IL-6 and IL-21 can further decrease Tfh cells in an IL-6/IL-21-independent manner (Seo et al., 2014).

On the other end of the spectrum, IL-2 effectively inhibits Tfh cell differentiation (Ballesteros-Tato et al., 2012; Johnston et al., 2012a; León et al., 2014). Upon commitment to the Tfh cell fate, pre-Tfh cells migrate towards the B cell zone, thus escaping the influence of IL-2 primarily abundant in the T cell zone (Papillion et al., 2019; Shi et al., 2018).

1.2.5 Differentiation of Tfh cells *in vitro*

Differentiation of naïve CD4⁺ T cells into effector cell subsets such as Th1, Th2, and Th17 has been performed in *in vitro* assays for many decades. However, while human Tfh cells can be easily generated *in vitro*, the *in vitro* generation of mouse Tfh cells has been controversial, with the consensus in the field that a robust and reliable assay is still missing (Crotty, 2019; Dong, 2021). Most papers used plate-bound anti-CD3 and anti-CD28 stimulation, in combination with IL-6 and IL-21 as well as blockade of IFN γ , IL-4, TGF β and occasionally IL-2 (Table 2). In a minimalistic system with only anti-CD3 and anti-CD28 stimulation, IL-6 and IL-21 alone was not sufficient to drive Tfh cell stimulation *in vitro* (Eto et al., 2011). Adding splenocytes as APCs improved Tfh cell differentiation, but concurrently increased background in the Th0, Th1, Th2, and Th17 differentiating conditions (Lu et al., 2011). Excessively increasing the APC to T cell ratio

improved Tfh differentiation (Gao et al., 2019). Interestingly, the role of TGF β in Tfh cell differentiation is ambiguous. Human Tfh cell differentiation is initiated by IL-12, IL-23 and TGF β (Locci et al., 2016; Schmitt et al., 2009, 2014). However, in mice, TGF β has mainly been reported to be a negative regulator of Tfh cell differentiation (McCarron & Marie, 2014; R. I. Nurieva et al., 2008, 2009) and the differentiation of IL-21-producing Th cells (Suto et al., 2008). Based on these initial publications, the addition of TGF β -blocking antibodies to murine Tfh cell *in vitro* cultures is quite common in currently used *in vitro* Tfh cell differentiation protocols. Reviewing 17 papers published between 2021 and 2022, which included an *in vitro* Tfh-skewing condition, revealed that in 12 articles anti-TGF β was added to the culture, and in five articles TGF β was neither blocked nor added (Table 2). Nevertheless, one report indicated that TGF β was required for Tfh differentiation in the lung mucosa *in vivo* (Marshall et al., 2015). In summary, it remains unclear what conditions induce murine Tfh cells *in vitro*.

Table 2. List of published studies from January 2021 to October 2022 that included at least one murine *in vitro* Tfh cell differentiation condition using mixtures of cytokines and cytokine-blocking antibodies.

Reference	Published online	TGF β	Plate format	T cell seeding density	APCs
(Jang et al., 2021)	2021 Feb 25	anti		1e6	-
(Alemán-García et al., 2021)	2021 Mar 8	anti	-	-	-
(Nian et al., 2021)	2021 Apr 9	--	96-Well	2e5	-
(Lin et al., 2021)	2021 Apr 19	anti	96-Well	2e5	-
(Fukuta et al., 2021)	2021 May 20	--	--	--	-
(Zheng et al., 2021)	2021 Jun 1	anti	96-Well	5e5	-
(Niogret et al., 2021)	2021 Jun 8	anti	-	-	-
(Guglielmo et al., 2021)	2021 Jul 14	anti	-	-	-
(Wang et al., 2021)	2021 Oct 1	anti	-	-	BMDCs
(Kuen et al., 2021)	2021 Oct 18	anti	-	-	-
(Wan et al., 2021)	2021 Dec 14	anti	96-Well	2e5	-
(Feng et al., 2022)	2022 Mar 02	anti	-	-	-
(Kim et al., 2022)	2022 Jun 8	anti	-	-	-
(Huang et al., 2022)	2022 Feb 10	anti	-	-	-
(Wu et al., 2022)	2022 Mar 28	--	-	5e5	-
(J. Li et al., 2022)	2022 Aug 28	--	96-Well	-	-
(C. Li et al., 2022)	2022 Oct 11	--	96-Well	5e5	B cells

In the column 'TGF β ', 'anti' refers to the usage of TGF β -blocking antibodies and '--' refers to that TGF β was neither added nor blocked. If information was available from the methods sections of the respective research articles, the used cell culture well plate format, the seeding density of the CD4⁺ T cells per well, and the type of APCs added to the culture is listed as well.

1.2.6 Transcription factor networks regulating Tfh cell differentiation

Cell fate commitment of T helper cells is driven by the actions of master transcription factors (O'Shea & Paul, 2010; Saravia et al., 2019; Zhu, 2018). The master transcription factors for Th1, Th2, Th17, and Treg cells are Tbet, Gata3, Rorgt, and Foxp3, respectively. They promote cell fate commitment by either inducing lineage-specifying genes or by inhibiting genes associated with alternative cell fates.

The transcription factor Bcl6 (B-cell lymphoma 6) is the master regulator of Tfh cells and its T cell-intrinsic expression is essential for Tfh cell differentiation and GC formation *in vivo* (Johnston et al., 2009; R. I. Nurieva et al., 2009; Yu et al., 2009). Functionally, Bcl6 is a transcriptional repressor, mediating the repression of a broad range of genes important for T cell migration pathways, TCR signaling pathways, and Th1, Th17, Th2, and Treg differentiation pathways (Choi & Crotty, 2021; Hatzi et al., 2015; R. I. Nurieva et al., 2009). Most prominently, it reciprocally inhibits its antagonist, Blimp-1 (encoded by *Prdm1*), which is induced via the IL-2-Stat5 pathway (Johnston et al., 2009, 2012b). CXCR5 expression generally coincides with Bcl6 expression (Baumjohann et al., 2011). However, it can also be initiated independently of Bcl6 under certain conditions (Liu et al., 2014).

The concept of a master transcription factor, however, is oversimplifying lymphocyte biology. T helper cells exhibit a high degree of flexibility and plasticity, allowing the expression of multiple master transcription factors, or phenotype switching (Nakayamada et al., 2012; Saravia et al., 2019). Besides the master transcription factor Bcl6, additional transcription factors are also required for optimal Tfh cell differentiation (Crotty, 2011; Vinuesa et al., 2016).

Stat3 (Signal transducers and activators of transcription 3) is the major signal transducer of IL-6 and IL-21. T cell-specific Stat3 deficiency greatly reduced the number of Tfh cells, resulting in defective GC B cell generation (R. I. Nurieva et al., 2008). However, Stat3 in cooperation with IRF4 potently induces Blimp-1, the antagonist of Bcl6 (Kwon et al., 2009).

BATF is a transcription factor belonging to the activator protein 1 superfamily, which includes Fos, Jun, and Atf proteins. Batf-deficient mice show reduced numbers of peripheral CD4⁺ T cells, with impaired differentiation of Th1, Th17 and Tfh cells (Betz et al., 2010).

c-Maf (encoded by *Maf*) induces IL-21 production upon Icos stimulation, and *Maf*-deficient mice have defective Tfh cell differentiation (Bauquet et al., 2008). For Th17 differentiation, c-Maf is not required; however, it improves the maintenance of Th17 cells after differentiation (Bauquet et al., 2008).

1.2.7 Tfh cell plasticity

Despite all factors driving Tfh cell commitment, Tfh cells are quite plastic. During *ex vivo* repolarization under Th1, Th2, and Th17 cell culture conditions, Tfh cells gained the ability to secrete the respective cytokine of the individual lineages, namely IFN γ , IL-4, and IL-17 (Lu et al., 2011). The chromatin at the sites of IFN γ , IL-4, and IL-17, as well as the master transcription factors *Tbx21*,

Gata3, and *Rorc*, showed histone marks associated with transcriptionally active/poised chromatin (Lu et al., 2011).

Depending on the type of invading pathogen, Tfh cells are tasked to fine-tune the antibody response (Crotty, 2011; Vinuesa et al., 2016). Dependent on the cytokine secreted, Tfh cells mediate B cell class switch recombination to different isotypes. For example, IL-4-secreting Tfh cells are required for switching to IgG1 (Reinhardt et al., 2009), while IFN γ mediates switching to IgG2a in type I responses (Toellner et al., 1998).

Production and secretion of IgA into the gut lumen is critical for the maintenance of the microbiota environment of the intestine (Pabst & Slack, 2019). For that purpose, the Peyer's patches continuously maintain active GCs. Fate tracking of Th17 cells showed that adoptively transferred Th17 cells preferentially homed to the gut and then were able to acquire a GC Tfh phenotype (Hirota et al., 2013). This inherent plasticity between Tfh and Th17 cells provides an intriguing starting point to explore Tfh cell plasticity.

2. Aims of the thesis

T helper subsets are critical and well-studied components of the mammalian immune system, categorized into subsets ranging nowadays from Th1 to Th22 (Dong, 2021; Sallusto, 2016). The ability to differentiate these subsets *in vitro* has greatly contributed to our current understanding of the immune system. For most CD4⁺ T cell subsets (i.e. Th1, Th2, Th17, Treg), reliable protocols for their differentiation *in vitro* exist. However, for the differentiation of murine Tfh cells, a reproducible and robust protocol is still missing, and this continues to be a serious knowledge gap in the field of Tfh cell biology (Crotty, 2019; Dong, 2021).

For the first part of this thesis, the aim was to close this gap of knowledge and to identify drivers for mouse Tfh cell differentiation, in order to establish a protocol for the *in vitro* generation of Tfh cells. The protocol was then to be further optimized, e.g. for improved CXCR5 and Bcl6 protein expression as well as for robustness and reproducibility. Subsequently, the *in vitro*-generated Tfh-like cells were to be validated for functional features of Tfh cells, such as chemotaxis and B cell interactions.

With the successful establishment of a protocol for *in vitro* Tfh cell generation, the next aim was the application of this system for probing unknown aspects of Tfh biology, in particular the molecular pathways that lead to Tfh cell differentiation.

3. Material and Methods

3.1 Resources tables

3.1.1 Mice

Mouse line	Source	Identifier
C57BL/6	Charles River or Janvier Laboratories	
Balb/c	LIMES Institute	
<i>Sh2d1a</i> ^{-/-} (B6.129S6- <i>Sh2d1a</i> ^{tm1Pls/J})	The Jackson Laboratory	JAX# 025754 (<i>Sh2d1a</i> ⁻ allele)
<i>Cd4-CreERT2</i> ⁺ <i>Cxcr5</i> ^{fl/fl} (B6.Cg- <i>Cd4</i> ^{tm1(cre/ERT2)Thbu} - <i>Cxcr5</i> ^{tm1.Namt})	(Alterauge et al., 2020)	
<i>Cd4-CreERT2</i> ⁺ <i>Bcl6</i> ^{fl/fl} <i>Rosa26</i> ^{fl-Stop-fl-YFP/fl-STOP-fl-YFP} (B6.Cg- <i>Cd4</i> ^{tm1(cre/ERT2)Thbu} - <i>Bcl6</i> ^{tm1.1Dent} - <i>Gt(ROSA)26Sor</i> ^{tm1(EYFP)Cos})	(Alterauge et al., 2020)	JAX# 023727 (<i>Bcl6</i> ^{fl/fl} allele)
GREAT/SMART17A (B6.Cg- <i>Ifng</i> ^{tm3.1Lky} - <i>Il17a</i> ^{tm1.1Lky})	(Price et al., 2012), kindly provided by Richard Locklsey	
<i>Cd4-CreERT2</i> ⁺ <i>Tgfb2</i> ^{fl/fl} <i>Rosa26</i> ^{fl-Stop-fl-YFP/fl-STOP-fl-YFP} (B6.Cg- <i>Ptprc</i> ^a <i>Pepe</i> ^b - <i>Cd4</i> ^{tm1(cre/ERT2)Thbu} - <i>Tgfb2</i> ^{tm1Karl} - <i>Gt(ROSA)26Sor</i> ^{tm1(EYFP)Cos})	This work, alleles kindly provided by Thorsten Buch and Caspar Ohnmacht	MGI 2183502 (<i>Tgfb2</i> ^{fl} allele) MGI 5549971 (<i>CreERT2</i> allele) JAX# 006148 (<i>Rosa26</i> ^{fl-Stop-fl-YFP} allele)
<i>Cd4-Cre</i> ⁺ <i>Stat3</i> ^{fl/fl} (B6.Cg- <i>Tg(Cd4-cre)1Cwi-Stat3</i> ^{tm2Aki} - <i>Foxp3</i> ^{tm1Kuch})	(Heink et al., 2017), kindly provided by Thomas Korn	MGI 2386448 (<i>Cd4-Cre</i> allele) MGI 1926816 (<i>Stat3</i> ^{fl} allele) MGI 3718527 (<i>Foxp3-GFP</i> allele)
<i>Cd4-Cre</i> ⁺ <i>IL6ra</i> ^{fl/fl} (B6.Cg- <i>Tg(Cd4-cre)1Cwi-Il6ra</i> ^{tm1.1Drew})	(Heink et al., 2017), kindly provided by Thomas Korn	MGI 2386448 MGI 4456449 (<i>IL6ra</i> ^{fl} allele)
<i>Cd4-Cre</i> ⁺ <i>gp130</i> ^{fl/fl} (B6.Cg- <i>Tg(Cd4-cre)1Cwi-Il6st</i> ^{tm1Wme} - <i>Foxp3</i> ^{tm1Kuch})	(Korn et al., 2008), kindly provided by Thomas Korn	MGI 2386448 MGI 1931239 (<i>gp130</i> ^{fl} allele) MGI 3718527
<i>Cd4-Cre</i> ⁺ <i>Mafl</i> ^{fl/fl} (B6.Cg- <i>Tg(Cd4-cre)1Cwi-Mafl</i> ^{tm2.1Cbm})	(Lee et al., 2001; Wende et al., 2012), kindly provided by Christian Neumann or Axel Kallies	MGI 2386448 MGI:5316775 (<i>Mafl</i> ^{fl} allele)

3.1.2 Viruses

Virus strains	Source
Lymphocytic choriomeningitis virus (LCMV), strain Armstrong	(Dutko & Oldstone, 1983)
Lymphocytic choriomeningitis virus (LCMV), strain Docile	Zinkernagel lab

3.1.3 Antibodies

3.1.3.1 Antibodies - Cell culture

Target Antigen	Clone	Vendor	Identifier
anti-CD3	145-2C11	Tonbo Biosciences	Cat# 70-0031-U500
anti-CD28	37.51	Tonbo Biosciences	Cat# 70-0281-U500
Goat Anti-Mouse IgM F(ab') ₂	Polyclonal	Jackson Immuno-Research Labs	Cat# 115-006-075 RRID: AB_2338474
anti-IFN γ	XMG1.2	Biolegend	Cat# 505834 RRID: AB_11150776
anti-IL4	11B11	Biolegend	Cat# 504122 RRID: AB_11150601
anti-TGF- β	1D11.16.8	BioXCell	Cat# BE0057 RRID: AB_1107757
anti-IL2	JES6-5H4	Biolegend	Cat# 503802 RRID: AB_315296

3.1.3.2 Antibodies – Surface staining

Target Antigen	Conjugate	Clone	Dilution	Vendor	Identifier
anti-CD16/32	–	93	1:100	Biolegend	Cat# 101302 RRID: AB_312801
anti-CD4	AF488	RM4-5	1:400	Biolegend	Cat# 100532 RRID: AB_493373
anti-CD4	BV510	RM4-5	1:400	Biolegend	Cat# 100559 RRID: AB_2562608
anti-CD4	BUV496	GK1.5	1:400	BD Biosciences	Cat# 612952 RRID: AB_2813886
anti-CD8	BV605	53-6.7	1:400	Biolegend	Cat# 100743 RRID: AB_2561352
anti-CD8	BUV737	53-6.7	1:400	BD Biosciences	Cat# 612759 RRID: AB_2870090
anti-CD19	APC	6D5	1:200	Biolegend	Cat# 115512 RRID: AB_313647
anti-I-A/I-E	BV421	M5/114.15.2	1:800	BD Bioscience	Cat# 562564 RRID: AB_2716857
anti-CD45.1	APC	A20	1:400	Biolegend	Cat# 110714 RRID: AB_313503
anti-CD45.2	PE-Cy7	104	1:400	Biolegend	Cat# 109830 RRID: AB_1186098
anti-CD62L	PE-Cy7	MEL-14	1:400	Tonbo Bioscience	Cat# 60-0621
anti-CD44	PerCP-Cy5.5	IM7	1:400	Biolegend	Cat# 103032 RRID: AB_2076204
anti-CXCR5	Biotin	L138D7	1:50	BioLegend	Cat# 145509 RRID: AB_2562125
anti-CXCR5	PerCP-ef710	SPRCL5		ThermoFisher	Cat# 46-7185-82 RRID: AB_2573837
anti-CD25	BV785	PC61.5	1:400	Biolegend	Cat# 102051 RRID: AB_2564131
anti-PD-1	PE-Cy7	RMP1-30		Biolegend	Cat# 109110 RRID: AB_572017
anti-PD-1	PE-eF610	J43		eBioscience	Cat# 61-9985-82 RRID: AB_2574688
anti-PD-1	BV711	29F.1A12	1:200	Biolegend	Cat# 135231 RRID: AB_2566158
anti-GL7	AF488	GL-7	1:200	eBioscience	Cat# 53-5902-82 RRID: AB_2016717
anti-IgG1	PE	RMG1-1	1:200	Biolegend	Cat# 406608 RRID: AB_10551618
anti-hNGFR	PE	ME20.4	1:200	Biolegend	Cat# 345106 RRID: AB_2152647
anti-TGF β R2	PE	polyclonal	1:20	R&D Systems	Cat# FAB532P-100UG

3.1.3.3 Antibodies – Transcription factor staining

Target Antigen	Conjugate	Clone	Dilution	Vendor	Identifier
anti-Bcl6	AF488	K112-91	1:50	BD Biosciences	Cat# 561524 RRID:AB_10716202
anti-Bcl6	PE	K112-91	1:50	BD Bioscience	Cat# 561522 RRID: AB_10717126
anti-Tbet	PE-Cy7	4B10	1:400	Biolegend	Cat# 644824 RRID: AB_2561761
anti-Gata3	PerCP-eF710	TWAJ	1:200	eBioscience	Cat# 46-9966-42 RRID: AB_10804487
anti-Rorgt	PE	Q31-378	1:200	BD Bioscience	Cat# 562607 RRID: AB_11153137
anti-Rorgt	APC	AFKJS-9	1:200	eBioscience	Cat# 17-6988-82 RRID:AB_10609207
anti-cMaf	AF488	sym0F1	1:200	ThermoFisher	Cat# 53-9855-82 RRID: AB_2811881
anti-cMaf	eF660	sym0F1	1:200	ThermoFisher	Cat# 50-9855-82 RRID: AB_2574388

3.1.3.4 Antibodies – Cytokine staining

Target Antigen	Conjugate	Clone	Dilution	Vendor	Identifier
anti-IL-17A	eF450	eBio17B7	1:400	eBioscience	Cat# 48-7177-82 RRID: AB_11149503
anti-IL-17A	BV650	TC11-18H10.1	1:400	Biolegend	Cat# 506930 RRID: AB_2686975
anti-IL-17A	BV785	TC11-18H10.1	1:400	Biolegend	RRID:AB_2629787
anti-IL-2	APC	JES6-5H4	1:200	BD Bioscience	Cat# 554429 RRID: AB_398555
anti-IL-2	PE	JES6-5H4	1:200	eBioscience	Cat# 12-7021-82 RRID:AB_466150
Recombinant Mouse IL-21R hFc Chimera Protein	–	–	1:50	R&D Systems	Cat# 596-MR-100
Goat Anti-human IgG F(ab') ₂	PE	Polyclonal	1:200	Jackson Immuno-Research Labs	Cat# 109-116098, RRID: AB_2337678

3.1.4 Chemicals, consumables, and recombinant proteins

Description	Vendor	Identifier
Cell culture related		
Dulbecco's PBS (w/o Mg ²⁺ , w/o Ca ²⁺)	Gibco	Cat# 14190144
RPMI 1640 Medium	Gibco	Cat# 11879020
FCS	Gibco	Cat# 10500-064 LOT 08Q6395K
HEPES	Gibco	Cat# 15630080
penicillin/streptomycin	Gibco	Cat# 15140122
sodium pyruvate	Gibco	Cat# 11360070
non-essential amino acid solution	Gibco	Cat# 11140050
β-mercaptoethanol	Gibco	Cat# 21985023
IL-12	Peprtech	Cat# 210-12
IL-4	Peprtech	Cat# 214-14
IL-6	Biolegend	Cat# 575706
IL-7	R&D Systems	Cat# 407-ML

IL-21	Biologend	Cat# 574504
TGF- β 1	Biologend	Cat# 763102
Cell culture plate 96-well for suspension cells, flat bottom	Sarstedt	Cat# 83.3924.500
Standard cell culture plate 96- well, round bottom	Sarstedt	Cat# 83.3925
Flow Cytometry related		
eF780 viability dye	eBioscience	Cat# 65-0865-14
7AAD	eBioscience	Cat# 00-6993-50
normal rat serum	Stemcell	Cat# 13551
Normal mouse serum	Thermo Fisher	Cat# 31881
Streptavidin-APC	Biologend	Cat# 405207
Streptavidin-BV421	Biologend	Cat# 405226
Streptavidin-BV650	Biologend	Cat# 405231
Phorbol 12-myristate 13-acetate (PMA)	Sigma-Aldrich	Cat# P1585
Ionomycin (calcium salt)	Sigma-Aldrich	Cat# I0634
4% PFA	Thermo Fisher	Cat# AA433689M
Albumin Fraktion V	Carl Roth	Cat# 8076.3
saponin	Sigma-Aldrich	Cat# 47036-250G-F
Protein Transport Inhibitor (containing Monensin, GolgiStop)	BD Bioscience	Cat# 554724 RRID: AB_2869012
123count eBeads Counting Beads	Thermo Fisher	Cat# 01-1234-42
OneComp eBeads Compensation Beads	Thermo Fisher	Cat# 01-1111-41
Others		
Recombinant Mouse CXCL13 (carrier-free)	Biologend	Cat# 583906
Transwell cell culture inserts	Corning Costar	Cat# 3421
Cell Trace Violet	Thermo Fisher	Cat# C34571
4-hydroxytamoxifen	Sigma-Aldrich	Cat# H7904
Tamoxifen	Sigma-Aldrich	Cat# T5648
Ethanol, absolute	Applichem	Cat# A1613
Corn oil	Sigma-Aldrich	Cat# C8267
STAT5 Inhibitor	Merck	Cat# 573108-10MG
Imject™ Alum Adjuvant	Thermo Fisher	Cat# 77161
NP-OVAL (Ovalbumin)	BioCat	Cat# N-5051
Trizol LS	Invitrogen	#10296028
chloroform	Sigma-Aldrich	Cat# 366927-100ML
Recombinant Cas9 protein	QB3 MacroLab, University of California, Berkeley	n/a
Poly-L- γ -glutamic acid sodium salt	Sigma-Aldrich	Cat# G1049-100MG
Quick Extract DNA Extraction solution	Lucigen	Cat# QE09050
24-well plates	Corning Costar	Cat# 3524

3.1.5 Commercial assays

Name	Vendor	Identifier
Foxp3 Transcription Factor Staining Buffer Set	Thermo Fisher	Cat# 00-5523-00
EasySep Mouse Naive CD4 ⁺ T Cell Isolation Kit	Stemcell	Cat# 19765
EasySep Mouse B Cell Isolation Kit	Stemcell	Cat# 19854
MojoSort Mouse CD4 Naïve T Cell Isolation Kit	Biologend	Cat# 480040
MojoSort Mouse CD4 Nanobeads	Biologend	Cat# 480070
CD4 ⁺ T Cell Isolation Kit, mouse	Miltenyi	Cat# 130-104-454
RNeasy Micro Kit	Qiagen	Cat# 74104
SensiFAST cDNA Synthesis Kit	Meridian Bioscience	Cat# BIO-65054

PrimeTime Gene Expression Master Mix	IDT	Cat# 1055772
P4 Primary Cell 96-well Nucleofector Kit	Lonza	Cat# V4SP-4096
Maxwell RSC miRNA Tissue Kit	Promega	Cat# AS1460
Agencourt RNAClean XP Beads	Beckman Coulter	Cat# A63987
SENSE mRNA-Seq Lib Prep Kit V2	Lexogen	Cat# A01161
Agencourt AMPure XP beads	Beckman Coulter,	Cat# A63880
3' mRNA-Seq Library Prep Kit FWD	Lexogen	Cat# 115
BD Mouse Immune Single-Cell Multiplexing Kit	BD	Cat# 633793
Qubit dsDNA HS Kit	ThermoFisher	Cat# Q32851
High-Sensitivity D5000 assay	Agilent	

3.1.6 Oligonucleotides

Name and Sequence	Vendor	Database
Alt-R CRISPR-Cas9 crRNA, 100 nmol	IDT	
Alt-R CRISPR-Cas9 tracrRNA, 100nmol	IDT (Cat# 1072534)	
Alt-R CRISPR-Cas9 Negative control crRNA #1	IDT (Cat# 1072544)	
<i>Cxcr5</i> sgRNA 5'-CCGTCGACTCCTCTCCATCC-3' Fw Primer 5'-CTCAACCGAGACCTTCCTGT -3' Rv Primer 5'-AACCAGGCTCTAGTTTCCGC -3'	IDT	Brie
<i>Cxcr5</i> sgRNA 5'- CCCGTTTCCTCTACCACATC-3' Fw Primer 5'-CTCAACCGAGACCTTCCTGT-3' Rv Primer 5'-CTCAACCGAGACCTTCCTGT-3'	IDT	VBC
<i>Cxcr5</i> sgRNA 5'- ATCACAAGCATCGGTAGTAG-3' Fw Primer 5'-CTCAACCGAGACCTTCCTGT-3' Rv Primer 5'-CTCAACCGAGACCTTCCTGT-3'	IDT	GuidePro
<i>Tgfb2</i> sgRNA 5'- CGTGAGGTACTCCTGCAGGT-3' Fw Primer 5'-GGGGATTGCCATAGCTGTCA-3' Rv Primer 5'-AGAGCTCTTGAGGTCCCTGT-3'	IDT	Brie
<i>Tgfb2</i> sgRNA GCAGACGGATGTCTACTCCA Fw Primer 5'-ACAATCGTTGGCATGGGAGA-3' Rv Primer 5'-CCATGCTTGAGACAGACAGC-3'	IDT	VBC
<i>Tgfb2</i> sgRNA 5'- CGGAAGTTCTAGAATCCAGG-3' Fw Primer 5'-ACAATCGTTGGCATGGGAGA-3' Rv Primer 5'-CCATGCTTGAGACAGACAGC-3'	IDT	GuidePro
<i>Bcl6</i> sgRNA GAGGGAAGGCAATATCATGG Fw Primer 5'-TACAGTGGCGACTCTGCTTG-3' Rv Primer 5'-TCTGGAACCATCCTTTCTGCAT-3'	IDT	Brie
<i>Bcl6</i> sgRNA 5'- CCAGTTTGTGTCACAGCAAC-3' Fw Primer 5'-TACAGTGGCCTGTCAACACC-3' Rv Primer 5'-TGGAGCATTCCGAGCAGAAG-3'	IDT	VBC
<i>Bcl6</i> sgRNA 5'- CTGTGAAATCTGTGGCACTC-3' Fw Primer 5'-GGTTTGTTCAGGTGAGCAGG-3' Rv Primer 5'-TCCAATTGCTGTGTACCCCT-3'	IDT	GuidePro
<i>Smad3</i> sgRNA 5'- CCATGAATTACGGGCCATGG-3' Fw Primer 5'-CTTAGGAGACGGCAGTCAA-3' Rv Primer 5'-CTCCTGAGTAGGTAGGAGGGG-3'	IDT	Brie
<i>Smad3</i> sgRNA 5'- ATGTGTCGCCTTGTAAGTTC-3' Fw Primer 5'-TACTACGAGCTGAACCAGCG-3' Rv Primer 5'-CCATTCAATGTCCTGTGGGC-3'	IDT	VBC

<i>Smad3</i> sgRNA TCACGTTATCTACTGCCGCC Fw Primer 5'-CTTAGGAGACGGCAGTCCAA-3' Rv Primer 5'-CTCCTGAGTAGGTAGGAGGGG-3'	IDT	GuidePro
<i>Stat3</i> sgRNA 5'-CCGTAGTGACAGAGAAGCAG-3' Fw Primer 5'-CTCCCCTTTGGATGGGATGG-3' Rv Primer 5'-CAAAGTCGTCCTGGAGGTTCT-3'	IDT	Brie
<i>Stat3</i> sgRNA 5'- GTGGGAAGAGTCTCGCCTCC-3' Fw Primer 5'-TAGCCAAGTTCACTCCACACC-3' Rv Primer 5'-GTTCACCCCTTCAGCAACACTG-3'	IDT	VBC
<i>Stat3</i> sgRNA 5'- ACCTGACTTTTCGTGGTAAAC-3' Fw Primer 5'-AGAGATGACGTTCCGAAGGG-3' Rv Primer 5'-TGGGCTTCATCTCTCACCCA-3'	IDT	GuidePro
<i>Batf</i> sgRNA 5'- CGGTGAGCTGTTTGATCTCT-3' Fw Primer 5'-GCCATCATGTACCACCAACC-3' Rv Primer 5'-GCCTTAAGTCCCTCTGACCA-3'	IDT	Brie
<i>Batf</i> sgRNA 5'-CTGTGCTCCGTGCTGGCCAG-3' Fw Primer 5'-GCCATCATGTACCACCAACC-3' Rv Primer 5'-GCCTTAAGTCCCTCTGACCA-3'	IDT	VBC
<i>Batf</i> sgRNA 5'- GGTGAAGGGTGTCCGCTTTC-3' Fw Primer 5'-GTCCTATTTTGAATAAGAGGAACG-3' Rv Primer 5'-GCAGCTCTTGCCCTCTACTA-3'	IDT	GuidePro
<i>Ikzf3</i> sgRNA TCATATTAACACTGCACACGG Fw Primer 5'-GGGATGGGCCTTACCTTAG-3' Rv Primer 5'-GGCCTCCACACTCAACTAGG-3'	IDT	Brie
<i>Ikzf3</i> sgRNA 5'- CTGAGATGGTCCCAGTCATC-3' Fw Primer 5'-GGATCCAGTGTGCAGCAATC-3' Rv Primer 5'-TATTGGGGGACAGACCTCGT-3'	IDT	VBC
<i>Ikzf3</i> sgRNA 5'- TAGATAGCTGATGGCGTTAT-3' Fw Primer 5'-GGATCCAGTGTGCAGCAATC-3' Rv Primer 5'-TATTGGGGGACAGACCTCGT-3'	IDT	GuidePro
<i>Maf</i> sgRNA GGTGTCGGCCGTGATCGCCG Fw Primer 5'-CCCTCTCCTGCAGCCCA-3' Rv Primer 5'-CGTTTTCTCGGAAGCCGTTG-3'	IDT	Brie
<i>Maf</i> sgRNA 5'- CCTTGCTGACCCCGCGCAGC-3' Fw Primer 5'-CCCTCTCCTGCAGCCCA-3' Rv Primer 5'-CGTTTTCTCGGAAGCCGTTG-3'	IDT	VBC
<i>Maf</i> sgRNA 5'- TCTTGAAGCGGCAGGACTGG-3' Fw Primer 5'-CCCTCTCCTGCAGCCCA-3' Rv Primer 5'-CGTTTTCTCGGAAGCCGTTG-3'	IDT	GuidePro

3.1.7 Deposited data

Name	Source	Identifier
Bulk RNA-seq 1 (Th1, Tfh (anti-TGF β), Tfh (TGF β))	This work	GEO: GSE198370
Bulk RNA-seq 2 (CXCR5+, IL17A+)	This work	GEO: GSE198374
Bulk RNA-seq 3 (Cell density)	This work	GEO: GSE197425
Bulk RNA-seq 4 (Maf KO)	This work	GEO: not deposited yet
Single-cell RNA-seq	This work	GEO: GSE197842
Mass cytometry proteomics	This work	PRIDE: PXD031913

3.1.8 Instruments

Name	Vendor	Location
BD LSRFortessa	BD Biosciences	CFFlowCyt Munich UKB Flow Core
BD FACSAria Fusion	BD Biosciences	CFFlowCyt Munich UKB Flow Core
BD FACSCanto II	BD Biosciences	CFFlowCyt Munich UKB Flow Core
HiSeq 1500	Illumina	LAFUGA Munich
NovaSeq 6000	Illumina	Life & Brain Center Bonn
Bioruptor	Diagenode	MPI Munich
EASY-nLC 1200 HPLC system	Thermo Fisher	MPI Munich
Q Exactive HF-X	Thermo Fisher	MPI Munich
BD Rhapsody	BD Biosciences	DZNE
Qubit Fluorometer	Thermo Fisher	DZNE
NextSeq 500	Illumina	DZNE
TapeStation 4200	Agilent Technologies	DZNE
Hemocytometer	INCYTO	DZNE
4D-Nucleofector	Lonza	Basel University Hospital

3.1.9 Software and algorithms

Name	Source
FlowJo, v10.8	Treestar
Prism, v8	GraphPad
Microsoft Word	Microsoft
Mendeley Reference Manager	Mendeley
Adobe Illustrator 2022	Adobe
Inkscape 1.2.1	Inkscape Project
Biorender.com	biorender.com
R, v4.1.2	(R Core Team, 2017)
RStudio, v2021.09.2	https://www.rstudio.com/
Galaxy, v22.01.rc1	(Afgan et al., 2018)
STAR 2.7.2b	(Dobin et al., 2013)
FeatureCount 1.6.4	(Liao et al., 2014)
Tidyverse v1.3.2	(Wickham et al., 2019)
ggplot2, v3.3.5	(Wickham, 2016)
DESeq2, v3.14	(Love et al., 2014)
DEP v1.20.0	(Zhang et al., 2018)
GSEA, v4.1.0	(Mootha et al., 2003; Subramanian et al., 2005)
Seurat, v4.1.0	(Stuart et al., 2019)
Xcalibur software	Thermo Fisher
MaxQuant (1.6.5.0)	(Cox & Mann, 2008)

3.2 Methods

3.2.1 Experimental animals

All mice used in this thesis are listed in table 2.1.1. Experimental groups were sex and age-matched. Mice were housed in individually ventilated cages under specific pathogen-free conditions. All animal experiments were performed in accordance with European regulation and federal law of Germany, either approved by the Regierung von Oberbayern or the Landesamt für Natur-, Umwelt und Verbraucherschutz NRW (for work in the Baumjohann lab), in accordance with the guidelines of the University of Melbourne Animal Ethics Committee (for work in the Kallies lab), or in accordance with federal and cantonal laws of Switzerland, approved by the Animal Research Commission of the Canton of Basel-Stadt (for work in the Jeker lab).

3.2.2 *In vitro* cell culture

We prepared single-cell suspensions by mincing spleens and peripheral lymph nodes between the frosted ends of two microscope slides. The cell suspensions were filtered through a fine mesh (Baumjohann & Ansel, 2015). Naïve CD4⁺ T cells were enriched from spleen and/or peripheral lymph node suspensions by negative selection using either Stemcell Technologies' EasySep™ Mouse Naïve CD4⁺ T Cell Isolation Kit or Biolegend's MojoSort™ Mouse CD4 Naïve T Cell Isolation Kit according to the manufacturers' instructions. The purity of naïve CD4⁺ T cells was consistently over 95%. 96-well flat-bottom tissue culture suspension plates were coated with 2 µg/ml anti-CD3 and 2 µg/ml anti-CD28 in 50 µl PBS overnight at 4°C. Plates were washed twice and naïve CD4⁺ T cells were cultured in 200 µl of complete medium (RPMI + 10% FCS + 10 mM HEPES + 100 U/ml penicillin/streptomycin + 1 mM sodium pyruvate + 1x non-essential amino acid solution + 50 nM β-mercaptoethanol) at 37 °C and 5% CO₂ for 3.5 days, if not stated otherwise. The following combinations of cytokines and cytokine-blocking antibodies were used: Th1 (20 ng/ml IL-12 and 10 µg/ml anti-IL-4), Th2 (40 ng/ml IL-4 and 10 µg/ml anti-IFNγ), Th17 (50 ng/ml IL-6, 5 ng/ml human TGFβ1, 10 µg/ml anti-IL-4, and 10 µg/ml anti-IFNγ), and Tfh (50 ng/ml IL-6, 25 ng/ml IL-21, 10 µg/ml anti-IL-4, and 10 µg/ml anti-IFNγ). If not stated otherwise, TGFβ was either blocked with anti-TGFβ antibodies at 10 µg/ml in Tfh (anti-TGFβ) cultures or TGFβ was added at 5 ng/ml to Tfh (TGFβ) cultures. Where indicated, 20 µg/ml anti-IL-2 or 100 µM of STAT5 inhibitor was added to the culture.

3.2.3 *In vitro* tamoxifen treatment

Where appropriate, purified naïve CD4⁺ T cells isolated from CD4-CreERT2 mice were incubated overnight in 200 µl cRPMI medium plus 4-hydroxytamoxifen. Cells were harvested on the next day and plated on anti-CD3/anti-CD28-coated plates as described above.

3.2.4 *In vivo* Tfh cell differentiation

Tamoxifen was dissolved in ethanol at a concentration of 1 g/ml and emulsified with corn oil at 56 °C in a water bath to a final concentration of 33 mg/ml. To generate induced control (*iTgfb2^{+/+}*) and conditional knock-out (*iTgfb2^{Δ/Δ}*) OT-II cells *in vivo*, CD45.1- and/or CD45.2-expressing OTII x CD4CreERT2⁺ x *Tgfb2^{+/+}* x *Rosa26^{fl-Stop-fl-YFP}* and OTII x CD4CreERT2⁺ x *Tgfb2^{fl/fl}* x *Rosa26^{fl-Stop-fl-YFP}* mice were treated with tamoxifen twice a day for two consecutive days with 5 mg tamoxifen in 150 μl corn oil by intragastric gavage. Three days after the start of the tamoxifen treatment, naïve CD4⁺ T cells were isolated from spleen and peripheral lymph node suspensions with the EasySep™ Mouse Naïve CD4⁺ T Cell Isolation Kit from Stemcell Technologies according to the manufacturer's instructions. OT-II cells were adjusted to 5x10⁴ cells in 100 μl PBS and injected into the tail vein of wildtype C57BL6/J recipient mice. On the following day, the mice were immunized intraperitoneally with a 1:1 mixture of 100 μg NP-OVA in PBS and Imject Alum in a total volume of 100 μl. On day 3.5 after immunization, the mice were sacrificed and CD4⁺ T cells in spleen and mesenteric lymph nodes were first enriched by positive selection using Miltenyi Biotec's CD4 (L3T4) MicroBeads and LS columns. Unfractionated (for quantification of total cell numbers) and enriched cell populations were then stained and analyzed by flow cytometry, utilizing antibodies against CD45.1 to identify adoptively transferred cells.

3.2.5 Flow cytometry

Cells were collected from cell cultures, washed, and stained in 96-well round bottom plates as previously described (Baumjohann & Ansel, 2015). Dead cells were excluded using Fixable Viability Dye eFluor™ 780. Unspecific binding was blocked by preincubating cells with 2 % normal mouse serum, 2 % normal rat serum, and anti-CD16/CD32 (1:100 dilution). For regular surface staining the antibodies listed in table 2.1.3.2 were used. Biotinylated anti-CXCR5 was used to stain CXCR5 for 30 min on ice, followed by washing and incubation with fluorophore-conjugated streptavidin for another 15 minutes on ice. For the detection of transcription factors, cells were fixed for 20 min at room temperature and permeabilized with the eBioscience™ Foxp3/Transcription Factor Staining Buffer Set and stained for 45 min in Perm/Wash buffer with the antibodies listed in table 2.1.3.3. For intracellular cytokine staining, cells were re-stimulated with 0.02 μM PMA and 1 μM ionomycin for 2h followed by addition of monensin for additional 2h. After surface staining, cells were then fixed for 20 min at room temperature and permeabilized with the eBioscience™ Foxp3/Transcription Factor Staining Buffer Set. Alternatively, cells were fixed with 4% PFA for 15min at room temperature and permeabilized with saponin for 5 min on ice. Antibodies in the table 2.1.3.4 were then used for intracellular cytokine detection. IL21R/Fc chimera was visualized with PE-conjugated affinity-purified F(ab')₂ fragment of goat anti-human Fcγ antibody. Samples were acquired on a BD FACSCanto II or a BD LSRFortessa. Cell sorting was performed on a BD FACSAriaFusion. Data were analyzed with FlowJo software and compensated with OneComp eBeads Compensation Beads.

3.2.6 Transwell migration assay

Naïve CD4⁺ T cells were cultured under Tfh (anti-TGFβ) or T_H (TGFβ) conditions for 3.5 days as described above. Cells were collected, washed, and adjusted to a concentration of 5x10⁶ cells/ml in chemotaxis medium (RPMI + 0,5% BSA + 10 mM HEPES + 100 U/ml penicillin/streptomycin + 1mM sodium pyruvate + 1x non-essential amino acid solution + 50 nM β-mercaptoethanol). 600 µl of chemotaxis medium containing 1 µg/ml CXCL13 was added to the lower chamber of transwell assay plates. Inserts were filled with 100 µl of the cell suspension and placed on top of the lower chamber. Additionally, cells were added to inserts in wells without the chemokine as a control for random migration and directly into wells containing the chemotaxis buffer as an input control. After incubation for 3 hours at 37°C and 5% CO₂, transmigrated cells were recovered from the lower chamber and stained for quantification by flow cytometry. Before acquisition, cells were resuspended in 150 µl flow buffer containing 7AAD, and 30 µl of 123count eBeads Counting Beads were added. The samples were acquired on a BD FACSCanto II flow cytometer. The Chemotatic Index was calculated by dividing the number of cells migrated to CXCL13 by the number of migrated cells in the absence of CXCL13. The % Net Migration was calculated by subtracting the number of cells that migrated to CXCL13 with the number of cells that migrated in the absence of CXCL13, divided by the number of cells in the input control.

3.2.7 B cell-T cell co-culture

Spleen and peripheral lymph nodes were harvested from wildtype C57BL/6J or SAP^{-/-} mice. Single-cell suspensions were prepared as described above. Naïve B cells were isolated using Stem-cell Technologies' EasySep™ Mouse B Cell Isolation Kit according to the manufacturer's instructions. Naïve CD4⁺ T cells were isolated and cultured under various T helper cell differentiation conditions for 3.5 days as described above. Cells were collected, washed, counted, and 3x10⁴ CD4⁺ T cells were co-cultured with 5x10⁴ naïve B cells in the presence of 2 µg/ml anti-CD3 antibodies and 5 µg/ml anti-IgM F(ab')₂ in cRPMI. After 3.5 days, cells were harvested, stained, and analyzed by flow cytometry as previously described (Sage et al., 2016).

3.2.8 Bulk RNA sequencing and GSEA

For Seq01 and Seq02, 3x10⁵ and 1x10⁵ live CD4⁺ T cells were sorted on a BD FACSAriaFusion using a 70-micron nozzle, respectively. RNA isolation and sequencing was performed by the LAGUGA platform in the Gene Center Munich. RNA was isolated using the Maxwell RSC miRNA Tissue Kit following the manufacturer's instructions and purified using Agencourt RNAClean XP Beads. For generating sequencing libraries, 100 ng RNA (RNA integrity number (RIN) > 8.0) was processed using the SENSE mRNA-Seq Lib Prep Kit V2 with half of the volume as described in the manual. The PCR products were purified with Agencourt AMPure XP beads. Sequencing was performed at LMU's Gene Center using a HiSeq1500 instrument with a read length of 50 nucleotides, single-end mode. For Seq03 and Seq04, 2x10⁵ *in vitro*-cultured T helper cell populations were sorted directly into 0.75 ml Trizol LS on a BD FACSAriaFusion using a 70-micron nozzle. 200 µl chloroform was added to 1ml of lysed cells and mixed by inverting. After incubation for 3

min, the samples were centrifuged for 15 min at 12,000 xg at 4 °C. The upper aqueous layer was transferred to a new tube, containing 200 µl chloroform. Then the upper aqueous layer was transferred to a new tube once more, and 1 volume of 70 % ethanol was added on top. After mixing by pipetting, each sample was transferred to a RNeasy spin column. The downstream RNA isolation was performed with the RNeasy kit according to the manufacturer's instructions. The bulk RNA-sequencing was performed by NGS core facility of the Medical Faculty at the University of Bonn. The sequencing library was generated according to manufacturer's guidelines with the 3' mRNA-Seq Library Prep Kit FWD with Unique Dual Indices using 50 ng total RNA as input. Libraries were single-end sequenced with 1x100bp on a S1 flow cell of an Illumina NovaSeq instrument to a depth of 10M raw reads on average at NGS Core Facility of University Hospital Bonn. All raw fastq data were mapped by Y.C. to the mouse genome (mm10) using STAR 2.7.2b. Count matrices were then generated using FeatureCount 1.6.4 with the gene annotation file for mm10. The count matrices were loaded into R. Sparsely detected genes with less than 10 counts over all samples were filtered out. Afterwards, libraries were normalized and differentially expressed genes were called with DESeq2. All plots were created using ggplot2. The GSEA plots were generated with software from UC San Diego and the Broad Institute.

3.2.9 MS-based proteomics

Live CD4⁺ T cells were sorted from *in vitro* cell cultures on day 3.5 with a BD FACSAriaFusion cell sorter at the BMC Core Facility Flow Cytometry using an 85-micron nozzle. 2-3x10⁵ (Tfh + anti-TGFβ) and 7-8x10⁵ (Tfh + 5ng/ml TGFβ) sorted cells were pelleted at 500 xg and shock-frozen with liquid nitrogen. The following procedures were performed by the Meissner lab in Munich (Winter et al., 2018): Cell pellets were resuspended in 50 µL of digestion buffer containing 1% sodium deoxycholate, 40 mM tris(2-carboxyethyl)phosphine and 40 mM 2-chloroacetamide in 100 mM Tris (pH 8.5), and immediately heated in a thermoshaker for 10 min at 95°C. Afterwards, samples were sonicated with a Bioruptor for 15 min at 4°C and digested with 1 µg LysC and 1 µg trypsin for 18 h at 37 °C, 1000 rpm. Samples were acidified by adding 300 µL of 1% trifluoroacetic acid (TFA) in isopropanol. Peptides were desalted using in-house made SDB-RPS StageTips and resuspended in 10 µL of buffer A* (2% acetonitrile, 0.1% TFA) for LC-MS. 500 ng peptides were analyzed with an EASY-nLC 1200 HPLC system coupled to a Quadrupole Orbitrap mass spectrometer (Q Exactive HF-X) via a nano-electrospray ion source. Peptides were loaded onto an in-house packed column (75 µm inner diameter, 50 cm length, packed with 1.9 µm C18 ReproSil beads (Dr. Maisch GmbH)). To elute peptides, a buffer system consisting of buffer A (0.5% formic acid) and buffer B (0.5% formic acid and 80% acetonitrile) was used with a linear gradient from 5% to 30% buffer B in 150 min at 300 nl/min flow. The temperature of the column was maintained at 60°C. The Mass spectrometer was operated using a data-dependent MS/MS method, collecting MS1 spectra (300 to 1650 m/z, R = 60 000, AGC target 3x10⁶, maximum injection time 20 ms) followed by 15 MS/MS scans with higher-energy collisional dissociation (200 to 2000 m/z, R = 15 000, normalized collision energy 27%, AGC target 1x10⁵, maximum injection time 28 ms, isolation window 1.4 m/z). Dynamic precursor exclusion of 30 s was enabled to minimize resequencing. Data were acquired using Xcalibur software. MS raw files were processed

using MaxQuant (1.6.5.0) and mass spectra were searched against the mouse UniProt FASTA database (July 2019) with an FDR of 1% at the protein and peptide level. A maximum of two missed cleavages and a minimum peptide length of 7 amino acids were allowed in the database search. Match between runs was enabled and the minimum ratio count for label-free quantification was set to 2. Proteins matches to the reverse database, matches only identified by site, and common contaminants were removed. Only proteins that are identified in at least 3 replicates of one condition were retained. Missing values were replaced from a Gaussian distribution (30% width and downshift by 1.8 standard deviations of measured values) and t-tests were applied with a permutation-based FDR of 5%. Data and statistical analysis were performed by Y.C. with DEP in R.

3.2.10 Single-cell RNA-sequencing

Naive CD4⁺ T cells were isolated from skin-draining lymph nodes of sex- and age-matched C57BL/6 mice using the EasySep™ Mouse Naïve CD4⁺ T Cell Isolation Kit from Stemcell Technologies according to the manufacturer's instructions. 2x10⁴ naïve CD4⁺ T cells were cultured under Tfh (2 ng/ml TGFβ) conditions as described above for 3.5, 1.5, 0.5, and 0 days. To minimize batch effects, all cells were harvested on the same day and further processed together. The harvested cells were stained with viability dye, CD4, CD8, I-A/I-E, CD62L and mouse sample hashtag antibodies. 2x10⁵ viable CD4⁺ T cells of each condition were sorted on a BD FACSAriaFusion at the UKB Flow Cytometry Core Facility using a 100-micron nozzle. Equal volumes of each sorted cell population were combined and the cell count was set to 1x10⁶ cell/ml. Whole transcriptome analysis was performed by the PRECISE platform of DZNE using the BD Rhapsody Single-Cell Analysis System. Cells corresponding to different time points were labelled with hashtag oligo (HTO)-conjugated anti-CD45 antibodies (BD Mouse Immune Single-Cell Multiplexing Kit). Pooled samples were diluted using BD Sample Buffer to a final volume of 615µL. Cell counting was performed using an INCYTO hemocytometer, and a total of 58,000 cells were loaded on a BD Rhapsody cartridge. Cell and bead loading, cell lysis, bead recovery, reverse transcription, and exonuclease treatment were performed according to the manufacturer's instructions (BD Biosciences). cDNA libraries were prepared using the BD Rhapsody mRNA Whole Transcriptome Analysis and Sample Tag Library Preparation Protocol, as per the manufacturer's recommendations (BD Biosciences). Quantification of the final libraries was done using a Qubit Fluorometer with the Qubit dsDNA HS Kit, whereas the size distribution of the cDNA library was assessed using the Agilent High-Sensitivity D5000 assay on a TapeStation 4200 system. Paired-end sequencing (2*75 cycles) was performed on a NextSeq 500 System (Illumina) using NextSeq 500/550 High Output Kits v2.5. Raw sequencing bcl files were demultiplexed using the Bcl2fastq2 V2.20. Sequencing adapters were trimmed and sequencing reads with a PHRED score >20 were filtered using Cu-tadapt 1.16. Subsequently, STAR was used to align reads against the GENCODE vM16 mouse reference genome. Drop-seq tools 2.0.0 were used to generate a UMI-corrected gene expression count matrix. HTO sequences associated with the anti-CD45 multiplexing antibodies were added to the reference genome to simultaneously allow for their retrieval during alignment. Downstream analysis was performed by Y.C with help from the PRECISE platform and Nicolás

Gutiérrez-Melo using the Seurat R package. The dataset was filtered to exclude cells with a UMI count below the inflection point on a UMI count-by-cell number plot. The dataset was further filtered to exclude cells expressing less than 500 genes, more than 4000 genes, or cells whose mitochondrial reads represented more than 10% of its total transcripts. Normalization and scaling were performed using the SCTransform function from Seurat. Principal component analysis, clustering, and non-linear dimensionality reductions were all performed using the standard Seurat workflow. Enrichment scores were calculated using the AddModuleScore function from Seurat. Th17 and Tfh signature scores were created based on the data generated by bulk RNAseq in this study or taken from the previously published dataset GSE11924 (Nurieva et al., 2008).

3.2.11 CRISPR in naïve CD4⁺ T cells

CRISPR experiments were performed by the Jeker lab in Basel. In some experiments, Luisa Bach provided help. Naive CD4⁺ T cells were isolated from skin-draining and mesenteric lymph nodes as well as spleens using the EasySep™ Mouse Naïve CD4⁺ T Cell Isolation Kit according to the manufacturer's instructions. To obtain enough cells for the experiments and to reduce variability, cells from 3-10 mice were pooled per experiment before the enrichment step. Purity was routinely checked by flow cytometry, with >95 % CD4⁺ cells and >90 % of CD62L⁺CD44⁻ cells. Isolated cells were stained with Cell Trace Violet (CTV) proliferation dye and cultured at 3x10⁶ cells/ml in 24-well plates for 24 hours in T cell medium supplemented with 5 ng/ml recombinant mouse IL-7. Guide RNAs (gRNAs) with highest predicted efficiencies were picked from the Brie library, VBC score (<https://www.vbc-score.org/>), and GuidePro (<https://bioinformatics.mdanderson.org/apps/GuidePro/>) webtool (Doench et al., 2016; He et al., 2021; Michlits et al., 2020). Cutting efficiencies were assessed using Sanger sequencing and the tracking indels by decomposition (TIDE) method (<http://shinyapps.datacurators.nl/tide/>) (Brinkman et al., 2014). Cas9 ribonucleoproteins (RNPs) were prepared according to previously described protocol (Dölz et al., 2021; Kornete et al., 2018). CRISPR RNA (crRNA) and trans-activating RNA (tracrRNA) were mixed in equimolar concentrations in a sterile microcentrifuge tube or PCR plate, incubated at 95°C for 5min and cooled down at room temperature for 10 minutes. Alternatively, previously prepared gRNAs were thawed and used downstream. 180 pmol (1.8 µl) of gRNA solution was taken for one transfection and mixed with 0.8x volume (1.44 µl) of 100 mg/ml of poly-L-glutamic acid (PGA) (Nguyen et al., 2020). As a negative control, tracrRNA was used without crRNA. 60pmol (1.5 µl) of recombinant Cas9 protein were added to gRNA-PGA solution for each electroporation. The resulting RNP solution was incubated for 20 min before electroporation according to a published protocol (Seki & Rutz, 2018). Plates containing T cell medium supplemented with 5 ng/ml recombinant murine (rm)IL-7 were prepared and warmed to 37 °C in an incubator. 48-well with 410 µl medium for 1-2x10⁶ cells/electroporation and 96-well with 110 µl medium for 6x10⁵ cells/electroporation. Cells were harvested from the plates, washed with PBS and adjusted to 6x10⁵ to 2x10⁶ cells/electroporation. Immediately before electroporation, cells were resuspended in 20µl of P4 primary cell buffer and mixed with RNP suspension by pipetting up and down and transferred to a Nucleocuvette Strip. Cells were electroporated on a 4D-Nucleofector X Unit using program DS137. After transfection, 80µl of prewarmed medium containing 5ng/ml rmlL-7 were added to

each well and 90µl of cell suspension were transferred to a previously prepared cell culture plate. After 3 days of culture, half of the medium was removed and exchanged for the same volume supplemented with 10ng/ml rmlL-7. On day 6 after electroporation, cells were harvested, washed three times with T cell medium, adjusted to 1×10^5 /ml and cultured on anti-CD3/anti-CD28-coated plates under various T helper cell differentiation conditions as outlined above. 3.5 days later, cells were harvested and stained with fluorophore-coupled antibodies as described above. Samples were acquired on a flow cytometer (BD LSRFortessa) and analyzed with FlowJo (v.10.8.0).

3.2.12 LCMV infections

LCMV experiments were performed by the Kallies lab in Melbourne. LCMV Armstrong was propagated on baby hamster kidney (BHK) cells and titrated on Vero African green monkey kidney cells according to the established protocol (Utzschneider et al., 2013). LCMV Armstrong was injected intraperitoneally into mice at 2×10^5 p.f.u. per mouse to establish an acute infection. LCMV Docile was propagated in BHK cells and titrated on Vero African green monkey kidney cells according to an established protocol (Battegay et al., 1991). Frozen stocks were adjusted with phosphate-buffered saline (PBS); 2×10^6 p.f.u. of LCMV Docile were injected intravenously.

3.2.13 Statistical analysis

All statistical analyses used are described in each corresponding figure legend. Analyses were performed with Prism 8 unless further specified.

4. Results

4.1 Validation of established T cell differentiation protocols

At the start of this project, the published protocols that were able to induce some levels of CXCR5 and Bcl6 protein expression *in vitro*, used *ex vivo* APCs as inducers of T cell activation and co-stimulation (Gao et al., 2019; Lu et al., 2011). The activation with APCs introduces a variety of uncertainties, such as variable interaction with surface molecules and secretion of cytokines. These uncertainties can lead to increased background in the non-Tfh conditions and higher variance in the resulting T cell differentiation (Lu et al., 2011). In order to more systematically probe the requirements for *in vitro* Tfh cell differentiation, we aimed to remove these uncertainties to more stringently control the culture conditions. We decided to culture naïve CD4⁺ T-cells isolated from peripheral lymph nodes and spleens of wildtype C57BL/6J mice with plate-bound anti-CD3 and anti-CD28, for TCR activation and co-stimulation, respectively, as in previous studies that failed to detect Bcl6 and CXCR5 protein expression (Eto et al., 2011; R. I. Nurieva et al., 2008). The culture was supplemented with differentiation mixtures, that contain polarizing cytokines and cytokine-neutralizing antibodies, which we adapted from published protocols for the generation of Th0, Th1, Th2, Th17, and Tfh-like cells (**Figure 1B**) (Eto et al., 2011; Lu et al., 2011). The cells were then differentiated in a 96-well plate for 3.5 days in a standard incubator (**Figure 1A**). In

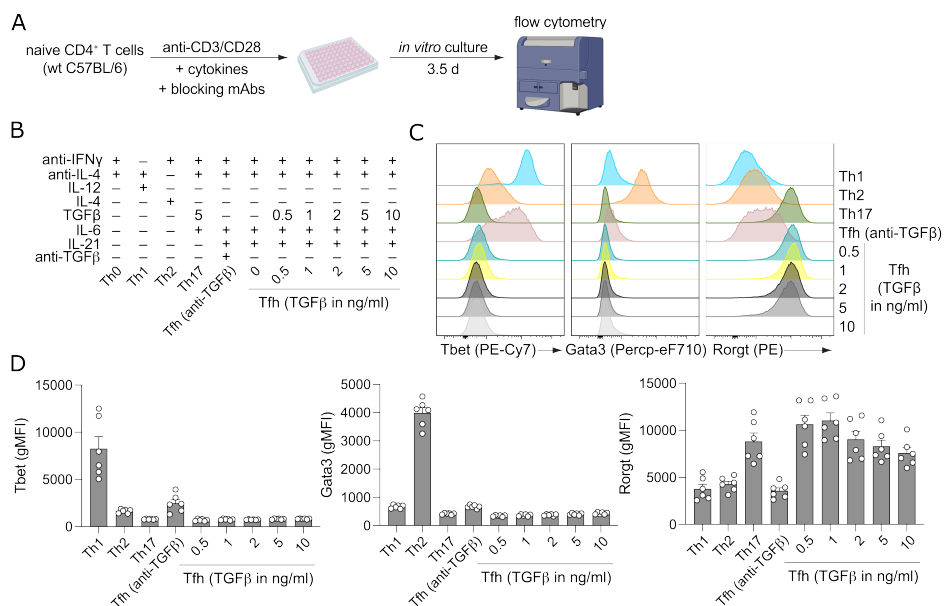


Figure 1: *In vitro* Th1, Th2, Th17, and Tfh differentiation of murine CD4⁺ T cells

(A) Experimental outline: Naïve CD4⁺ T cells (4×10^4) isolated from spleen and peripheral lymph nodes of wildtype C57BL/6 mice were cultured *in vitro* in anti-CD3/CD28-coated 96-well flat-bottom cell culture plates for 3.5 days under various T helper cell differentiation conditions. Cells were then analyzed by flow cytometry.

(B) The combinations of cytokines and cytokine-blocking antibodies used for *in vitro* T helper cell differentiation.

(C) Representative flow cytometry histogram plots showing Tbet, Gata3, and Rorgt protein expression by live CD4⁺ T cells cultured for 3.5 days under the indicated polarizing T helper cell differentiation conditions.

(D) Quantification of the gMFIs of Tbet, Gata3, and Rorgt of live CD4⁺ T cells.

The data are representative of more than five independent experiments with mean \pm SEM displayed of $n = 6$ biological replicates.

accordance with the literature (Saravia et al., 2019), the master transcription factors Tbet, Gata3, and Rorgt were upregulated in Th1, Th2, Th17 conditions, respectively (**Figure 1C, 1D**).

4.2 TGF β induces CXCR5 and Bcl6 protein expression in activated murine CD4⁺ T cells *in vitro*

Looking into the Tfh hallmark proteins, as expected we did not observe CXCR5 protein expression in Th0, Th1 and Th2 differentiation conditions (**Figure 2A, 2B**). Bcl6 gMFI was slightly increased in the Th1 cell condition, as previously reported (Oestreich et al., 2011), but did not result in increased frequencies of Bcl6-positive cells (**Figure 2A, 2B**). In the previously published Tfh-like cell culture (Eto et al., 2011; Lu et al., 2011; R. I. Nurieva et al., 2008), which contains a TGF β -neutralizing antibody, we observed neither CXCR5 nor Bcl6 protein expression (**Figure 2A, 2B**). This differentiation condition will be termed “Tfh (anti-TGF β)” for simplicity reasons, despite not generating Tfh-like cells (**Figure 1B**). Surprisingly, exchanging the TGF β -neutralizing antibody with an increasing dose of TGF β resulted in a dose-dependent and robust increase in CXCR5 and Bcl6 protein expressions (**Figure 2A, 2B**). This Tfh-like differentiation condition will be termed “Tfh (TGF β)” (**Figure 1B**). We further observed strong CXCR5 and Bcl6 protein expression in the Th17 differentiating condition (**Figure 2A, 2B**). The Th17 differentiating condition was similar to the Tfh (5 ng/ml TGF β) condition with the only difference that the former lacked exogenous IL-21 (**Figure 1B**). Likewise, Rorgt was expressed in the Th17 and all Tfh cell cultures that included TGF β and IL-6 (**Figure 1C, 1D**). Furthermore, we observed high T-bet expression in the Tfh (anti-TGF β) condition (**Figure 1C, 1D**).

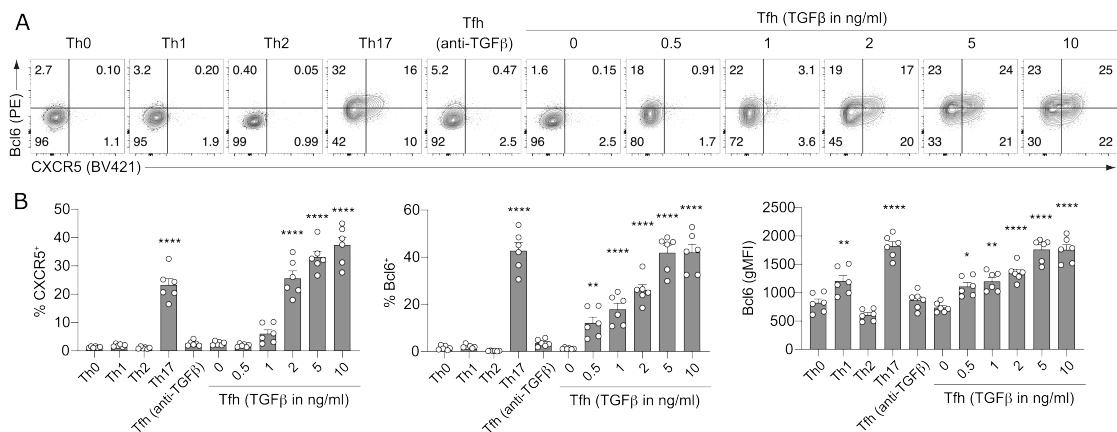


Figure 2: CXCR5 and Bcl6 expression of *in vitro* differentiated cells

(A) Representative flow cytometry contour plots showing the expression of CXCR5 and Bcl6 by live wildtype C57BL/6 CD4⁺ T cells after 3.5 days of culture.

(B) Quantification of frequencies of CXCR5⁺ and Bcl6⁺ cells as well as of Bcl6 gMFI of live CD4⁺ T cells. The Data are representative of more than five independent experiments and display mean \pm SEM with n = 6 biological replicates. (B) One-way ANOVA with Dunnett's multiple comparison test against Th0 condition: *p < 0.05; **p < 0.01; ***p < 0.001; ****p < 0.0001

We next combined our *in vitro* T cell culture with tamoxifen-induced knockout of CXCR5 in naïve CD4⁺ T cells (*Cd4-CreERT2⁺ Cxcr5^{fl/fl}; iCxcr5 Δ/Δ*) and the appropriate control (*Cd4-CreERT2⁺*

Cxcr5^{+/+}; *iCxcr5*^{+/+}). The knockout of CXCR5 resulted in complete ablation of CXCR5 expression, validating the fidelity of the CXCR5 staining (**Figure 3A, 3B, 3C**).

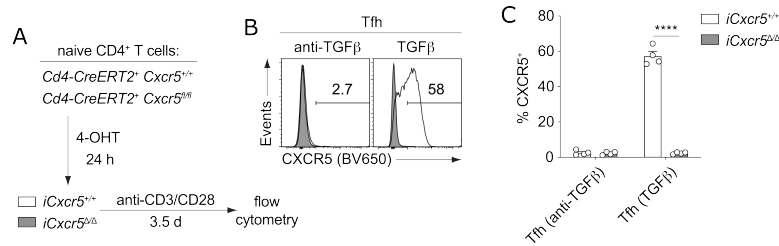


Figure 3: Validation of CXCR5 expression

(A) Experimental outline: Naïve 4-hydroxytamoxifen (4-OHT)-treated CD4⁺ T cells isolated from *Cd4-CreERT2*⁺ *Cxcr5*^{+/+} (*iCxcr5*^{+/+}) and *Cd4-CreERT2*⁺ *Cxcr5*^{fl/fl} (*iCxcr5*^{Δ/Δ}) mice were differentiated *in vitro*.

(B) Representative flow cytometry histogram plots showing the expression of CXCR5 by live CD4⁺ T cells after 3.5 days of culture.

(C) Quantification of the frequency of CXCR5⁺ cells among live CD4⁺ T cells.

The data are representative of two independent experiments with mean ± SEM displayed of n = 4 biological replicates; Unpaired t-test: *p < 0.05; **p < 0.01; ***p < 0.001; ****p < 0.0001.

In order to exclude batch-dependent effects from the fetal bovine serum (FBS) used in the culture, we independently reproduced the results of the Tfh cell culture with FBS from different lots and different sources/vendors in four different labs across two continents. Besides my own work in the Baumjohann lab in Munich and Bonn, the protocol was also validated by the Heissmeyer lab in Munich, the Jeker lab in Basel, and the Kallies lab in Melbourne. Furthermore, the induction of CXCR5 and Bcl6 protein expression by TGFβ *in vitro* was not restricted to C57BL/6 mice, but was also confirmed in CD4⁺ T cells from BALB/c mice (**Figure 4A, 4B, 4C**). While the effect of TGFβ on the induction of CXCR5 was weaker in CD4⁺ T cells derived from BALB/c mice, Bcl6 expression was comparable between BALB/c and C57BL/6 mice (**Figure 4A, 4B, 4C**). In summary, TGFβ induced the Tfh cell hallmark proteins CXCR5 and Bcl6 *in vitro* in both Tfh (TGFβ) and Th17-differentiating conditions.

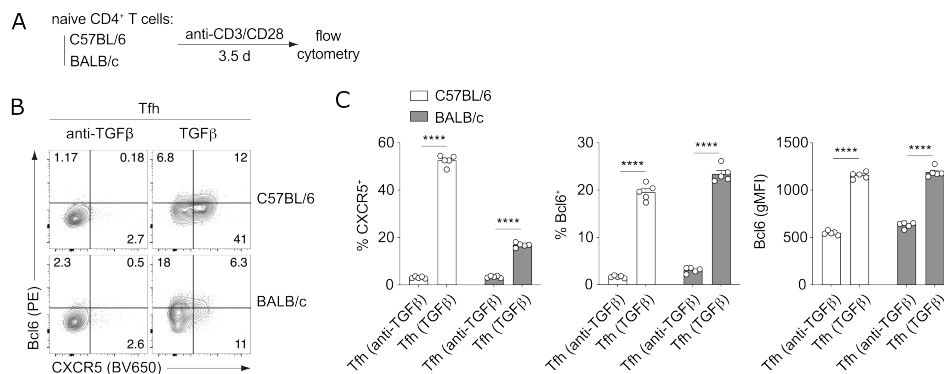


Figure 4: TGFβ induces CXCR5 and Bcl6 expression in CD4⁺ T cells in Balb/c mice

(A) Experimental outline: Naïve CD4⁺ T cells isolated from C57BL/6 and BALB/c mice were differentiated *in vitro*.

(B) Representative flow cytometry histogram plots showing the expression of CXCR5 and Bcl6 by live CD4⁺ T cells after 3.5 days of culture.

(C) Quantification of the frequency of CXCR5⁺ and Bcl6⁺ cells as well as the Bcl6 gMFI of live CD4⁺ T cells. The data are representative of two independent experiments with mean ± SEM displayed of n = 5 biological replicates; Unpaired t-test: *p < 0.05; **p < 0.01; ***p < 0.001; ****p < 0.0001.

4.3 TGF β -induced CXCR5 and Bcl6-expressing cells share transcriptional and proteomic features of *bona fide* Tfh cells

In order to gain more insight into the identity and phenotype of our *in vitro* differentiated Tfh-like cells, we performed bulk RNA-sequencing on *in vitro*-differentiated CD4⁺ T cells cultured under Th1, Tfh (anti-TGF β), and Tfh (TGF β) conditions (**Figure 5A, 5B**). Principal component analysis showed that the difference between the Th1 and Tfh (TGF β) population contributed to the majority of variance (85 %) within this system. The Tfh (anti-TGF β) population introduced an additional 14 % of variance. While the Tfh (anti-TGF β) showed some resemblance with the Th1 condition with a distance of 28.7% of total variance, Tfh (TGF β) was distinctly different from both Th1 and Tfh (anti-TGF β) with a distance of 85.0 % and 61.0 % of total variance, respectively (**Figure 5C**).

Looking into differentially regulated genes between Tfh (anti-TGF β) and Tfh (TGF β), various genes that associate with different T helper cell subsets differed significantly (**Figure 5D, 5E**). The Tfh hallmark genes *Cxcr5* and *Bcl6* were significantly upregulated within the Tfh (TGF β) condition compared to Tfh (anti-TGF β), similar to other Tfh-associated genes, such as *Pdcd1* (encoding PD-1), *Tcf7* (encoding Tcf1), *Tox*, *Tox2*, and *Il21*. However, *Icos*, a characteristic marker of Tfh cells, was downregulated with addition of increasing doses of TGF β (R. I. Nurieva et al., 2008; Schmitt et al., 2014; Suto et al., 2008). The Tfh (anti-TGF β) condition, on the other hand, resembled more the expression pattern of Th1 cells, exhibiting significantly increased expression of *Tbx21* (encoding Tbet), *Il12rb2*, *Il2ra*, *Cxcr3*, and *Prdm1* (encoding the Bcl6-antagonizing transcription factor Blimp-1). As the Tfh (TGF β) condition closely resembles the Th17 condition, with the addition of IL-21, the Tfh (TGF β) compared to Tfh (anti-TGF β) cells expressed markers of Th17 cells, such as *Il17a*, *Il17f*, *Ccl20*, *Rora*, *Rorc*, and *Ahr* (**Figure 5D, 5E**).

Comparing the transcriptome of the *in vitro*-generated Tfh-like cells to previously published signature gene sets of *ex vivo* T cells (R. I. Nurieva et al., 2008), confirmed the resemblance of Tfh (TGF β) with *ex vivo* mature Tfh cells, and Tfh (anti-TGF β) with *ex vivo* mature Th1 cells (**Figure 5F**). Within the multi-staged process of Tfh differentiation (Baumjohann & Fazilleau, 2021), the culture of 3.5 days correlates with the pre-Tfh stage. We therefore choose a dataset of *in vivo*-generated pre-Tfh cells, compared to Th1 cells within the same time frame, and converted the top 200 significantly differentially expressed genes to a gene signature dataset for GSEA (Choi et al., 2015). This gene set supported that Tfh (TGF β) were also transcriptomically closer related to *bona fide* Tfh cells in the pre-Tfh stage than Tfh (anti-TGF β) cells, whose transcriptome was more Th1-like (**Figure 5G**).

In order to confirm the RNA-sequencing findings on the protein level, we performed a proteomics analysis comparing Tfh (anti-TGF β) with Tfh (TGF β) (**Figure 6A, 6B**). The Tfh (TGF β) population was enriched for proteins associated with Tfh cells such as Bcl6 and Tcf1 (encoded by *Tcf7*), and Th17 cells such as Rorgt (encoded by *Rorc*), Mt1, Mt2, IL-17F, and Ahr (**Figure 6C**). In the Tfh (anti-TGF β) population, Th1 marker such as T-bet and IL-2Ra were enriched (**Figure 6C**).

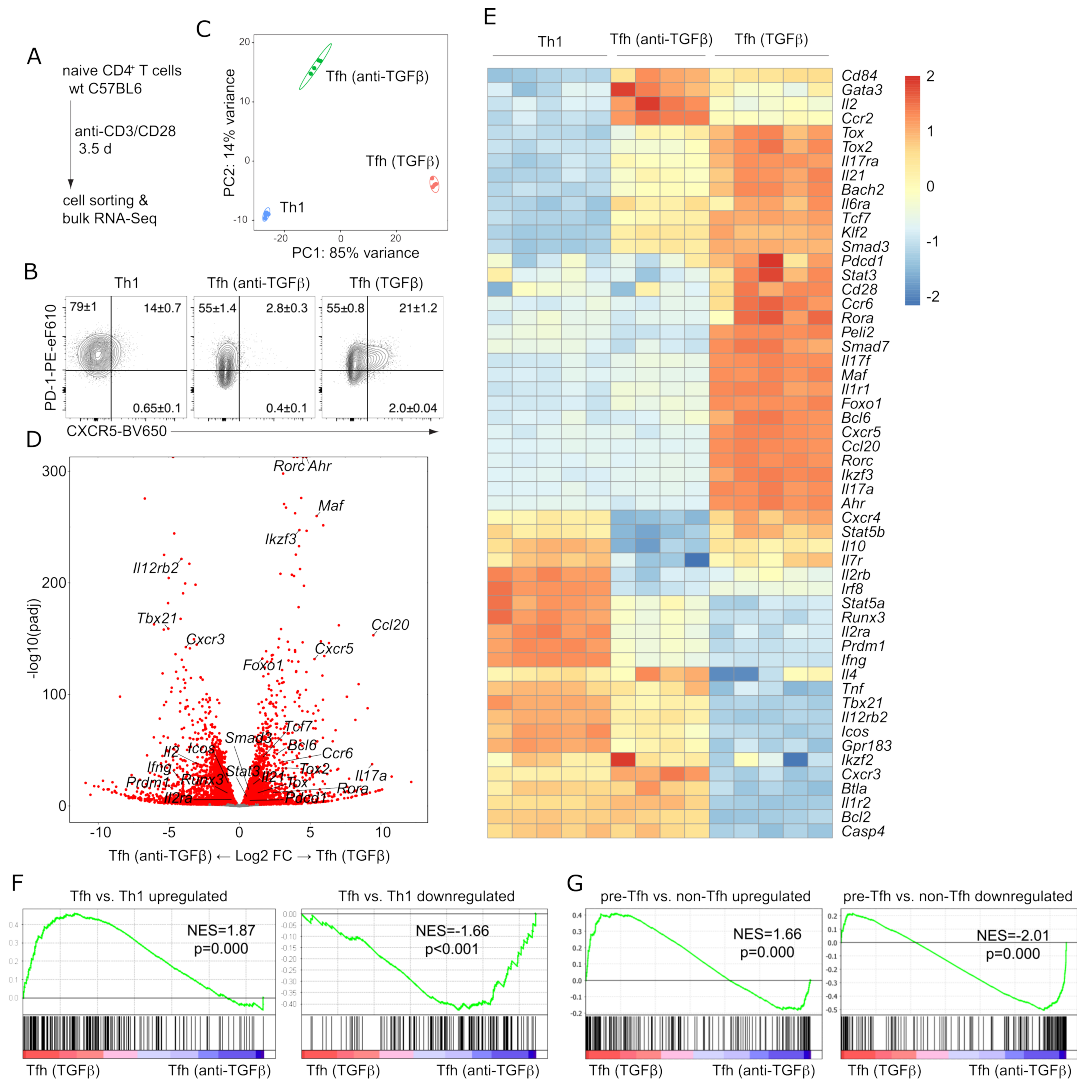


Figure 5: TGF β -induced CXCR5-expressing cells have transcriptomic features of Tfh cells

(A) Experimental outline: Naïve CD4⁺ T cells (5×10^4) were cultured *in vitro* in anti-CD3/CD28-coated 96-well flat-bottom plates for 3.5 days under Th1, Tfh (anti-TGF β), and Tfh (TGF β) differentiation conditions. Live CD4⁺ T Cells were then sorted for bulk RNA-seq.

(B) Shown are representative flow cytometry contour plots of sorted cells.

(C) PCA analysis of the bulk RNA-seq data. Each dot represents one sample.

(D) Volcano plot of differentially expressed genes between Tfh (anti-TGF β) and Tfh (TGF β) cell populations. Selected relevant genes are indicated. The red dots depict significantly up- or downregulated genes.

(E) Heatmap of selected genes and their expression in sorted Th1, Tfh (anti-TGF β), and Tfh (TGF β) cell populations.

(F) GSEA of previously published genes (GSE11924) that are up- and downregulated in mature Tfh versus Th1 cells in the *in vitro*-differentiated Tfh (anti-TGF β) versus Tfh (TGF β) cell populations.

(G) GSEA of previously published (GSE67334) early Th1 versus early Tfh signatures in the *in vitro*-differentiated Tfh (TGF β) versus Tfh (anti-TGF β) cells.

The Data are from one experiment with 4-5 mice per group. While the RNA-sequencing was performed by the LAFUGA platform in Munich, all analyses and visualizations depicted in panels A-G were performed by myself. Statistics are calculated using DESeq2 (D) and GSEA (F, G). * $p < 0.05$; ** $p < 0.01$; *** $p < 0.001$

In summary, we could show that *in vitro* TGF β -induced Tfh-like cells were transcriptomically and proteomically clearly distinct from Th1 and Tfh (anti-TGF β) cells and that they resembled *bona fide* Tfh cells, however, with additional characteristics of Th17 cells.

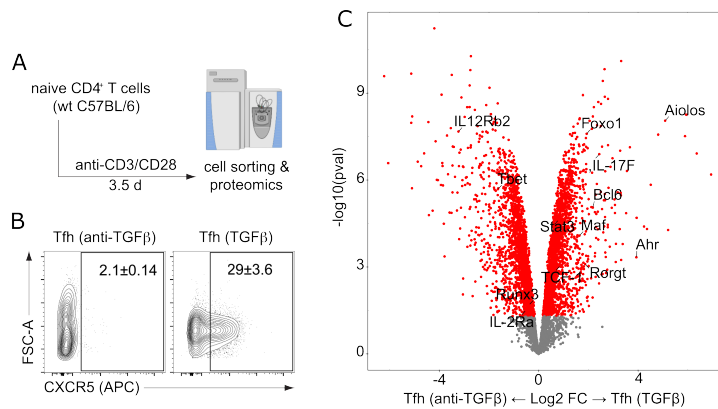


Figure 6: Proteomic analysis of CXCR5-expressing cells confirms features of Tfh cells

(A) Experimental outline: Naive C57BL/6 CD4⁺ T cells (5×10^4) were cultured *in vitro* in anti-CD3/CD28-coated plates for 3.5 days under Tfh (anti-TGF β) and Tfh (TGF β) differentiation conditions. Live CD4⁺ T Cells were then sorted for proteomics.

(B) Shown are representative flow cytometry contour plots of sorted cells.

(C) Volcano plot of differentially expressed proteins between Tfh (anti-TGF β) and Tfh (TGF β) cell populations. Selected relevant proteins are indicated. The red dots depict significantly up- or downregulated proteins.

The Data are from one experiment with 4-5 mice per group. The proteomics analysis was performed by the Meissner lab in Munich. Statistics were calculated using DEP.

4.4 TGF β -induced CXCR5⁺Bcl6⁺ Tfh cells are functional

Since the key function of Tfh cells is to provide help to B cells in the B cells zone, we tested their ability to migrate towards CXCL13, the main chemotactic attractant for B cells as well as Tfh cells, which is mediated by CXCR5. In a transwell migration assay, naive CD4⁺ T cells cultured in the Tfh (TGF β) condition efficiently migrated towards the CXCL13 gradient (**Figure 7A, 7B**). Cells that were differentiated in the Tfh (anti-TGF β) condition, and thus did not express CXCR5, showed no directional migration towards the CXCL13 gradient (**Figure 7B**).

In order to assess the ability of the *in vitro*-differentiated cells to provide help to B cells, we modified an established T-B cell co-culture protocol (Sage et al., 2016) (**Figure 8A**). We evaluated the *in vitro*

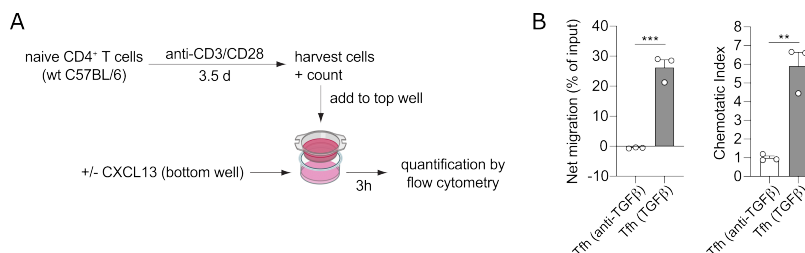


Figure 7: TGF β -induced CXCR5 expressing cells migrate toward a CXCL13 gradient in a transwell migration assay

(A) Experimental outline: *In vitro*-generated Tfh (anti-TGF β) and Tfh (TGF β) cells were placed into the upper compartment of a transwell chamber and migrated cells were quantified by flow cytometry 3h later.

(B) The net migration corresponds to the percentage of input cells that directionally migrated towards the CXCL13 gradient, excluding random migration. The chemotactic index corresponds to the ratio of the number of cells that migrated towards the CXCL13 gradient versus a control without the chemokine gradient.

The Data are representative of two independent experiments, with $n = 2-3$ mice per experiment. Unpaired t-test. ** $p < 0.01$; *** $p < 0.001$.

differentiated cells on their ability to support B cell activation, assessed by expression of the activation marker GL-7, and to induce class-switching to IgG1. Cells differentiated in the Th1 cell condition did not support B cell class-switching, and only inadequately activated B cells, indicated by a slight increase in GL-7 expression (**Figure 8B**). Similarly, the Tfh (anti-TGF β) cells, differentiated in the absence of TGF β , while being capable of activating B cells, they failed to induce class-switching (**Figure 8B**). T cells differentiated in both Tfh (TGF β) and Th17 conditions were able to potently activate B cells and induce their class-switching, resulting in a GL-7 and IgG1 double-positive B cells population (**Figure 8B**). *In vitro*-differentiated Th2 cells were able to support both B cell activation and class-switching. However, compared to the Tfh (TGF β) and Th17 conditions, the Th2 cells induced class-switching indistinguishably in both activated GL-7⁺ and in non-activated GL-7⁻ B cells (**Figure 8B**). As Th2 cells are known to produce high amounts of IL-4, this might be a direct effect of high amounts of IL-4 secreted by the Th2 cells, independently of cognate interactions between T and B cells (**Figure 8B**).

In order to assess the requirements for T-B specific interactions, we used a mouse model deficient for SAP (a SLAM-associated protein encoded by *Sh2d1a*). SAP-deficiency disrupts the function of surface molecules that support T-B cell interaction but does not affect cytokine production (Cannons et al., 2006). While SAP-deficient Th2 still potently induced B cell activation and class-switching, SAP-deficient TGF β -induced Tfh (TGF β) and Th17 cell populations were not able to induce B cell class-switching (**Figure 8B**). Further, without the support of T-B cell interaction, the Tfh (anti-TGF β), Tfh (TGF β) and Th17 cell populations were strongly diminished in their ability to support B cell activation compared to the Th2 cells, which showed only a reduction in GL-7 expression levels in the IgG1⁺ B cells (**Figure 8B**). This highlights the contact-dependent B cell helper function of TGF β -induced CD4⁺ T cells present in Th17 and Tfh cell cultures.

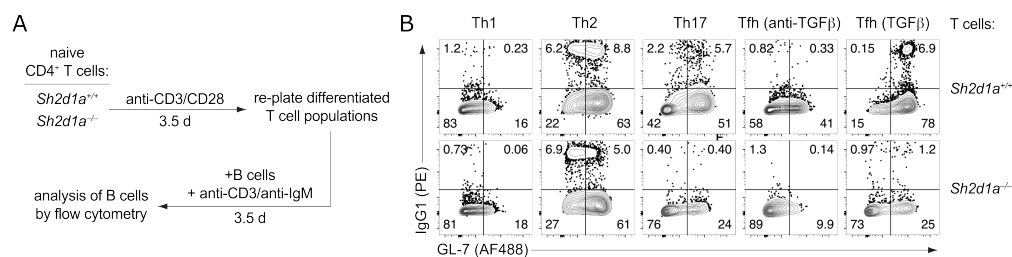


Figure 8: TGF β -induced Tfh-like cells provide critical help to B cells in an *in vitro* T-B cell co-culture assay

(A) Experimental outline: Naïve CD4⁺ T cells from *Sh2d1a*^{+/+} and *Sh2d1a*^{-/-} mice were differentiated *in vitro* into various T helper cell subsets for 3.5 days as described in Figure 1. Differentiated T cells were then co-cultured with purified total B cells with addition of anti-CD3 and anti-IgM. After 3.5 days, the cultured B cells were analyzed by flow cytometry.

(B) Representative flow cytometry plots showing the frequency of activated (GL7⁺) and class-switched (IgG1⁺) wildtype B cells after 3.5 days of co-culture with *in vitro*-differentiated wildtype (*Sh2d1a*^{+/+}) or SAP-deficient (*Sh2d1a*^{-/-}) T helper cell subsets. Gated on live CD4⁺CD19⁺MHC-II⁺ B cells.

The Data are representative of four independent experiments, with n = 2-3 mice per experiment.

4.5 TGF β signaling is required for CXCR5 and Bcl6 expression

To gain additional insights into the kinetics and requirements of *in vitro* Tfh cell differentiation, we observed the course of CXCR5 protein expression over time (**Figure 9A, 9B**). Upon stimulation, CXCR5 protein expression was evident after 12 hours in the cultures containing TGF β , reaching the peak of CXCR5 expression by day 1.5 after stimulation (**Figure 9A, 9B**). After the peak of expression, CXCR5 protein expression rapidly decreased in the Tfh (1 ng/ml TGF β) condition, while in the Tfh (5 ng/ml TGF β) condition, containing a higher concentration of the TGF β , the decrease was considerably slower (**Figure 9A, 9B**). We next looked into the requirement of TGF β for the induction of CXCR5 and Bcl6, by delaying the addition of TGF β into the culture (**Figure 9A, Figure 9C**). Adding TGF β 12 hours after the start of the culture halved the percentage of CXCR5-expressing cells and noticeably decreased Bcl6 protein expression (**Figure 9A, Figure 9C**).

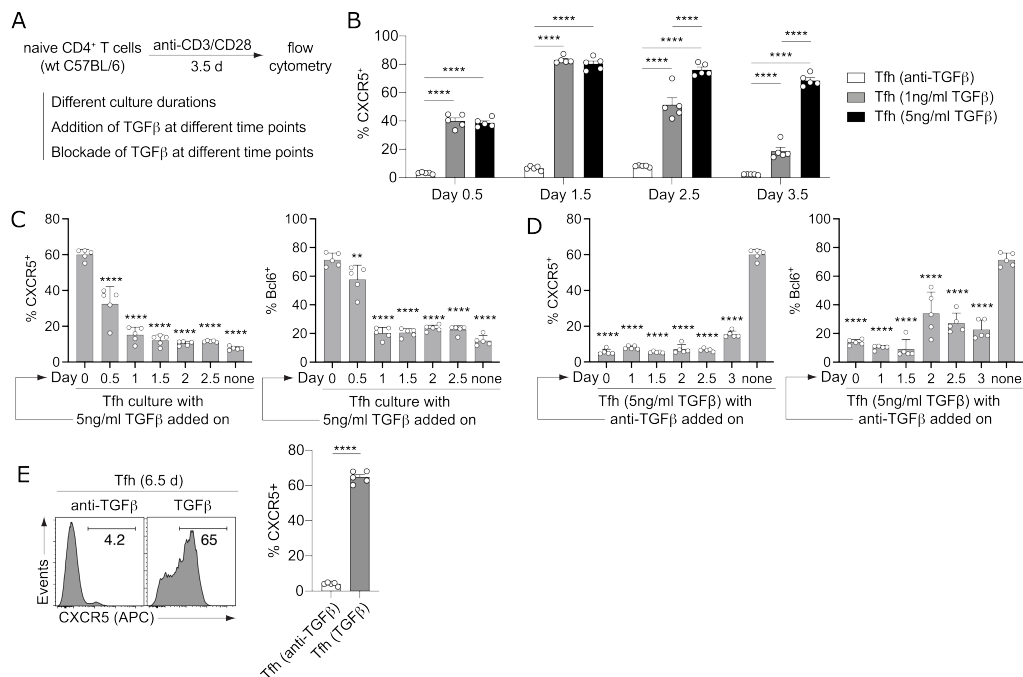


Figure 9: Continuous TGF β availability is required for the maintenance of CXCR5 expression

(A) Experimental outline: Naïve CD4⁺ T cells (4×10^4) were cultured *in vitro* in anti-CD3/CD28-coated plates for up to 3.5 days under different Tfh-polarizing differentiation conditions. Additionally, TGF β was added or blocked at the indicated time points. Live CD4⁺ T cells were then analyzed by flow cytometry.

(B) Quantification of the frequency of CXCR5⁺ cells among live CD4⁺ T cells on day 0.5, 1.5, 2.5 and 3.5 after the start of the *in vitro* culture.

(C) Quantification of the frequencies of CXCR5⁺ and Bcl6⁺ cells among live CD4⁺ T cells after 3.5 days of *in vitro* Tfh cell differentiation, in which TGF β was either added at the start of the culture ('Day 0') or on days 0.5, 1, 1.5, 2, or 2.5.

(D) Quantification of the frequencies of CXCR5⁺ and Bcl6⁺ cells among live CD4⁺ T cells after 3.5 days of culture under Tfh (TGF β) conditions, in which neutralizing anti-TGF β antibody was added at day 1, 1.5, 2, 2.5, or day 3 of culture or not at all ('none').

(E) Quantification of the frequency of CXCR5⁺ cells among live CD4⁺ T cells on day 6.5 after the start of the *in vitro* culture. The cells were splitted on day 3.5 by removing half of the cells/volume and replacing it with fresh medium and cytokines.

The Data in (B, C, D), and (E) are representative of four and two independent experiments, respectively, with the mean \pm SEM displayed for 5 mice per group. (B) Two-way ANOVA with Tukey's multiple comparison test (**** < 0.0001). (C, D) One-way ANOVA with Dunnett's multiple comparison test against 'Day 0' or 'none'. (E) Unpaired t-test ** $p < 0.01$; *** $p < 0.001$.

Delaying the addition of TGF β by 24 hours or more after stimulation resulted in a decrease of CXCR5 and Bcl6 protein expression to the level of Tfh (anti-TGF β), included here as a negative control for CXCR5 and Bcl6 expression (**Figure 9A, Figure 9C**). In order to assess the requirement of TGF β for the maintenance of CXCR5 protein expression, we removed TGF β at different time points from the culture using a TGF β -neutralizing antibody (**Figure 9A, Figure 9D**). Removing TGF β for 12 hours already completely abolished CXCR5 protein expression (**Figure 9A, Figure 9D**). Bcl6 protein expression showed a significant decrease 12 hours after TGF β -neutralization, but reaching the baseline compared to Tfh (anti-TGF β) only after 2 days without TGF β (**Figure 9A, Figure 9D**). In contrast, CXCR5 protein expression could be maintained in long-term cultures containing TGF β for at least 6.5 days (**Figure 9E**). These experiments showed that TGF β was essential for both the induction and the maintenance of CXCR5 protein expression *in vitro*.

4.6 *In vivo* relevance of TGF β signaling for Tfh cell differentiation

To test the relevance of the TGF β pathway for Tfh cell differentiation in an *in vivo* setting, we adopted a mouse model with a CD4-specific tamoxifen-induced knockout of *Tgfr2*, which encodes a major TGF β receptor. We treated naïve CD4⁺ cells from *Cd4-CreERT2⁺ Tgfr2^{fl/fl}* and *Cd4-CreERT2⁺ Tgfr2^{+/+}* mice overnight with 4HO-Tamoxifen to generate the knockout *iTgfr2 Δ/Δ* and the respective control *iTgfr2^{+/+}* cells (**Figure 10A**). The generated knockout cells were then subjected to the Th17, Tfh (anti-TGF β), and Tfh (TGF β) cell cultures (**Figure 10A**). Control T cells (*iTgfr2^{+/+}*) cultured in Th17 and Tfh (TGF β) conditions expressed CXCR5 and Bcl6, while in the same condition CXCR5 and Bcl6 expression was reduced to the level of the negative control (Tfh (anti-TGF β)) for the induced *Tgfr2* knockouts (*iTgfr2 Δ/Δ*) (**Figure 10B, 10C**).

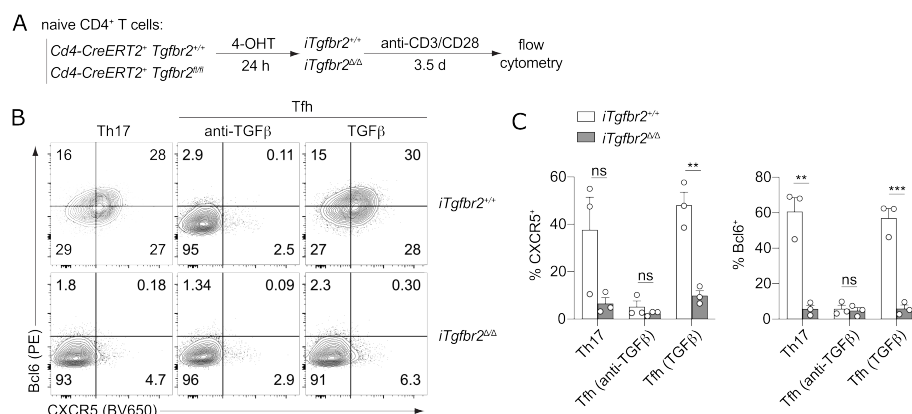


Figure 10: CD4⁺ T cells from *Tgfr2* knockout mice resemble the Tfh (anti-TGF β) condition *in vitro*
(A) Experimental outline: Naïve *Cd4-CreERT2⁺ Tgfr2^{+/+}* (*iTgfr2^{+/+}*) and *Cd4-CreERT2⁺ Tgfr2^{fl/fl}* (*iTgfr2 Δ/Δ*) CD4⁺ T cells were treated with 4-hydroxytamoxifen for 24 h and differentiated under T helper cell-polarizing conditions for 3.5 days *in vitro*.
(B) Representative contour plots of flow cytometry showing the expression of CXCR5 and Bcl6 by live CD4⁺ T cells.
(C) Quantification of the frequencies of CXCR5⁺ and Bcl6⁺ cells among live CD4⁺ T cells.

The data are representative of three independent experiments with the mean \pm SEM displayed for 3 mice per group. Unpaired t-test ** $p < 0.01$; *** $p < 0.001$.

After confirming the critical role of T cell-intrinsic TGF β signaling for *in vitro* differentiation of murine Tfh cells, we test and validate these *in vitro* findings *in vivo*. We choose the adoptive co-transfer of both induced *Tgfr2* knockout and control cells followed by intraperitoneal immunization with NP-ovalbumin (NP-OVA) and alum as adjuvant. To this end, we crossed an OVA-specific TCR-transgenic OT-II allele and congenic CD45 alleles into *Cd4-CreERT2⁺ Tgfr2^{+/+}* (*iTgfr2^{+/+}*) and *Cd4-CreERT2⁺ Tgfr2^{fl/fl}* (*iTgfr2 $\Delta\Delta$*) mice. We verified that *Tgfr2* protein expression was efficiently ablated in tamoxifen-treated *Cd4-CreERT2⁺ Tgfr2^{fl/fl}* (*iTgfr2 $\Delta\Delta$*) mice compared to *Cd4-CreERT2⁺ Tgfr2^{+/+}* (*iTgfr2^{+/+}*) (**Figure 11A, 11B**). The transferred *iTgfr2 $\Delta\Delta$* cells showed a significant reduction in CXCR5^{hi}Bcl6^{hi} Tfh cells compared to co-transferred control *iTgfr2^{+/+}* cells (**Figure 11C, 11D, 11E**). This showed that the *in vitro*-observed TGF β -mediated induction of Tfh cells is also relevant *in vivo*.

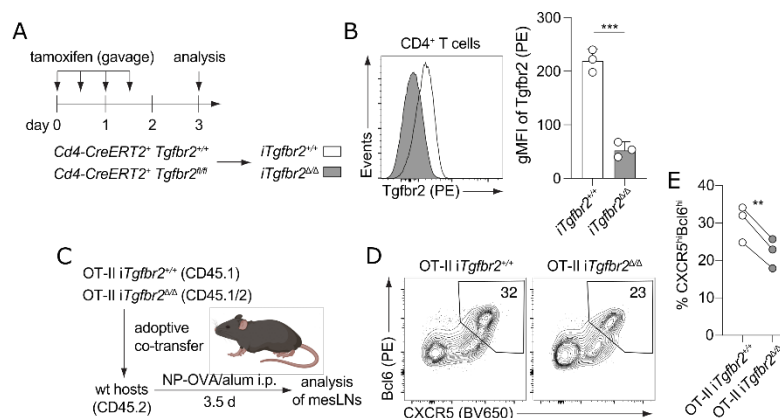


Figure 11: TGF β signaling is required for optimal Tfh cell differentiation *in vivo*

(A) Experimental outline: *Cd4-CreERT2⁺ Tgfr2^{+/+}* (*iTgfr2^{+/+}*) and *Cd4-CreERT2⁺ Tgfr2^{fl/fl}* (*iTgfr2 $\Delta\Delta$*) mice were treated with tamoxifen for four times on two consecutive days and analyzed three days after the first dose of tamoxifen administration.

(B) Representative flow cytometry histogram plots showing *Tgfr2* protein expression in *ex vivo* live CD4⁺ T cells. Quantification of the gMFI is displayed in the bar graph.

(C) Experimental outline: OT-II *iTgfr2^{+/+}* CD45.1 and OT-II *iTgfr2 $\Delta\Delta$* CD45.1/2 cells were generated as in (A) and co-transferred into wild type hosts. On the following day, the hosts were immunized by intraperitoneal injection of NP-OVA in alum. 3.5 days after immunization, the transferred T cells from the mesenteric lymph node were analyzed by flow cytometry.

(D) Representative flow cytometry plots showing transferred control and *iTgfr2 $\Delta\Delta$* CD4⁺ T cells stained for Bcl6 and CXCR5 and gated on CXCR5^{hi}Bcl6^{hi} Tfh cells.

(E) Quantification of the Tfh cells is displayed in the bar graph.

Data in (B, D, E) are representative of three independent experiments, respectively, with the mean \pm SEM displayed for 3 mice per group. (B) Unpaired t-test with *** $p < 0.001$. (D) Paired t-test with ** $p < 0.01$.

4.7 Differential IL-6 and Stat3 signaling requirements for the induction of CXCR5 and Bcl6

Besides TGF β , IL-6 was required for the efficient induction of CXCR5 and Bcl6 protein expression in the Th17 and Tfh (TGF β) conditions (**Figure 1B, 2A, 2B**). In order to further assess the role of IL-6 for Tfh cell differentiation, we looked into IL-6 receptor knockout mice. The functional IL-6 receptor in mice is encoded by GP130 and IL6ra (Johnson et al., 2018). We cultured naïve CD4⁺ T cells from both Il6ra and gp130-deficient mice, as well as the respective controls, in the Th17, Tfh (anti-TGF β), and Tfh (TGF β) differentiation conditions (**Figure 12A**). In the control cells, CXCR5 and Bcl6 protein expression were upregulated in the Tfh (TGF β) and Th17 conditions containing TGF β , but not in the Tfh (anti-TGF β) condition (**Figure 12B, 12C**). While in the Tfh (TGF β) condition CXCR5 and Bcl6 protein expression was nearly unchanged in IL6a or GP130-deficient cells, we observed a strong reduction of CXCR5 expression in the Th17 condition (**Figure 12B, 12C**). As the sole difference between the two conditions was the addition of IL-21 in the Tfh (TGF β) condition (**Figure 1B**), these results indicated that IL-21 was sufficient to induce CXCR5 expression in the absence of IL-6. This finding is in line with previous reports that IL-6 and IL-21 have redundant functions in Th17 cell differentiation *in vivo* (Korn et al., 2007; R. Nurieva et al., 2007). Expression of IL-17A and IL-21 in the Th17 condition was dependent on IL-6 signaling through IL6ra and GP130 (**Figure 12E, 12F**). While IL-17A expression was absent in the Tfh (anti-TGF β) cultures of control (Il6ra^{fl/fl}, gp130^{fl/fl}), Il6ra ^{$\Delta\Delta$} , and gp130 ^{$\Delta\Delta$} cells, IL-21 was strongly produced by these cells (**Figure 12E, 12F**). With the addition of TGF β in the Tfh (TGF β) condition, we observed, in line with previous reports (R. I. Nurieva et al., 2008; Suto et al., 2008), a decrease in production of IL-21, albeit the production of IL-21 was not entirely abrogated (**Figure 12E, 12F**). Disruption of the IL-6 signaling in the Il6ra and Gp130 knockout cells further impaired the IL-21 production (**Figure 12E, 12F**). As both IL-6 and IL-21 signal downstream through the transcription factor Stat3 (Johnson et al., 2018), we looked into the phenotype of the Stat3 knockout. CXCR5 protein expression as well as IL-17A and IL-21 cytokine production were abrogated in Th17 as well as Tfh (TGF β)-differentiating conditions (**Figure 12D, 12G**). Interestingly, however, Bcl6 expression was not completely diminished (**Figure 12D**). In summary, we confirmed that TGF β induced CXCR5 protein expression with redundant functions for IL-6 and IL-21, but dependent on Stat3 downstream signaling. Bcl6 protein expression required TGF β , but was not dependent on IL-6 or IL-21 Signaling via Stat3.

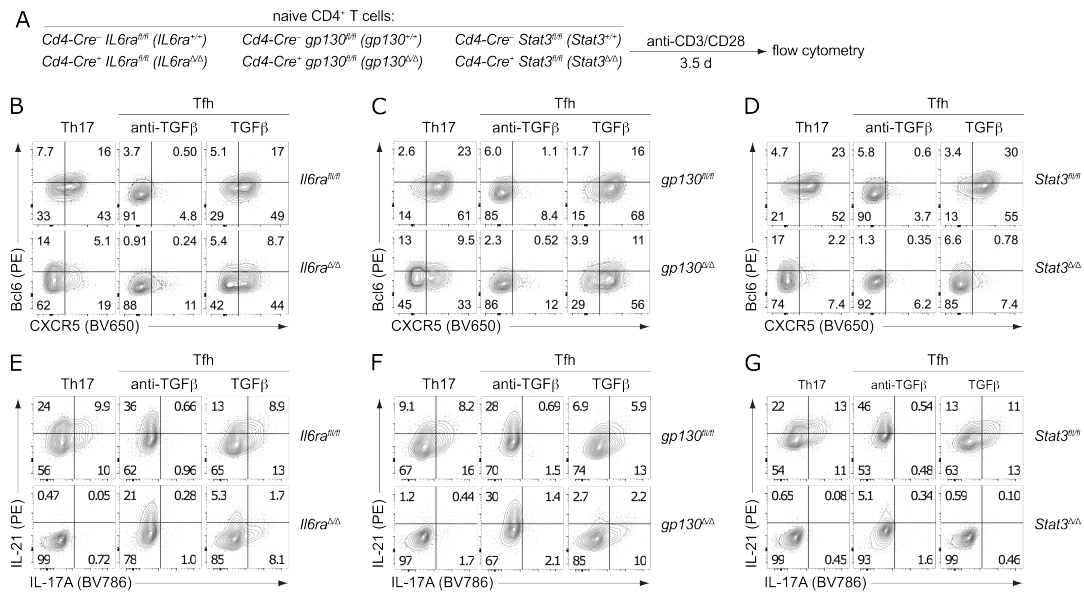


Figure 12: Induction of CXCR5 and Bcl6 protein expression requires Stat3 signaling

(A) Experimental outline: Naïve CD4⁺ T cells of the indicated genotypes were cultured *in vitro* in anti-CD3/CD28-coated plates for 3.5 days under various T helper cell differentiation conditions. Cells were then analyzed by flow cytometry.

(B-D) Representative flow cytometry contour plots showing CXCR5 and Bcl6 expression of live CD4⁺ T cells of the indicated genotypes.

(E-G) Representative flow cytometry contour plots showing IL-17A and IL-21-producing cells of the indicated genotypes cultured for 3.5 days and restimulated with PMA/ionomycin in the presence of monensin.

Data in (B, D, E, G) and (C, F) are representative of three and two independent experiments, respectively, with *n* = 2-5 mice per experiment.

4.8 Cell density-mediated IL-2 production inhibits Tfh cell differentiation *in vitro*

During the process of optimization of the *in vitro* Tfh cell differentiation protocol, one successful optimization step that yielded a significant increase in CXCR5 and Bcl6 protein expression was the reduction of cell density in the cell culture. This could be achieved by either splitting the cells on day 2 two of culture (data not shown) or by reducing the numbers of cells seeded on day 0 (**Figure 13A**). With decreasing seeding cell densities, we observed a strong upregulation of CXCR5 and Bcl6 protein expression in Tfh (TGFβ) cultures (**Figure 13A**). On the other hand, regardless of the seeding cell densities, no CXCR5 protein expression could be detected in the Tfh (anti-TGFβ) conditions (**Figure 13A**). However, Bcl6 protein expression, while being lower compared to the Tfh (TGFβ) condition, increased slightly with lower seeding cell densities (**Figure 13A**).

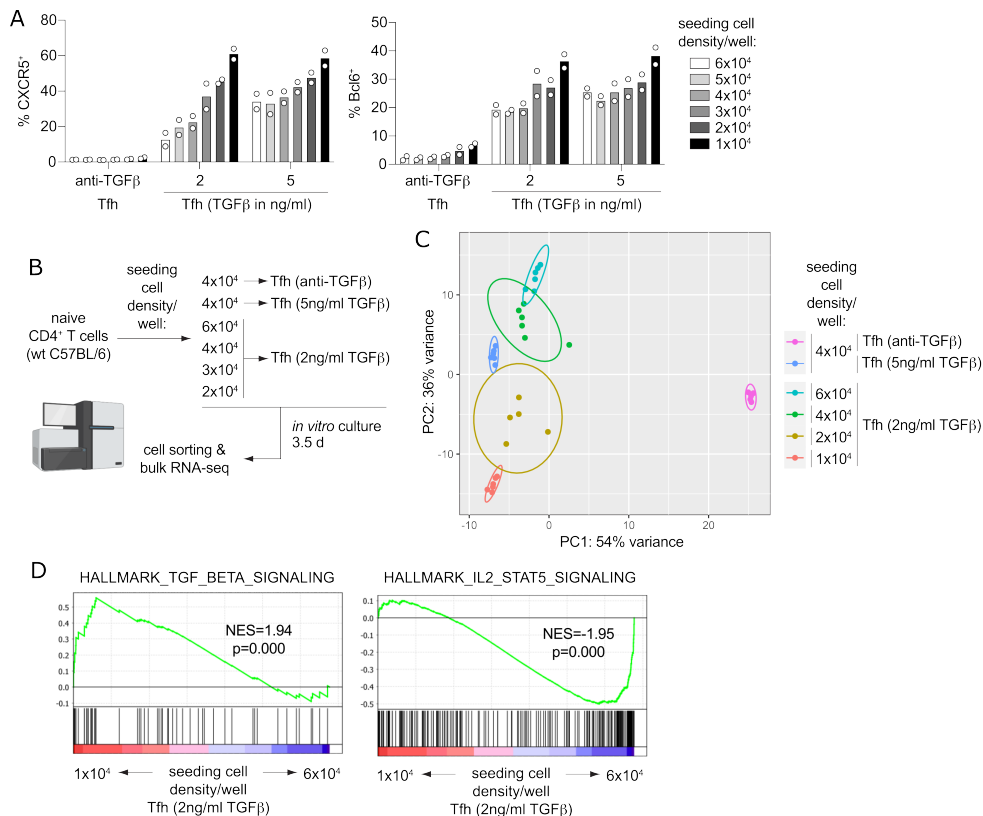


Figure 13: Increased cell density causes reduction in CXCR5 and Bcl6 protein expression *in vitro*

(A) Quantification of the frequencies of CXCR5⁺ and Bcl6⁺ cells by live CD4⁺ T cells on day 3.5 after *in vitro* differentiation of wildtype C57BL/6 CD4⁺ T cells at different cell seeding densities.

(B) Experimental outline: Naive CD4⁺ T cells were differentiated under Tfh (2ng/ml TGFβ) conditions with varying cell seeding densities per well of a 96-well flat-bottom plate: 6x10⁴, 4x10⁴, 2x10⁴, and 1x10⁴ cells. Tfh (anti-TGFβ) and Tfh (TGFβ) conditions with 4x10⁴ cells each served as controls. After 3.5 days in culture, live CD4⁺ T cells were sorted and subjected to bulk RNA-seq.

(C) PCA of the bulk RNA-seq data. Each dot represents one sample.

(D) GSEA of the MSigDB Hallmark genes that are upregulated in response to TGFβ and IL-2 signaling in *in vitro* differentiated Tfh (2ng/ml TGFβ) cells in the context of low (1x10⁴) versus high (6x10⁴) cell seeding densities.

Data in (A) are representative of three independent experiments, with the mean of 2 mice per group shown. Data in (C, D) are from one experiment with 5-6 mice per group. RNA-seq was performed by the NGS core facility of the Medical Faculty at the University of Bonn, the resulting data was analyzed and visualized by me. Statistics are calculated using GSEA (D). *p < 0.05; **p < 0.01; ***p < 0.001

For most of our experiments, we used an optimized starting cell seeding density of 4x10⁴ cells per well of a 96-well flat-bottom plate. The reduction of cell density also eliminated the need to change medium within the 3.5-day cell culture period (data not shown). In order to gain insights into the molecular pathways affected by seeding cell densities, we cultured Tfh (2ng/ml TGFβ) with varied seeding cell densities (6x10⁴, 4x10⁴, 2x10⁴, 1x10⁴). Tfh (anti-TGFβ) and Tfh (5ng/ml TGFβ) conditions at our standard 4x10⁴ seeding cell density served as controls (**Figure 13B**). Differentiated cells were purified and subjected to bulk RNA-seq. The presence or absence of TGFβ contributed to the largest variance, while the difference in seeding cell density contributed to an additional 36% of the total variance (**Figure 13C**). Looking deeper into the biological processes by GSEA, we observed that with increasing cell density, TGFβ signaling was declining, while IL-2/Stat5 signaling increased (Liberzon et al., 2015) (**Figure 13D**), thus providing a link between seeding cell density, Tfh cell-antagonizing IL-2/Stat5 signaling, and the differentiation of Tfh cells *in vitro*.

IL-2 strongly inhibits Tfh cells *in vivo* (Ballesteros-Tato et al., 2012; Ditoro et al., 2018; Johnston et al., 2012). We are able to reproduce this result *in vitro*, as exogenous IL-2 diminished CXCR5 and Bcl6 in Tfh (TGF β) cultures (**Figure 14A**). In contrast, neutralization of IL-2 using a blocking antibody resulted in increased CXCR5⁺ cell frequencies in Tfh (TGF β) cultures (**Figure 14B**). Using a small molecule inhibitor of STAT5, the downstream signaling factor in the IL-2 signaling pathway, resulted in increased CXCR5 expression levels in the Tfh (TGF β) condition (**Figure 14C**). Looking into the producers of IL-2 in the cell cultures, we found that in both Tfh (anti-TGF β) and Tfh (TGF β) conditions a population capable of producing IL-2 was detectable already on day 0.5 after stimulation (**Figure 14D**). The frequency of the IL-2-producing population in the Tfh (anti-TGF β) condition was greater

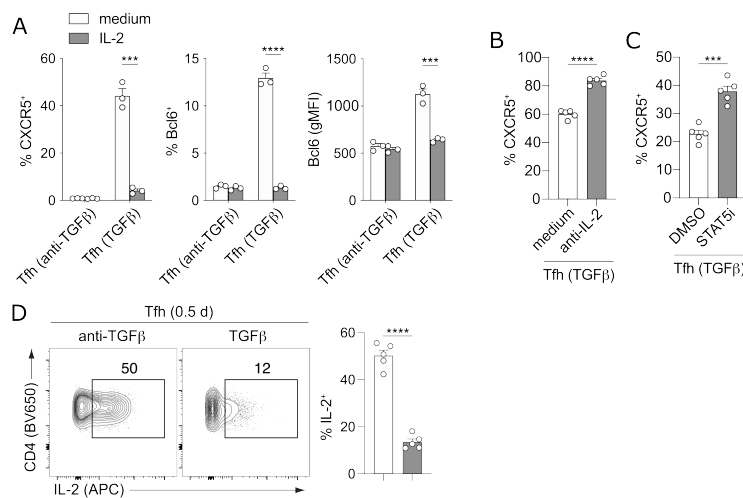


Figure 14: IL-2 reduces CXCR5 and Bcl6 expression in the *in vitro* Tfh culture

(A) Quantification of the frequencies of CXCR5⁺ and Bcl6⁺ positive cells as well as of Bcl6 gMFI among live CD4⁺ T cells after *in vitro* differentiation, either without ('medium') or with the addition of 300U/ml IL-2.

(B) Quantification of the frequency of CXCR5⁺ cells by live CD4⁺ T cells on day 3.5 after *in vitro* differentiation, either without ('medium') or with the addition of a neutralizing anti-IL-2 antibody.

(C) Quantification of the frequency of CXCR5⁺ cells by live CD4⁺ T cells on day 3.5 after *in vitro* differentiation, with the addition of a STAT5 inhibitor ('STAT5i') or DMSO control.

(D) Representative flow cytometry contour plots showing live IL-2-producing CD4⁺ T cells cultured for 0.5 days under Tfh (anti-TGF β) and Tfh (TGF β) conditions and restimulated with PMA/ionomycin in the presence of monensin. Quantification of the frequencies of IL-2⁺ cells among live CD4⁺ cells is displayed on the right. The Data in (A-D) are representative of three independent experiments each, with the mean \pm SEM of 3 (A), and 5 mice (B, C, D) per group shown. (A-D) Unpaired t-test with **p < 0.01; ***p < 0.001; ****p < 0.0001.

than the one in CD4⁺ T cells from the Tfh (TGF β) condition (**Figure 14D**). Taken together, these results highlighted the inhibitory function of IL-2 on Tfh cells.

With increased cell density resulting in less TGF β -signaling and more IL-2 signaling, we next wanted to dissect the causality of these two effects. As *iTgfb2* $\Delta\Delta$ cells mimic the Tfh (anti-TGF β) condition, intrinsically producing more IL-2, we cultured naïve *iTgfb2*^{+/+} and *iTgfb2* $\Delta\Delta$ CD4⁺ T cells either separately or together as co-cultures in Tfh (anti-TGF β) or Tfh (TGF β) conditions (**Figure 15A**). No CXCR5 protein expression was detected in the Tfh (anti-TGF β) single- or co-culture conditions (**Figure 15B**). In separate cultures of the Tfh (TGF β) condition, CXCR5 protein expression was observed in the culture with *iTgfb2*^{+/+} cells, but not in the culture with *iTgfb2* $\Delta\Delta$ cells (**Figure 15B**). However, culturing *iTgfb2*^{+/+} and *iTgfb2* $\Delta\Delta$ cells together, resulted in reduced CXCR5 protein expression of *iTgfb2*^{+/+} cells similar to those levels detected in *iTgfb2* $\Delta\Delta$ cells in

the same culture (**Figure 15B**). CXCR5 protein expression of the co-cultured cells matched the expression of separately cultured *iTgfb2^{ΔΔ}* cells (**Figure 15B**). In the co-culture, the effect on Bcl6 protein expression was similar to that observed for CXCR5 (**Figure 15B**). This indicated that *iTgfb2^{ΔΔ}* had a dominant negative effect over *iTgfb2^{+/+}* cells in the co-culture. CD25 was upregulated in *iTgfb2^{ΔΔ}* cells cultured under Tfh (TGFβ) conditions, whereas *iTgfb2^{+/+}* gained high levels of CD25 expression when co-cultured with *iTgfb2^{ΔΔ}* cells (**Figure 15B**). These data indicated that an increase in cell density or reduction of TGFβ within the media resulted in increased production of IL-2, which had a dominant negative effect on the Tfh differentiation *in vitro*.

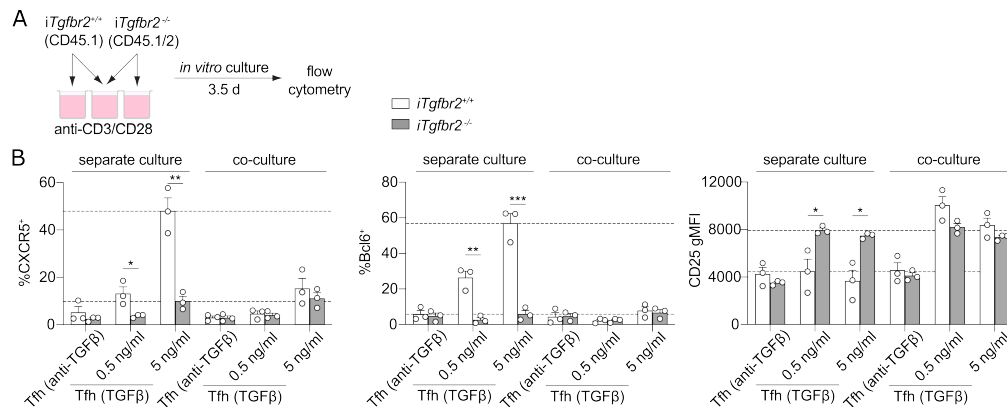


Figure 15: In a co-culture setting, *iTgfb2^{+/+}* cells assume the phenotype of *iTgfb2^{ΔΔ}* cells
(A) Experimental outline: 4×10^4 4-hydroxytamoxifen-treated naïve *Cd4-CreERT2⁺ Tgfb2^{+/+}* (*iTgfb2^{+/+}*) and *Cd4-CreERT2⁺ Tgfb2^{fl/fl}* (*iTgfb2^{ΔΔ}*) $CD4^+$ T cells were cultured in Tfh (anti-TGFβ) and Tfh (TGFβ) differentiation conditions for 3.5 days. The cells were cultured either separately or as a co-culture with a 1:3 ratio.
(B) Quantification of the frequencies of CXCR5⁺ and Bcl6⁺ cells as well as of Bcl6 and CD25 gMFI of live $CD4^+$ T cells on day 3.5 of culture, as determined by flow cytometry. Dashed lines indicate mean expression levels of separately cultured *iTgfb2^{+/+}* and *iTgfb2^{ΔΔ}* Tfh (TGFβ) cells.
 The Data are representative of three independent experiments, with the mean \pm SEM of 3 mice per group shown. Unpaired t-test with ** $p < 0.01$; *** $p < 0.001$; **** $p < 0.0001$.

4.9 TGFβ-induced CXCR5-expressing cells are distinct from Th17 cells

As both Th17 and Tfh (TGFβ) cells were capable to induce and maintain CXCR5 and Bcl6 expression efficiently, we looked into the Th17 identity of these cells. Both populations showed high expression of the Th17 master transcription factor RORgt and the Th17-defining cytokine IL-17A (**Figure 1B, 1C, 16A**). The co-existence of both Tfh phenotype (Bcl6⁺CXCR5⁺) and Th17 phenotype (RORgt⁺IL-17⁺) suggested that Th17 and Tfh cell fate was either overlapping or competing. In order to assess this, we used an IL-17A mRNA reporter mouse, *Il17a^{Smart}*, in order to differentiate between IL-17A⁺ Th17 and CXCR5⁺ Tfh cell fates without the need of fixation or restimulation (Price et al., 2012). As both the concentration of TGFβ and the cell density of the culture were affecting both IL-17A and CXCR5 expression in a reversed manner, we titrated both parameters with the aim to generate similar percentages of both CXCR5⁺IL-17A⁻ Tfh and IL-17A⁺CXCR5⁻ Th17 cells (**Figure 16B, 16C**).

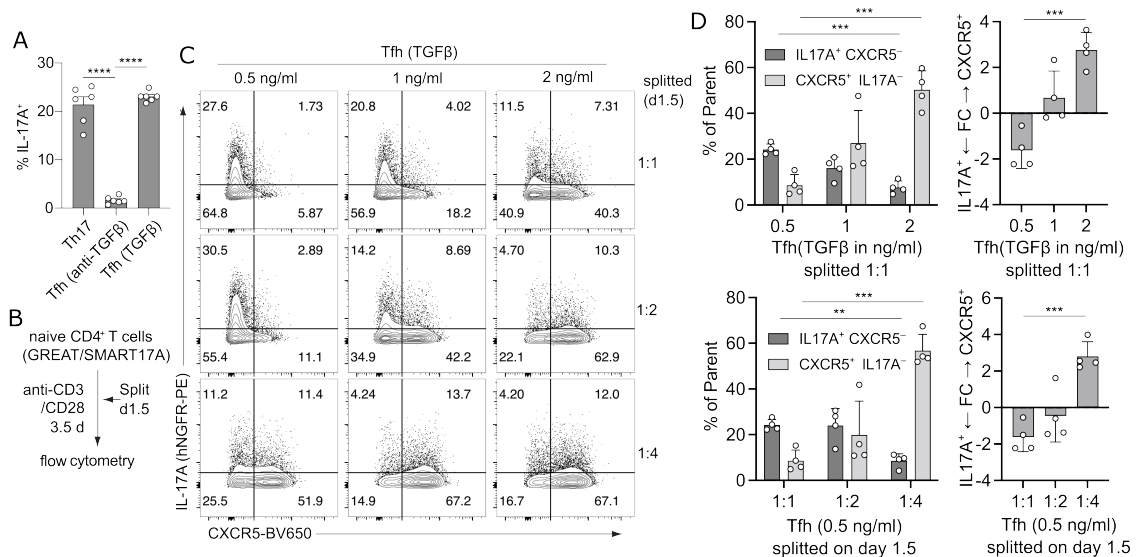


Figure 16: *In vitro* Tfh cell culture gives rise to distinct CXCR5⁺ and IL-17A⁺ cell populations

(A) Quantification of IL-17A-producing CD4⁺ T cells that were cultured for 3.5 days under the indicated polarizing T helper cell differentiation conditions and were then restimulated with PMA/ionomycin in the presence of monensin.

(B) Experimental outline: Naïve CD4⁺ T cells (5x10⁴) from GREAT/SMART-17A reporter mice were cultured *in vitro* in anti-CD3/CD28-coated plates for 3.5 days under Tfh differentiation conditions with the indicated amount of TGFβ for 3.5 days. The cells were splitted on day 1.5.

(C) Representative contour plots of flow cytometry showing CXCR5 and IL-17A expression of live CD4⁺ T cells.

(D) Quantification of the frequencies of CXCR5⁺ and IL-17A⁺ cells among live CD4⁺ T cells. The log₂ fold change between CXCR5⁺ and IL-17A⁺ cells is displayed on the right.

Data in (A) are representative of more than five independent experiments and display mean ± SEM with n = 6 biological replicates. Data in (B, C) are representative of four independent experiments, with mean ± SEM with 4 mice per group. (A, D) One-way ANOVA with Tukey's multiple comparison test (**p < 0.01; ***p < 0.001; ****p < 0.0001).

We cultured naïve CD4⁺ T cells from the reporter mice in the Tfh (1 ng/ml) condition, sorted CXCR5⁺IL-17A⁻ Tfh and IL-17A⁺CXCR5⁻ Th17 cells 3.5 days later and subjected them to bulk RNA-sequencing. (**Figure 17A, 17B**). The CXCR5⁺IL-17A⁻ population expressed more Tfh cell markers, such as *Bcl6*, *Cxcr5*, *Tcf7*, *Tox*, and *Tox2*, whereas the CXCR5⁻IL-17A⁺ population expressed Th17 markers, such as *Scd1*, *Mt1*, *Mt2*, *Il17a*, *Il17f*, *Ccl20*, and *Il23r* (**Figure 17C, 17D**). Comparing with published gene signatures of *ex vivo* Tfh and Th17 cells with GSEA analysis further confirmed the Tfh and Th17 identity of the CXCR5⁺IL-17A⁻ and IL-17A⁺CXCR5⁻ populations, respectively (R. I. Nurieva et al., 2008) (**Figure 17E**).

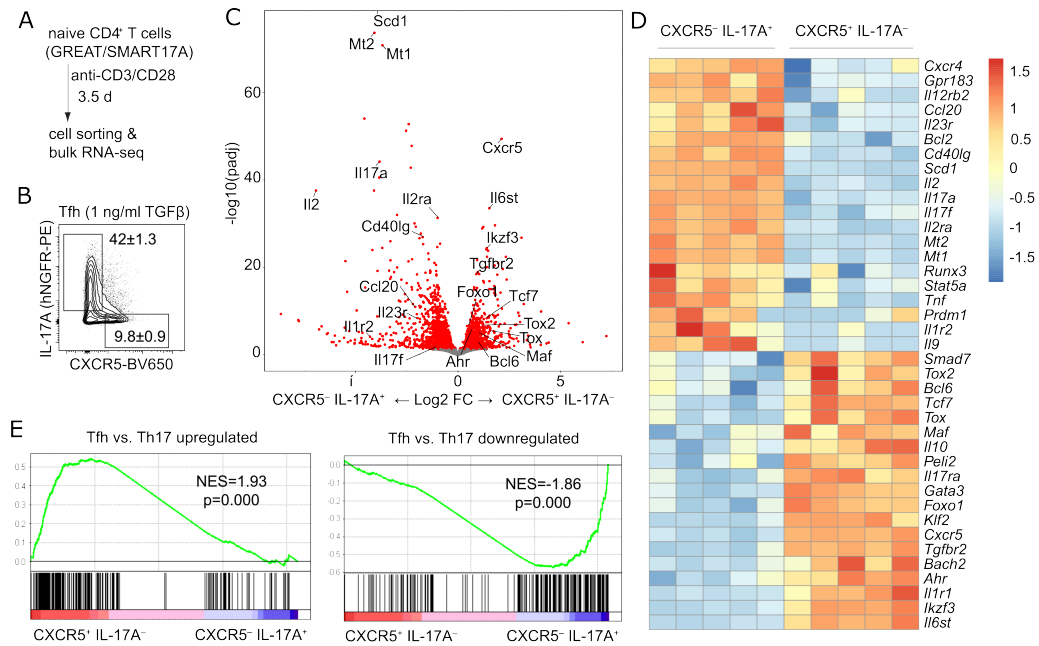


Figure 17: *In vitro*-generated CXCR5⁺ and IL-17A⁺ cells are transcriptomically distinct and resemble Tfh and Th17 cells

(A) Experimental outline: Naïve CD4⁺ T cells (2×10^4) from GREAT/SMART-17A reporter mice were cultured *in vitro* in anti-CD3/CD28-coated plates for 3.5 days under Tfh (1 ng/ml TGF β) differentiation conditions to better induce IL-17⁺ and CXCR5⁺ cells. CXCR5⁺IL-17A⁺ Th17 and CXCR5⁺IL-17A⁻ Tfh cells were then sorted for bulk RNA-seq.

(B) Shown is a representative flow cytometry contour plot with indicated gates used for sorting.

(C) Volcano plot of differentially expressed genes between Th17 and Tfh cells. Selected relevant genes are indicated. The red dots depict significantly up- or downregulated genes.

(D) Heatmap of selected genes and their expression in the sorted Th17 and Tfh cells.

(E) GSEA of previously published genes (GSE11924) that are up- or downregulated in mature Tfh versus Th17 cells in the *in vitro* differentiated Th17 and Tfh cells.

The Data are from one experiment with 5 mice per group. While the RNA-sequencing was performed by the LAFUGA platform in Munich, all analyses and visualizations depicted in panels A-D were performed by myself. Statistics are calculated using DESeq2 (C) and GSEA (E). * $p < 0.05$; ** $p < 0.01$; *** $p < 0.001$

In order to further assess the heterogeneity and composition of the two cell populations within the Tfh (TGF β) condition, we performed a single-cell RNA-sequencing experiment on day3.5-sorted viable Tfh (2 ng/ml TGF β) cells (**Figure 18A**). In the UMAP, Tfh and Th17 cells segregated into distinct populations using the CXCR5⁺IL-17A⁻ Tfh and IL-17A⁺CXCR5⁻ Th17 cell signatures from the bulk RNA-sequencing (**Figure 17A, 18B**). This mapping also overlapped with the previous published Th17 and Tfh cell signatures (R. I. Nurieva et al., 2008) (**Figure 18C**). In conclusion, these data showed that in the Tfh (TGF β) and Th17-differentiating cell culture conditions distinct populations of CXCR5⁺ Tfh and IL-17A⁺ Th17 cells were generated, thus revealing the high heterogeneity within the cell culture.

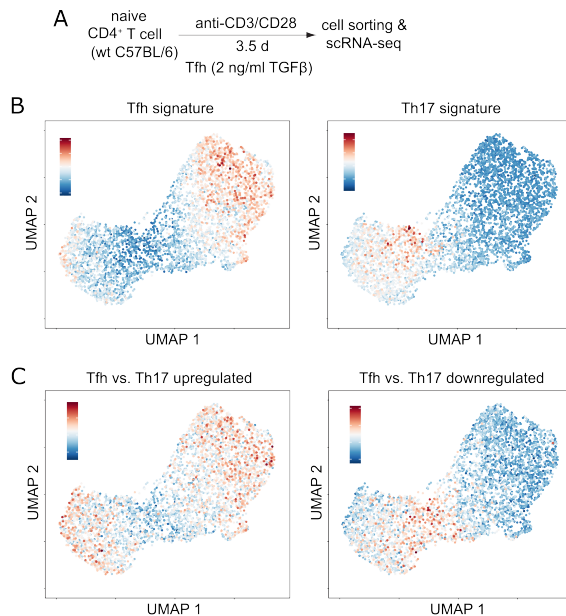


Figure 18: scRNA-sequencing confirms two distinct cell populations within Tfh (TGF β) *in vitro* cell cultures

(A) Naive CD4⁺ T cells (1×10^4) from wildtype C57BL/6 mice were cultured *in vitro* in anti-CD3/CD28-coated plates for 3.5 days under Tfh (2ng/ml TGF β) differentiation conditions. Live CD4⁺ T cells were then sorted for single-cell RNA-seq.

(B) The Th17 and Tfh signatures from the bulk RNA-seq experiment in **Figure 17** were superimposed on the scRNA-seq data. Each dot represents one cell.

(C) Published Th17 and Tfh signatures (GSE11924) were superimposed on the scRNA-seq data. Each dot represents one cell.

The Data are from one experiment with 3 mice per group. The single cell whole transcriptome analysis was performed together with the PRECISE platform of DZNE.

4.10 Identification of Tfh cell fate deciders with an arrayed CRISPR/Cas9 screen

CRISPR/Cas9 is a powerful and versatile tool for genome editing. To be able to dissect the early molecular events during Tfh cell differentiation, a system is required that can interrogate gene expression of potential target genes already in naive T cells. To this end, we implemented a CRISPR/Cas9 workflow that is compatible with our *in vitro* Tfh cell culture (**Figure 19A**). We first validated the fidelity of this approach by comparing the CRISPR/Cas9-generated knockout cells with cells derived from genetically-targeted mouse models. For each gene of interest, we generated and tested three different guide RNAs in our culture system. Guides against *Cxcr5* efficiently reduced CXCR5 protein expression without affecting Bcl6 expression and knocking out *Tgfb2* abolished both CXCR5 and Bcl6 expression (**Figure 19B, 19C**). Ablation of *Bcl6* resulted in a reduction of Bcl6 protein expression in two guides (**Figure 19B, 19C**). For the third guide, the deletion of the Zink finger domain interfered with the negative autoregulation of Bcl6, resulting in an elevated expression of truncated but dysfunctional Bcl6 protein (Wang et al., 2002). The Ablation of *Bcl6* with all three guides did not affect CXCR5 expression (**Figure 19B, 19C**). These results were confirmed using a knockout mouse model with *Cd4-CreERT2⁺ Bcl6^{fl/fl} (iBcl6 $\Delta\Delta$)* CD4⁺ T cells (**Figure 20A, 20B, 20C**). Perturbing *Smad3*, the canonical downstream signaling molecule of TGF β , resulted in the loss of

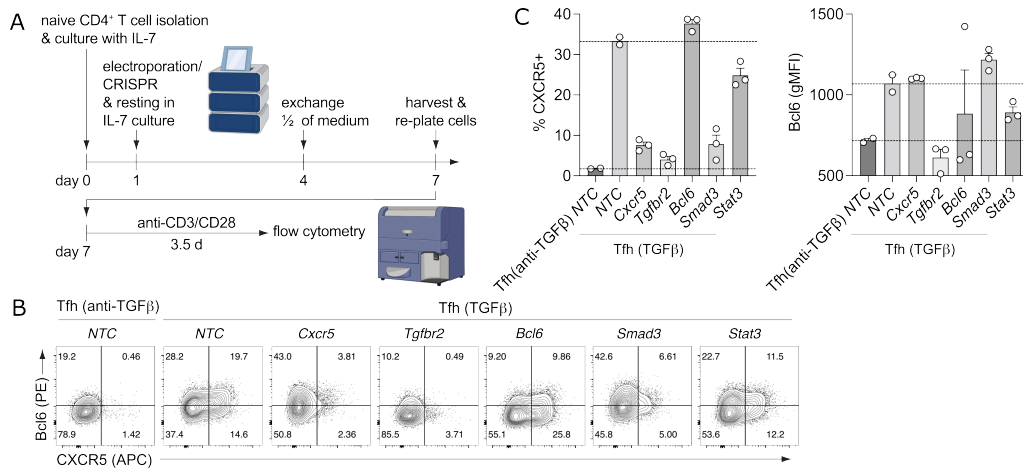


Figure 19: Efficient generation of CRISPR/Cas9-generated gene knockout CD4⁺ T cells

(A) Experimental outline: Naïve CD4⁺ T cells pooled from several C57BL/6 mice were cultured overnight in IL-7-supplemented T cell medium followed by electroporation with ribonucleoprotein complexes. After 6 days of resting in the IL-7 culture, cells were transferred to anti-CD3/CD28-coated plates, cultured for 3.5 days under various T helper cell differentiation conditions, then analyzed by flow cytometry.

(B) Representative flow cytometry contour plots of the CRISPR/Cas9-generated knockout CD4⁺ T cells for the indicated target genes, stained for CXCR5 and Bcl6. Gated on live CD4⁺ cells. *NTC*, non-targeting control.

(C) Quantification of the frequencies of CXCR5-positive cells and gMFI of Bcl6. Each dot represents an individual guide RNA used for CRISPR/Cas9-mediated knockout. Dashed lines indicate the mean frequency of CXCR5⁺ cells and mean Bcl6 expression levels of *NTC* (anti-TGFβ) and Tfh (TGFβ) cells. The Data are representative of three independent experiments, with mean ± SEM with 2-3 gRNAs per group. CRISPR experiments were performed by the Jeker lab in Basel.

CXCR5 protein expression without influencing Bcl6 protein expression (**Figure 19B, 19C**). This indicated that TGFβ signaling through Smad3 was required for CXCR5 induction, whereas TGFβ-induced Bcl6 protein expression was mediated through a Smad3-independent pathway.

After we validated the power and versatility of the CRISPR/Cas9 approach, we utilized this system to investigate the potential connections between the Tfh and Th17 developmental pathways. We selected several of the significantly differentially expressed genes from the bulk RNA-seq data (**Figure 5D, 5E, 17C, 17D**) as candidates for a CRISPR/Cas9 screen, including Aiolos (*Ikzf3*), *c-Maf*

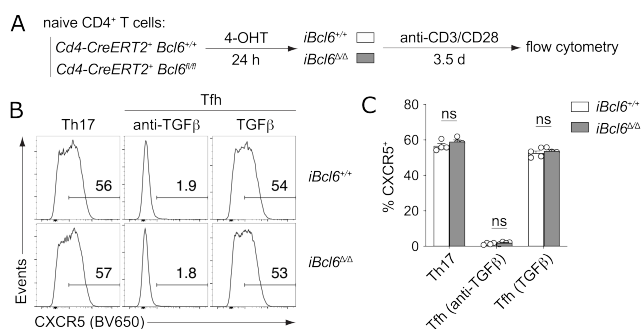


Figure 20: TGFβ-induced CXCR5 expression is independent of Bcl6

(A) Experimental outline: 4-hydroxytamoxifen (4-OHT)-treated naïve CD4⁺ T cells (5×10^4) isolated from *Cd4-CreERT2⁺ Bcl6^{+/+}* (*iBcl6^{+/+}*) and *Cd4-CreERT2⁺ Bcl6^{fl/fl}* (*iBcl6^{Δ/Δ}*) mice were differentiated *in vitro* for 3.5 days under T helper cell subset-polarizing conditions.

(B) Representative flow cytometry histogram plots showing the frequency of CXCR5⁺ cells among live CD4⁺ T cells after 3.5 days of culture.

(C) Quantification of the frequencies of CXCR5⁺ cells among live CD4⁺ T cells.

The Data are representative of three independent experiments, with mean ± SEM with $n = 4$ biological replicates. Unpaired t-test with * $p < 0.05$; ** $p < 0.01$; *** $p < 0.001$; **** $p < 0.0001$

(*Maf*), and *Batf*. *c-Maf* and *Aiolos* were strongly expressed in the Th17 and Tfh (TGF β) conditions compared to the Th1 and Tfh (anti-TGF β) conditions, *Batf* was inversely expressed (**Figure 21A**). While in the conditions containing TGF β mRNA of *c-Maf* and *Aiolos* were significantly enriched in the CXCR5⁺IL-17A⁻ population compared to the IL-17A⁺CXCR5⁻ cell population (**Figure 17C, 17D**). We observed a reduction in IL-17A production with no change in CXCR5 protein expression for *Batf* knockout samples, whereas IL-17A was slightly increased and CXCR5 protein expression was reduced for *Ikzf3* knockout samples (**Figure 12B, 21D**). In contrast, ablation of *c-Maf* resulted in the complete absence of CXCR5 with a strong increase of IL-17A production (**Figure 21B, 21C, 21D**). Regarding IL-2 expression, we observed strong IL-2 production in the Tfh (anti-TGF β) condition as well as in the *Tgfb2* knockout cell cultures (**Figure 21E**). IL-2 production in *Maf* knockouts was slightly elevated compared to the non-targeting control (NTC), but showed no distinct positive population (**Figure 21E**).

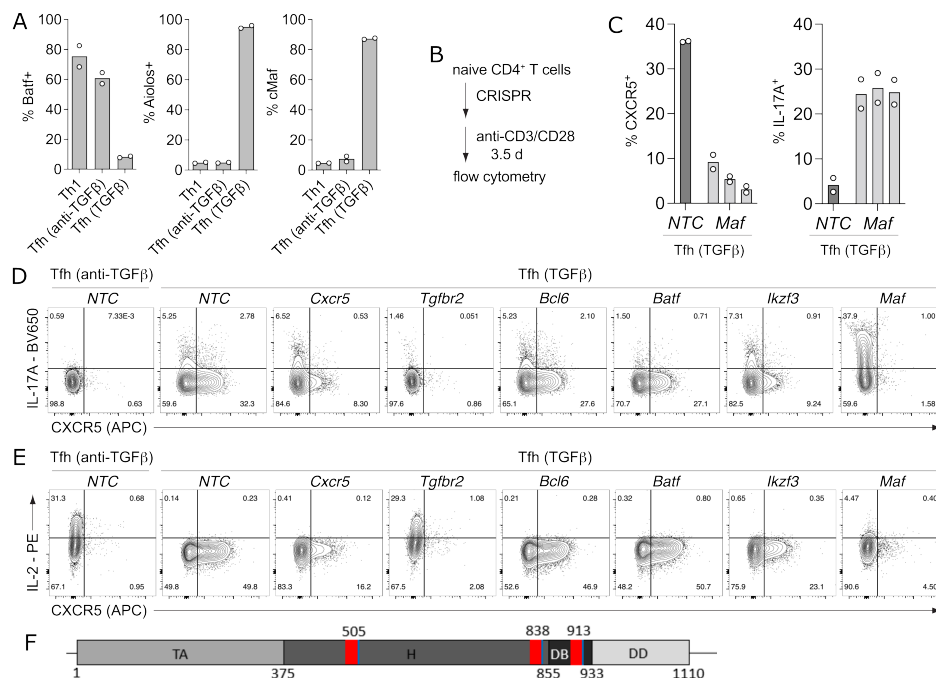


Figure 21: Arrayed CRISPR/Cas9 screen to identify transcription factors driving Tfh versus Th17 cell differentiation

(A) Quantification of the frequencies of *Batf*, *Aiolos*, and *c-Maf*-positive cells in live CD4⁺ T cells that were differentiated for 3.5 days *in vitro*, as assessed by flow cytometry.

(B) Experimental outline: Naïve CD4⁺ T cells were cultured as described in Figure 19. In brief, naïve CD4⁺ T cells were electroporated with ribonucleoprotein complexes and cultured in anti-CD3/CD28-coated plates under various T helper cell differentiation conditions. Cells were analyzed on day 3.5 by flow cytometry.

(C) Quantification of the frequencies of CXCR5⁺ and IL-17A⁺ cells among live CD4⁺ T cells. Each bar represents an individual guide RNA used for CRISPR/Cas9-mediated knockout.

(D, E) Representative flow cytometry contour plots of the CRISPR/Cas9-generated knockout CD4⁺ T cell for the indicated target genes stained for CXCR5 and IL-17A (**D**) or CXCR5 and IL-2 (**E**). Gated on live CD4⁺ cells.

(F) Schematic of the *Maf* gene locus. The target locations of three different guide RNAs are indicated. Abbreviations: transactivation domain (TA), hinge region (H), dimerization domain (DD), DNA-binding domain (DB). Numbers indicate nucleotide positions from transcription start site.

The Data in (A) are representative of three independent experiments, with the mean of 2 mice per group shown. Data in (C,D) are representative of three independent experiments, with mean with 2 biological replicates per gRNA. Data in (E) are representative of two independent experiments. CRISPR experiments were performed by the Jeker lab in Basel.

As c-Maf and Bcl6 have been previously shown to cooperatively regulate human Tfh cells (Kroenke et al., 2012), we next assessed the role of c-Maf and Bcl6 in more detail. Deletion of *Maf* resulted in a reduction in the expression of Bcl6 protein (**Figure 22A, 22B**), whereas c-Maf protein expression was not affected by the loss of Bcl6 (**Figure 22C**). Furthermore, we observed an increase in IL-17A-production and a decrease in CXCR5 expression in cells after knockout of *Maf*, while ablation of *Bcl6* did not result in any changes in cytokine production or CXCR5 expression (**Figure 21D**). Together this indicates that the TGF β -induced CXCR5 expression was driven by c-Maf, independently of Bcl6, these findings implied that c-Maf functioned as a switch between Tfh and Th17 cell fate.

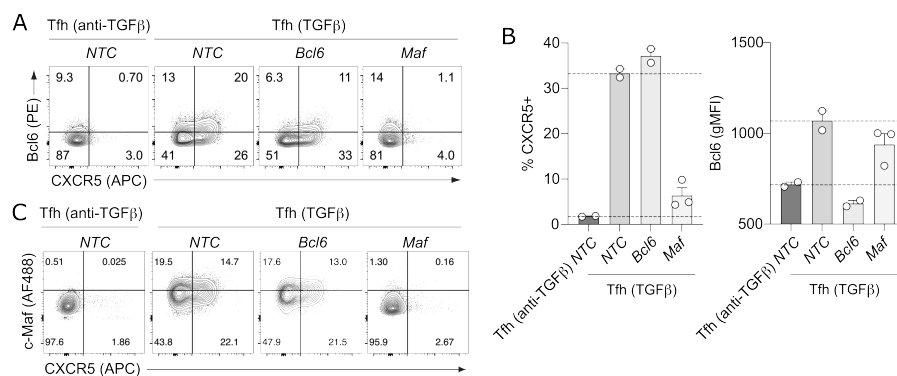


Figure 22: c-Maf expression is independent of Bcl6

(A) Representative flow cytometry contour plots of the CRISPR/Cas9-generated knockout CD4⁺ T cells for the indicated target genes stained for CXCR5 and Bcl6. Gated on live CD4⁺ cells.

(B) Quantification of the frequencies of CXCR5-positive cells and gMFI of Bcl6. Each dot represents an individual guide RNA used for CRISPR/Cas9-mediated knockout. Dashed lines indicate the mean frequency of CXCR5⁺ cells and mean Bcl6 expression levels of NTC-treated Tfh (anti-TGF β) and Tfh (TGF β) cells.

(C) Representative flow cytometry contour plots of the CRISPR/Cas9-generated knockout CD4⁺ T cells for the indicated target genes stained for CXCR5 and c-Maf. Gated on live CD4⁺ cells.

Data in (A, B, C) are representative of three independent experiments each, with mean \pm SEM with 2-3 gRNAs per group in (B). CRISPR experiments were performed by the Jeker lab in Basel.

4.11 c-Maf functions as a switch factor determining Tfh versus Th17 cell fates

In order to validate the results from the CRISPR/Cas9 screen, we cultured *Ma^f Δ* CD4⁺ T cells with the respective controls under Tfh (TGF β) conditions. In accordance with the CRISPR/Cas9 data, *Ma^f Δ* cells failed to upregulate CXCR5 protein expression, coinciding with increased frequencies of IL-17A⁺ cells (**Figure 23A, 23B**). We next cultured *Ma^f Δ* CD4⁺ cell with the respective control (*Ma^f^{fl/fl}*) in Tfh (anti-TGF β), Tfh (1 ng/ml TGF β), and Tfh (5 ng/ml TGF β) conditions, and subjected the sorted CD4⁺ T cells to bulk RNA-sequencing (**Figure 23A, 23C**).

Since c-Maf is not expressed in the Tfh (anti-TGF β) condition (**Figure 21A**), in the PCA the *Ma^f Δ* and *Ma^f^{fl/fl}* samples cultured in the Tfh (anti-TGF β) condition clustered together (**Figure 23C**). With increasing amounts of TGF β in the culture, we observed a shift of both the *Ma^f Δ* and *Ma^f^{fl/fl}* populations along the PC1 axis, concurrently with a divergence of both populations in the PC2 axis (**Figure 23C**). GSEA analysis of the Tfh (5 ng/ml TGF β) condition finally confirmed that the

Tfh signature is enriched in the control, while the Th17 signature was enriched in the knockout, thus supporting that c-Maf regulated Tfh versus Th17 cell fate as a switch factor (**Figure 23D**).

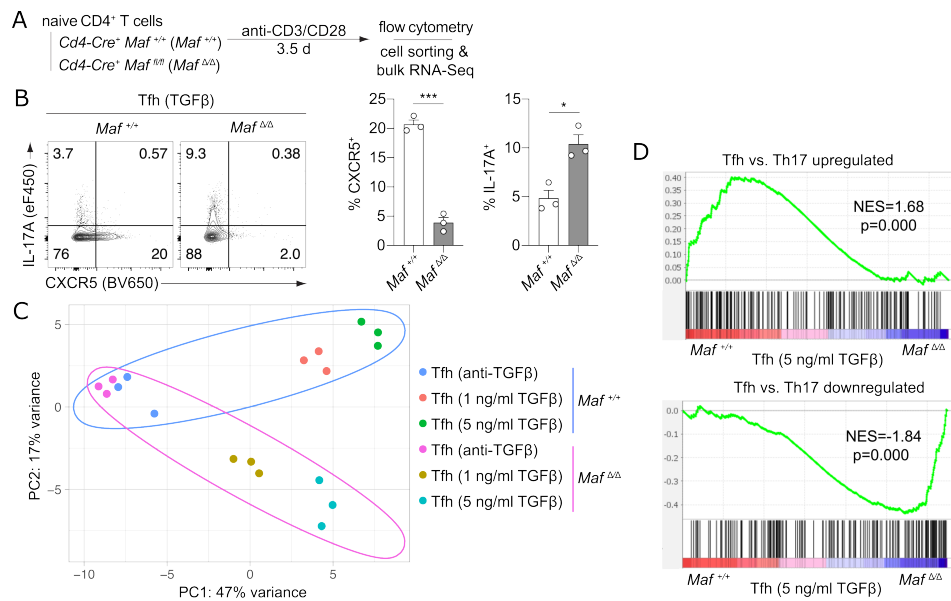


Figure 23: Absence of c-Maf shifts the phenotype from Tfh towards Th17 in the Tfh (TGF β) cell culture

(A) Experimental outline: Naïve *Cd4-Cre⁺ Maf^{+/+} (Maf^{+/+})* and *Cd4-Cre⁺ Maf^{fl/fl} (Maf $\Delta\Delta$)* CD4⁺ T cells were cultured *in vitro* in anti-CD3/CD28-coated plates for 3.5 days under different Tfh-polarizing differentiation conditions. Cells were then analyzed by flow cytometry, or live CD4⁺ T cells were sorted and subjected to bulk RNA-seq.

(B) Representative flow cytometry contour plots of CXCR5 expression and IL-17A production following restimulation with PMA/ionomycin in the presence of monensin were measured on day 3.5 by flow cytometry. Shown are representative flow cytometry contour plots as well as quantification of the frequency of CXCR5⁺ and IL-17A⁺ cells among live CD4⁺ T cells.

(C) PCA of the bulk RNA-seq data. Each dot represents one sample. Ellipses surround all *Maf^{+/+}* and *Maf $\Delta\Delta$* samples, respectively.

(D) GSEA of previously published genes (GSE11924) that are up- or downregulated in mature Tfh versus Th17 cells in the *in vitro* differentiated Th17 and Tfh cells.

Data in (B) are representative of three independent experiments, with mean \pm SEM with 3 mice per group. The Data in (C, D) are from one experiment with 3 mice per group. While the RNA-sequencing was performed by the NGS core facility of the Medical Faculty at the University of Bonn, all analyses and visualizations depicted in panels A-D were performed by myself. Statistics were calculated using GSEA (D). (B) Unpaired t-test with * $p < 0.05$; ** $p < 0.01$; *** $p < 0.001$

c-Maf was also highly expressed in CXCR5^{hi}PD-1^{hi} GC Tfh cells *in vivo* following acute lymphocytic choriomeningitis virus (LCMV) infection (**Figure 24A, 24B**). T cell-specific knockout of *Maf* diminished the frequencies of CXCR5^{hi}Bcl6^{hi} GC Tfh cells among GP66-specific CD4⁺ T cells following acute LCMV infection (**Figure 24A, 24C**), as well as the frequencies of CXCR5^{hi}Bcl6^{hi} GC Tfh cells among total CD4⁺ T cells following chronic LCMV infection (**Figure 24A, 24D**). Concurrently with the decrease in Tfh cell frequencies, an increase in Th17 cell frequencies was observed, as identified by an increase in Rorgt⁺ and IL-17A⁺ cells in activated CD44⁺PD1⁺ CD4⁺ T cells following acute LCMV infection (**Figure 24A, 24E, 24F**). Given that the immune response against LCMV infection is normally Th1 and Tfh, but not Th17 cell-restricted (Baumjohann et al., 2013), these *in vivo* experiments further support the role of c-Maf as a switch factor between Th17 and Tfh cell fates.

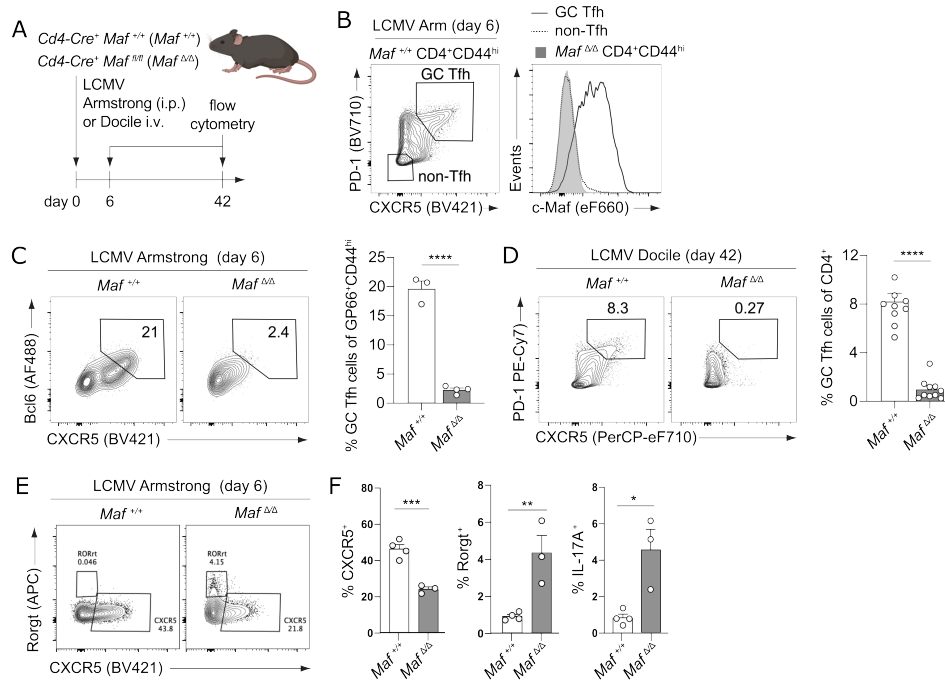


Figure 24: T cell-specific absence of Maf results in reduced Tfh cell and concurrently increased Th17 cell frequencies *in vivo*

(A) Experimental outline: *Maf*^{+/+} and *Maf*^{Δ/Δ} mice were infected with LCMV Armstrong or LCMV Docile to induce acute or chronic infections, respectively. Splenic CD4⁺ T cells were analyzed on day 6 (acute LCMV infection) or day 42 (chronic LCMV infection) post-infection by flow cytometry.

(B) Gating strategy to identify GC Tfh and non-Tfh cells. Histogram of c-Maf expression among GC Tfh compared to non-Tfh cells as well as *Maf*^{Δ/Δ} live CD4⁺ T cells.

(C) Representative flow cytometry contour plots of live control (left) and *Maf*^{Δ/Δ} CD4⁺ T cells (right) stained for Bcl6 and CXCR5 on day 6 post LCMV Armstrong infection. Gated on GP66-tetramer-positive CD44^{hi} cells. Quantification of the frequency of GC Tfh cells is shown in the bar graph.

(D) Representative flow cytometry contour plots of live control (left) and *Maf*^{Δ/Δ} CD4⁺ T cells (right) stained for PD-1 and CXCR5 on day 42 post LCMV Docile infection. Quantification of the frequency of GC Tfh cells is shown in the bar graph.

(E) Representative flow cytometry contour plots of live control (left) and *Maf*^{Δ/Δ} CD4⁺ T cells (right) stained for Rorgt and CXCR5 on day 6 post LCMV Armstrong infection.

(F) Quantification of the frequency of CXCR5⁺, Rorgt⁺, IL-17A⁺ positive cells.

Data in (B, C, E, F) are from one experiment each, with 3-4 mice per group. Data in (D) are pooled from two independent experiments with 9-10 mice per group. LCMV experiments were performed by the Kallies lab in Melbourne. Unpaired t-test with **p* < 0.05; ***p* < 0.01; ****p* < 0.001; *****p* < 0.0001.

5. Discussion

5.1 Improved *in vitro* culture recapitulates early *in vivo* differentiation of mouse Tfh cells

The present work established a robust *in vitro* differentiation protocol for murine Tfh cells from naïve CD4⁺ T cells. In an APC-free system using plate-bound anti-CD3/anti-CD28, it was shown that TGF β synergized with IL-6 and IL-21 to induce CXCR5 as well as Bcl6 protein expression in activated murine CD4-positive T cells *in vitro*. This finding is contradictory to the current state-of-the-art, which for many years has implied an inhibitory function of TGF β on Tfh cell differentiation. This conception primarily arose from two publications stating that TGF β repressed IL-21 production (R. I. Nurieva et al., 2008; Suto et al., 2008), which is an important cytokine produced by Tfh cells. While it has been shown previously that Tfh cells produce large quantities of IL-21 (Chtanova et al., 2004; R. I. Nurieva et al., 2008; Vogelzang et al., 2008), IL-21 can also be produced by various other T helper cell populations such as Th1 (Chtanova et al., 2004), Th2 (Wurster et al., 2002), Th17 (Korn et al., 2007; R. Nurieva et al., 2007), and NKT cells (Coquet et al., 2007). Hence, Tfh cells cannot be identified solely by the production of IL-21; additional markers are required, most commonly Bcl6, CXCR5, and PD-1 (Eisenbarth et al., 2021). Importantly, quantification of Bcl6 and CXCR5 protein expression using flow cytometry often proves to be a challenge, sometimes showing weak separation, and thus making it difficult to clearly distinguish positive and negative populations. While reliable staining protocols for the identification of Tfh cells by protein markers are now available (Baumjohann & Ansel, 2015), others prefer to quantify CXCR5 and Bcl6 mRNA by qPCR instead (R. I. Nurieva et al., 2008; Wan et al., 2021). The genome-wide correlation between protein and mRNA expression are quite poor though, with a squared Pearson correlation coefficient of about 0.40, indicating that mRNA quantification is able to predict changes in protein expression in only 40 % of cases (de Sousa Abreu et al., 2009; Vogel & Marcotte, 2012). This discrepancy is likely due to some combination of post-transcriptional regulation and measurement noise, such as in the case of CXCR5 and Bcl6 (Choi & Crotty, 2021; Vogel & Marcotte, 2012).

In order to better assess CXCR5 and Bcl6 protein expression, we applied optimizations as described before (Baumjohann & Ansel, 2015). For Bcl6 staining, fixation at room temperature enhanced the separation of positive versus negative populations. For CXCR5 staining, we used streptavidin to enhance the signal. The tetrameric structure of streptavidin enables three biotinylated anti-CXCR5 antibodies to crosslink on a plane, thereby strongly increasing the avidity of the antibodies (Hudson & Kortt, 1999). The improved methods for detection allowed us to pick up even small changes in CXCR5 and Bcl6 expression. The *in vitro*-generated Tfh-like cells showed key properties of *bona fide* Tfh cells, including chemotaxis towards CXCL13, the ligand of CXCR5, and supportive abilities towards B cells. The *in vitro* differentiation process also recapitulated important *in vivo* differentiation aspects of Tfh cells. For example, we confirmed and extended our

knowledge on the inhibitory function of IL-2 on Tfh cell differentiation (Ballesteros-Tato et al., 2012; Ditoro et al., 2018; Johnston et al., 2012).

5.2 TGF β in human versus mouse Tfh cell differentiation

Mouse and human Tfh cells express an almost identical set of signature molecules, with high percentages of overlapping gene expression profiles (Crotty, 2011). One notable exception is CXCL13; while human Tfh cell produces high quantities of CXCL13 (Kim et al., 2004; Rasheed et al., 2006), it is not produced by murine Tfh cells (Crotty, 2011).

Further evolutionary divergence between human and mouse Tfh cell biology has been shown for the cytokines required for their generation. While in mouse IL-6 is a potent inducer of IL-21 production and Tfh differentiation (Eto et al., 2011; R. I. Nurieva et al., 2008; Suto et al., 2008), it has limited effect in driving both human IL-21 production and Tfh differentiation (Schmitt et al., 2009, 2013). In contrast, IL-12 appears to be critical for the generation of human Tfh cells (Ma et al., 2009; Schmitt et al., 2009), while in mouse it only has minor effects on IL-21 expression (Nakayama et al., 2011; Suto et al., 2008). Contrary to murine Tfh cell differentiation, TGF β has been previously shown to promote human Tfh cell differentiation (Locci et al., 2016; Schmitt et al., 2014). Our finding that TGF β potently induces Tfh cell features in mouse CD4⁺ T cells indicates that human and mouse Tfh cell differentiation may not be as different as previously thought, and that our murine model of *in vitro* Tfh cell differentiation might generate new insights that are relevant for our understanding of the human immune system as well.

5.3 Cell density-mediated effects on Tfh cell differentiation

We showed that seeding density critically alters the efficiency of *in vitro* Tfh cell differentiation. Increased cell density in the culture negatively affected Tfh cell differentiation, reducing both CXCR5 and Bcl6 protein expression. This effect was especially prevalent in the Tfh cell cultures containing lower concentrations of TGF β , involving increased IL-2 pathway signaling in combination with reduced TGF β pathway signaling. Tfh cell differentiation *in vivo* exhibits a similar effect, increasing the amount of adoptively transferred CD4⁺ T cells from 5e3 to 2.5e4 to 1e5 resulted in a stepwise decrease in the frequency of Tfh cells within the transferred cells (Lee et al., 2021). We compared two approaches to reduce cell density within the cell culture. First, starting with a uniformly high seeding density, followed by splitting the cells on day 2 in order to reduce cell density. The second approach reduced the cell density directly by reducing the cells initially seeded. As both approaches provided similar results, the second approach was preferred as it cuts down on the number of plates and cells required, while providing sufficient quantity of cells for analysis. A seeding density of 4e4 allowed culturing the cells for 3.5 days without the need to change the media.

Out of 17 papers that applied a Tfh-skewing *in vitro* condition and were published between 2021 and 2022, only five publications provided an unambiguous description of the seeding density (Table 2; page 25). Three cases used a seeding density of 2×10^5 cells in a 96-well format. Two cases further increased the seeding density to 5×10^5 cells in a 96-well format (Table 2; page 25). This seeding density is much higher than the optimized density of 4×10^4 per well in a 96-well format established in this thesis, which resulted in the loss of the CXCR5 and Bcl6-inducing effect of TGF β .

The reduction of cell density increases the distance between cells, and therefore might reduce paracrine signaling of IL-2, resulting in enhanced Tfh cell differentiation. Mathematical modeling of IL-2 signaling through CD25 revealed feedback regulation causing an all-or-nothing response (Busse et al., 2010). The activation threshold of this feedback loop exhibits random variation from cell to cell (Busse et al., 2010), which might result in spontaneous activation of this feedback loop. The paracrine IL-2 signaling is strongly distance-dependent, as secreted IL-2 is constantly captured by the IL-2 receptor (CD25) expressed by the same but also by adjacent cells (Ditiro et al., 2018). In order for the IL-2 signal to propagate to adjacent cells, cells expressing CD25 have to be within the paracrine signaling distance of 60 μm from a source of IL-2 (Busse et al., 2010). Naïve T cells and Tfh cells, which do not express the high-affinity receptor CD25, may require even closer distances to a potential source of IL-2 to respond to the secreted IL-2. This highlights the benefits of the reduced cell density in the Tfh cell culture, as it hinders the paracrine signaling of IL-2.

TGF β inhibits IL-2 expression *in vitro* in a Smad3-dependent manner (McKarns et al., 2004). Similarly, CD4⁺ T cell culture under Tfh cell-polarizing conditions in the presence of TGF β produced reduced amounts of IL-2, with both the frequency of IL-2-producing cells as well as the quantity of IL-2 produced on a per-cell basis being reduced, albeit IL-2 production was not abrogated completely. Therefore, the effect of TGF β firstly limits potential sources of IL-2. Secondly, by reducing the quantity of IL-2 being produced, TGF β allowed for higher cell density without increasing the potential for paracrine IL-2 signaling. Increased cell density might have also caused increased consumption of TGF β , and thereby hampering the maintenance of CXCR5 expression.

IL-2 was capable of averting growth suppression mediated by TGF β in a dose-dependent manner, however, excessive amounts of IL-2 are not able to completely negate the effect of TGF β (Kehrl et al., 1986). Co-culturing Tgfr2 wildtype and knockout CD4⁺ T cells mimicked the spontaneous activation of the positive feedback loop of IL-2 in a partial population of the cultured cells, namely the Tgfr2 knockout cells. Tgfr2 wildtype cells, despite possessing competent TGF β signaling, assumed the same level of CD25 and CXCR5 expression as the Tgfr2 knockout cells. This finding supported our model and strongly indicated the dominance of a trans-effect mediated by IL-2 signaling. While TGF β has been shown to restrict IL-2 responsiveness by reducing CD25 expression *in vitro* (Marshall et al., 2015), the effect described in that study could also be explained by this model by circumventing a positive feedback loop of IL-2-induced upregulation of CD25 (Busse et al., 2010).

A further mechanism of directional, paracrine delivery of IL-2 is via homotypic interaction with multifocal synapses between T cells mediated by LFA-1 (Sabatos et al., 2008). The paracrine signaling of IL-2 within the culture can be obstructed by the addition of Treg cells. Treg cells act as a potent sink for IL-2, and they are capable of disrupting the autocrine IL-2 signaling of T cells within a distance of 10 μm (Busse et al., 2010). A similar phenomenon has been described *in vivo* that excess IL-2 can be quenched by DCs (Li et al., 2016) and Treg cells (León et al., 2014), thus promoting Tfh cell differentiation. While IL-2 strongly inhibits Tfh cell differentiation, the effect of TGF β has to include more facets than solely the suppression of IL-2. On day 0.5 of the Tfh cell culture, CXCR5 was expressed only in the conditions containing TGF β . During this early time point, the effect of IL-2 can be assumed to be minimal. Furthermore, both blocking IL-2 and inhibiting its downstream signaling molecule Stat5 were able to enhance Tfh cell differentiation, however, only in the presence of TGF β . This implies that the initial cell fate commitment requires TGF β signaling in some form or another. Stat5 inhibition resulted in a stronger enhancement of Tfh cell differentiation as compared to IL-2 blocking. This is likely due to either autocrine delivery of IL-2 or the forming of homotypic synapses between T cells, allowing for IL-2 delivery without interference of the IL-2 blocking antibody in the cell culture medium, while the small molecule inhibitor was capable to diffuse into the cell and thereby directly inhibiting IL-2 signaling intracellularly. In summary, a major obstacle of the *in vitro* Tfh cell culture is to manage IL-2 production by activated CD4⁺ T cells, which can be counteracted by reducing cell density within the cell culture to restrict IL-2 signaling and thereby enhancing Tfh differentiation.

5.4 APC-based systems of Tfh cell differentiation

Other attempts to differentiate Tfh cells *in vitro* relied on APC-based culture systems, for instance co-culturing OT-II cells with T cell-depleted, mitomycin C-treated splenocytes with OVA₃₂₃₋₃₃₉ peptide (Lu et al., 2011). This approach generated about 20% CXCR5-positive Tfh-like cells. However, utilizing T-cell-depleted splenocytes, with a largely diverse cell composition, might produce results that vary strongly between experiments and within experiments. Between biological replicates, cell composition may vary considerably, with the frequency of splenic DCs ranging from 3.49% to 5.67% with a mean of $4.24 \pm 0.707\%$ in male C57BL/6J mice (Jackson Laboratory, 2007). The Complement-mediated cell depletion and mitomycin C-treatment add unnatural stress on the APCs, facilitating cell death (Fulda et al., 2010). An entangled network of possible interaction between different cell types and their different cytokine secretion pattern might obscure crucial interaction or cytokines driving Tfh differentiation. Consequently, the controls of Th0, Th1, Th2, and Th17 conditions showed a high background with up to 10% CXCR5-positive cells (Lu et al., 2011). A more recent attempt improved the previous approach by stimulation of the APC with LPS and the increase of the APC:T cell ratio (Gao et al., 2019). The increase of this ratio to 500:1 concurrently resulted in the generation of higher frequencies of CXCR5⁺ Tfh-like cells, potentially due to a decrease in inhibition or competition between T cells, similarly to the effects seen by reduction of the seeding density in the work of this thesis. Of note, DCs or Treg cells within the

splenocytes might act as a potential sink for IL-2, thereby enhancing Tfh cell differentiation (León et al., 2014; Li et al., 2016).

5.5 Limitations of *in vitro* culture systems

In vitro differentiation of T cells is a powerful model system that has been used for many decades; however, it cannot fully recapitulate all aspects of the complex *in vivo* immune response to infectious agents or other naturally occurring stimulants. *In vivo* differentiated cells may undergo different pathways of differentiation compared to those established *in vitro*. For *in vitro* Th2 cell differentiation, IL-4 signaling through its mediator Stat6 is essential (Zhu et al., 2001). However, *in vivo*, IL-4 or Stat6 deletion had only minor effects on the number or the timing of the appearance of Th2 cells (van Panhuys et al., 2008).

In vivo, TCR stimulation is mediated via pulses with longer periods of signal deprivation while migrating from one DC to another and serial triggering of the TCR (Valitutti et al., 1995). Both cannot be easily imitated in an APC-free culture system. The various stages of *in vivo* T cell differentiation are compartmentalized. This means that during differentiation a T cell migrates to different areas within the lymph node (for example, Tfh cells migrating from the T cell zone to the T:B cell zone and into the follicles) or even leaves the lymph node (for example, Th1 or Th2 cells emigrating to peripheral tissues). The change in environment results in compartmentalization, where different signals are provided to and blocked from the cell, thus allowing a natural progression. Both Th1 and Th2 cell differentiation have potential positive feedback loops, where the secreted effector molecule can in turn cause an enhanced differentiation of that phenotype (Seder et al., 1992). Similarly, Th17 cells produce IL-21 to promote and sustain Th17 lineage commitment (Wei et al., 2007). While *in vivo* the locations of priming and effector function are anatomically segregated, a separation *in vitro* of naïve cells from effector cells is difficult or not possible. For Th1, Th2, Th17 *in vitro* cultures, the key cytokines produced by these cells further drive the respective cell fate commitment. In contrast, for the Tfh cell culture, we have shown that IL-2-producing cells could become prevalent within the culture, potentially undermining Tfh cell differentiation. While the limitations imposed by the IL-2 feedback loop might be overcome *in vivo* with the involvement of other cell types such as Treg or DCs, or *in vitro* by the addition of splenocytes, which contain Treg and DCs, we here showed another feasible approach through the reduction of cell density within the cell culture.

5.6 *In vivo* sources of TGF β

Tfh cell differentiation is characterized by a multistep process, in which Tfh cells continuously interact with different APCs (Baumjohann & Fazilleau, 2021). In our *in vitro* differentiation model, Tfh cells required constant TGF β availability. During the priming process, the primary source of active TGF β is likely to be provided by DCs. TGF β is secreted by various cell types, particularly in epithelial-rich tissues, such as skin or intestines. TGF β is secreted in a latent complex of ho-

modimers of TGF β , bound to the latency-associated peptide (LAP) or TGF β -binding proteins associated with the extracellular matrix (Munger & Sheppard, 2011). Both cDC1 and cDC2 are capable of activating latent TGF β , though through different enzymes: cDC1 preferentially express integrin $\alpha\beta 8$ to form $\alpha\beta 8$, enabling them to activate latent TGF β (Boucard-Jourdin et al., 2016), whereas cDC2 are able to cleave latent TGF β through the metalloprotease MMP-9 (Brown et al., 2019). *In vivo* immunization and allergy models indicate that cDC2 are predominantly responsible for Tfh cell activation (Briseño et al., 2018; Krishnaswamy et al., 2017; Sakurai et al., 2021). However, during viral infection integrin $\alpha\beta 8$ on cDC1 are required for RV-specific IgA responses, while dispensable for steady-state immune homeostasis (Nakawesi et al., 2020). This highlights that the priming and source of TGF β is context-dependent rather than dependent on the DC subset. After initial cell fate commitment, pre-Tfh cells enter the follicle and migrate into the light zone of the GC (Baumjohann & Fazilleau, 2021). In order to maintain CXCR5 expression by Tfh cells in our *in vitro* cell culture model, a constant source of TGF β was required. Interestingly, B cells require TGF β in order to cycle between light and dark zones within GCs (Albright et al., 2019). Using B cell-specific ablation of *Tgfbr1*, it was shown that GC B cells in the light zone required TGF β signaling to transition into the dark zone (Albright et al., 2019). The source of active TGF β in the light zone is likely to be follicular dendritic cells (Albright et al., 2019; Suzuki et al., 2010).

5.7 Adoptive transfer of Th17 cells and the development of ectopic lymphoid follicles

Th17 and Tfh cells appear to exhibit high plasticity. Th17 cells that homed to Peyer's patches acquired a Tfh-like phenotype and supported antigen-specific IgA responses in GCs (Hirota et al., 2013). Similarly, in this thesis, we have shown that under Th17-polarizing conditions *in vitro* a significant number of cells acquired characteristics of Tfh cells, such as expression of CXCR5 and Bcl6. This finding sheds light on previous reports that described an ability of *in vitro*-generated Th17 cells to provide efficient help to B cells both *in vitro* and *in vivo* (Mitsdoerffer et al., 2010). Interestingly, in an EAE setting adoptively transferred *in vitro*-differentiated Th17 cells induced ectopic lymphoid follicles in the central nervous system (Peters et al., 2011). B cell entry into lymph nodes requires non-redundantly both CCR7 and CXCR4, reducing or blocking their downstream signaling reduced B cell accumulation in the lymph nodes about 90% compared to the control (Okada et al., 2002). Additional CXCR5 expression did not contribute to entry into lymph nodes, while enhancing entry into Peyer's patches by twofold (Okada et al., 2002). CXCR5 signaling is however crucial for the retention of B cells and organization of lymphoid follicles (Ansel et al., 2000; Förster et al., 1996). These findings imply that adoptively transferred Tfh cells, which downregulate CCR7 during activation, might not be able to enter the lymph node through the HEV. Unable to home to GCs, the adoptively transferred T cells might accumulate in proximity of their cognate antigen, for instance in the CNS for MOG-specific Tfh cells. Further work is needed to decipher the precise contributions of Th17 versus Tfh cells in the development of ectopic lymphoid follicles.

5.8 Role of Bcl6 and c-Maf in Tfh and Th17 differentiation

The *in vitro* differentiation of mouse Tfh cells provides a powerful system to study the underlying molecular pathways. The strong plasticity between Tfh and Th17 cells is intriguing, and in this thesis, we aimed at dissecting what drives the cell fate commitment between them. Il17a^{Smart} mice are a transcriptional reporter for IL-17A and reliably report T cells with the potential to produce IL-17A (Price et al., 2012). Using this system, we sorted either CXCR5⁺ or hNGFR2-positive cells, which have committed to Tfh and Th17 cell fates, respectively, and identified potential drivers of bifluctuation between them. Interestingly, by increasing the dose of TGF β we also observed CXCR5-positive cells with the potential ability to produce IL-17A, as described in Bauquet et al., 2008. In order to screen the potential drivers of Tfh versus Th17 bifluctuation, we adopted and validated a gene editing approach with CRISPR/Cas9 in naïve CD4⁺ T cells (Dölz et al., 2021; Kornete et al., 2018; Nguyen et al., 2020; Seki & Rutz, 2018). For each gene of interest, we generated three guide RNAs targeting different regions to exclude domain-specific differences between the knockouts. All genes of interests showed similar phenotypes with the respective three guide RNAs, with the exception of Bcl6. For the Bcl6 knockout, we captured the negative autoregulation of Bcl6. The truncation of Bcl6, resulting in the lack of the Zink finger domain, nicely recapitulated the findings described in (Wang et al., 2002), showing elevated expression of the truncated but dysfunctional Bcl6. Tfh cells are highly plastic *in vivo*, as previously shown in a LCMV infection setting in which the induced loss of Bcl6 in established Tfh cells resulted in the loss of CXCR5 expression and transdifferentiation of ex-Tfh cells into Th1-like cells (Alterauge et al., 2020). Reducing the environmental factors present *in vivo* to a minimum *in vitro*, allowed us to confirm that CXCR5 can be expressed independently of Bcl6 (Liu et al., 2014).

In the arrayed CRISPR/Cas9 screen, we showed that both CXCR5 and IL-17A could be reduced individually by the knockout of *Ikzf3* and *Batf*, respectively. However, most intriguingly, knockout of *Maf* resulted in a reduction of CXCR5 and Bcl6 expression, concurrently with an increase in IL-17A expression. We were able to confirm this finding in Cd4-Cre *Maf*^{fl/m} mice, both *in vitro* and *in vivo*. c-Maf plays a critical role in Tfh cell differentiation. Loss of *Maf* results in defective Tfh cell differentiation *in vivo* in a protein immunization setting (Andris et al., 2017). In human T cells, *Maf* overexpression resulted in increased expression of CXCR5 and IL-21 (Kroenke et al., 2012). In contrast, the role of c-Maf in Th17 cell differentiation is more ambiguous. Th17 cells show high levels of *Maf* transcripts (Imbratta et al., 2020). However, c-Maf is not required for early Th17 cell differentiation (Bauquet et al., 2008). In Th17 cells, c-Maf was shown to drive IL-10 production (Xu et al., 2009) and to repress IL-2 production (Gabryšová et al., 2018), driving the cell fate decision towards a more anti-inflammatory Th17 phenotype (Aschenbrenner et al., 2018). While IL-2 levels in our *Maf* knockout cells were not increased, we observed elevated CD25 expression levels. These findings suggest that c-Maf functions as a switch factor for Tfh versus Th17 cell fate decisions. The developmental program between Tfh and Th17 shows a remarkable degree of similarities. Both populations are induced by IL-6 and IL-21 (Korn et al., 2007; R. I. Nurieva et al., 2008; Suto et al., 2008), and are inhibited by IL-2 (Ballesteros-Tato et al., 2012; Laurence et al., 2007). Both populations were shown to be able to produce both IL-21 and IL-17 (Bauquet et al.,

2008). Here, we present c-Maf as an additional transcription factor, beside Bcl6 and Rorgt, that drives the divergence between the two CD4⁺ T cell populations. Nevertheless, several questions remain unanswered and will be addressed in the future. At what time does c-Maf exert its effect? Does it only drive early cell fate commitment or can it also mediate plasticity between matured Tfh and Th17 at later time points? Does it have a directionality? Can Th17 cells be converted in Tfh cells by overexpression of Maf?

5.9 Summary and future directions

The work presented in this thesis has established the *in vitro* requirements for the induction of murine CXCR5 and Bcl6-expressing Tfh cells in an APC-free culture system. By utilizing complementary cell culture assays and gene knockout approaches of various signaling pathways, we revealed that Tfh and Th17 cells exhibit distinct but overlapping requirements for their generation and that c-Maf acts as a switch factor for their cell fates (**Figure 25**). Using the novel *in vitro* Tfh culture, we have focused in this work primarily on the group 3 Tfh cells. Future directions include also studying the plasticity and function within group 1 Tfh, group 2 Tfh, and T follicular regulatory (Tfr) cells. In addition, more efforts should aim at characterizing the ability of the *in vitro*-generated Tfh cells to provide help to B cells *in vivo*.

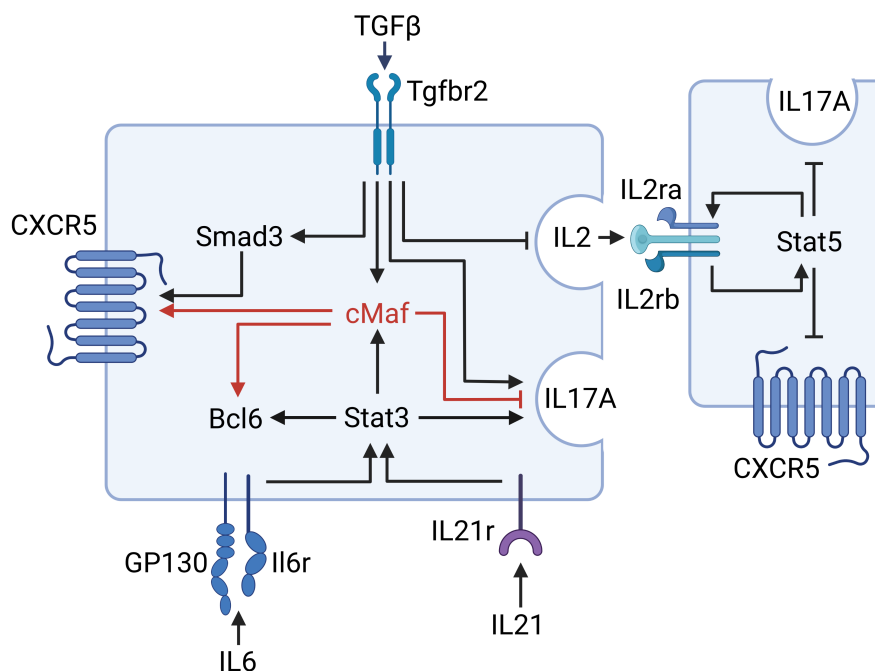


Figure 25: Intra- and inter-cellular signaling pathways in murine *in vitro*-cultured Tfh cells

References

- Acharya, K. R., & Ackerman, S. J. (2014). Eosinophil Granule Proteins: Form and Function. *Journal of Biological Chemistry*, 289(25), 17406–17415. <https://doi.org/10.1074/JBC.R113.546218>
- Acosta-Rodriguez, E. v., Rivino, L., Geginat, J., Jarrossay, D., Gattorno, M., Lanzavecchia, A., Salustio, F., & Napolitani, G. (2007). Surface phenotype and antigenic specificity of human interleukin 17–producing T helper memory cells. *Nature Immunology* 2007 8:6, 8(6), 639–646. <https://doi.org/10.1038/ni1467>
- Aderem, A., & Underhill, D. M. (1999). Mechanisms of phagocytosis in macrophages. *Annu. Rev. Immunol.*, 17, 593–623. <https://doi.org/10.1146/annurev.immunol.17.1.593>
- Afgan, E., Baker, D., Batut, B., van den Beek, M., Bouvier, D., Ech, M., Chilton, J., Clements, D., Coraor, N., Grüning, B. A., Guerler, A., Hillman-Jackson, J., Hiltemann, S., Jalili, V., Rasche, H., Soranzo, N., Goecks, J., Taylor, J., Nekrutenko, A., & Blankenberg, D. (2018). The Galaxy platform for accessible, reproducible and collaborative biomedical analyses: 2018 update. *Nucleic Acids Research*, 46(W1), W537–W544. <https://doi.org/10.1093/NAR/GKY379>
- Aggarwal, S., & Gurney, A. L. (2002). IL-17: prototype member of an emerging cytokine family. *Journal of Leukocyte Biology*, 71(1), 1–8. <https://doi.org/10.1189/JLB.71.1.1>
- Akiba, H., Takeda, K., Kojima, Y., Usui, Y., Harada, N., Yamazaki, T., Ma, J., Tezuka, K., Yagita, H., & Okumura, K. (2005). The Role of ICOS in the CXCR5+ Follicular B Helper T Cell Maintenance In Vivo. *The Journal of Immunology*, 175(4), 2340–2348. <https://doi.org/10.4049/JIMMUNOL.175.4.2340>
- Albright, A. R., Kabat, J., Li, M., Raso, F., Reboldi, A., & Muppidi, J. R. (2019). TGFβ signaling in germinal center B cells promotes the transition from light zone to dark zone. *The Journal of Experimental Medicine*, 216(11), 2531–2545. <https://doi.org/10.1084/JEM.20181868>
- Alemán-García, Y. P., Vaquero-García, R. M., Flores-Fernández, R., Fuentes-Pananá, E. M., Gorocica-Rosete, P., Pizaña-Venegas, A., Chávez-Sánchez, L., Blanco-Favela, F., Legorreta-Haquet, M. v., & Chávez-Rueda, A. K. (2021). Prolactin Increases the Frequency of Follicular T Helper Cells with Enhanced IL21 Secretion and OX40 Expression in Lupus-Prone MRL/lpr Mice. *Journal of Immunology Research*, 2021. <https://doi.org/10.1155/2021/6630715>
- Allen, J. E., & Wynn, T. A. (2011). Evolution of Th2 Immunity: A Rapid Repair Response to Tissue Destructive Pathogens. *PLoS Pathogens*, 7(5). <https://doi.org/10.1371/JOURNAL.PPAT.1002003>
- Alterauge, D., Bagnoli, J. W., Dahlström, F., Bradford, B. M., Mabbott, N. A., Buch, T., Enard, W., & Baumjohann, D. (2020). Continued Bcl6 Expression Prevents the Transdifferentiation of Established Tfh Cells into Th1 Cells during Acute Viral Infection. *Cell Reports*, 33(1), 108232. <https://doi.org/10.1016/J.CELREP.2020.108232>

- Andris, F., Denanglaire, S., Anciaux, M., Hercor, M., Hussein, H., & Leo, O. (2017). The transcription factor c-Maf promotes the differentiation of follicular helper T cells. *Frontiers in Immunology*, 8(APR), 480. <https://doi.org/10.3389/FIMMU.2017.00480/BIBTEX>
- Ansel, K. M., Ngo, V. N., Hyman, P. L., Luther, S. A., Förster, R., Sedgwick, J. D., Browning, J. L., Upp, M., & Cyster, J. G. (2000). A chemokine-driven positive feedback loop organizes lymphoid follicles. *Nature* 2000 406:6793, 406(6793), 309–314. <https://doi.org/10.1038/35018581>
- Aschenbrenner, D., Foglierini, M., Jarrossay, D., Hu, D., Weiner, H. L., Kuchroo, V. K., Lanzavecchia, A., Notarbartolo, S., & Sallusto, F. (2018). An immunoregulatory and tissue-residency program modulated by c-MAF in human TH17 cells. *Nature Immunology* 2018 19:10, 19(10), 1126–1136. <https://doi.org/10.1038/s41590-018-0200-5>
- Ballesteros-Tato, A., León, B., Graf, B. A., Moquin, A., Adams, P. S., Lund, F. E., & Randall, T. D. (2012). Interleukin-2 Inhibits Germinal Center Formation by Limiting T Follicular Helper Cell Differentiation. *Immunity*, 36(5), 847–856. <https://doi.org/10.1016/J.IMMUNI.2012.02.012>
- Bartleson, J. M., Viehmann Milam, A. A., Donermeyer, D. L., Horvath, S., Xia, Y., Egawa, T., & Allen, P. M. (2020). Strength of tonic T cell receptor signaling instructs T follicular helper fate decisions. *Nature Immunology*, 21(11), 1384. <https://doi.org/10.1038/S41590-020-0781-7>
- Battegay, M., Cooper, S., Althage, A., Bänziger, J., Hengartner, H., & Zinkernagel, R. M. (1991). Quantification of lymphocytic choriomeningitis virus with an immunological focus assay in 24- or 96-well plates. *Journal of Virological Methods*, 33(1–2), 191–198. [https://doi.org/10.1016/0166-0934\(91\)90018-U](https://doi.org/10.1016/0166-0934(91)90018-U)
- Baumjohann, D., & Ansel, K. M. (2015). Tracking early T follicular helper cell differentiation in vivo. *Methods in Molecular Biology (Clifton, N.J.)*, 1291, 27. https://doi.org/10.1007/978-1-4939-2498-1_3
- Baumjohann, D., & Fazilleau, N. (2021). Antigen-dependent multistep differentiation of T follicular helper cells and its role in SARS-CoV-2 infection and vaccination. *European Journal of Immunology*, 51(6), 1325–1333. <https://doi.org/10.1002/EJI.202049148>
- Baumjohann, D., Kageyama, R., Clingan, J. M., Morar, M. M., Patel, S., de Kouchkovsky, D., Bannard, O., Bluestone, J. A., Matloubian, M., Ansel, K. M., & Jeker, L. T. (2013). The microRNA cluster miR-17~92 promotes TFH cell differentiation and represses subset-inappropriate gene expression. *Nature Immunology* 2013 14:8, 14(8), 840–848. <https://doi.org/10.1038/ni.2642>
- Baumjohann, D., Okada, T., & Ansel, K. M. (2011). Cutting Edge: Distinct Waves of BCL6 Expression during T Follicular Helper Cell Development. *The Journal of Immunology*, 187(5), 2089–2092. <https://doi.org/10.4049/JIMMUNOL.1101393>
- Baumjohann, D., Preite, S., Reboldi, A., Ronchi, F., Ansel, K. M., Lanzavecchia, A., & Sallusto, F. (2013). Persistent antigen and germinal center B cells sustain T follicular helper cell responses and phenotype. *Immunity*, 38(3), 596–605. <https://doi.org/10.1016/J.IMMUNI.2012.11.020>

- Bauquet, A. T., Jin, H., Paterson, A. M., Mitsdoerffer, M., Ho, I. C., Sharpe, A. H., & Kuchroo, V. K. (2008a). The costimulatory molecule ICOS regulates the expression of c-Maf and IL-21 in the development of follicular T helper cells and TH-17 cells. *Nature Immunology* 2008 10:2, 10(2), 167–175. <https://doi.org/10.1038/ni.1690>
- Bauquet, A. T., Jin, H., Paterson, A. M., Mitsdoerffer, M., Ho, I. C., Sharpe, A. H., & Kuchroo, V. K. (2008b). The costimulatory molecule ICOS regulates the expression of c-Maf and IL-21 in the development of follicular T helper cells and TH-17 cells. *Nature Immunology* 2008 10:2, 10(2), 167–175. <https://doi.org/10.1038/ni.1690>
- Bettelli, E., Carrier, Y., Gao, W., Korn, T., Strom, T. B., Oukka, M., Weiner, H. L., & Kuchroo, V. K. (2006). Reciprocal developmental pathways for the generation of pathogenic effector TH17 and regulatory T cells. *Nature*, 441(7090), 235–238. <https://doi.org/10.1038/NATURE04753>
- Betz, B. C., Jordan-Williams, K. L., Wang, C., Kang, S. G., Liao, J., Logan, M. R., Kim, C. H., & Taparowsky, E. J. (2010). Batf coordinates multiple aspects of B and T cell function required for normal antibody responses. *Journal of Experimental Medicine*, 207(5), 933–942. <https://doi.org/10.1084/JEM.20091548>
- Bossaller, L., Burger, J., Draeger, R., Grimbacher, B., Knoth, R., Plebani, A., Durandy, A., Baumann, U., Schlesier, M., Welcher, A. A., Peter, H. H., & Warnatz, K. (2006). ICOS Deficiency Is Associated with a Severe Reduction of CXCR5+CD4 Germinal Center Th Cells. *The Journal of Immunology*, 177(7), 4927–4932. <https://doi.org/10.4049/JIMMUNOL.177.7.4927>
- Boucard-Jourdin, M., Kugler, D., Endale Ahanda, M.-L., This, S., de Calisto, J., Zhang, A., Mora, J. R., Stuart, L. M., Savill, J., Lacy-Hulbert, A., & Paidassi, H. (2016). β 8 Integrin Expression and Activation of TGF- β by Intestinal Dendritic Cells Are Determined by Both Tissue Microenvironment and Cell Lineage. *The Journal of Immunology*, 197(5), 1968–1978. <https://doi.org/10.4049/JIMMUNOL.1600244/-DCSUPPLEMENTAL>
- Bretscher, P., & Cohn, M. (1970). A Theory of Self-Nonself Discrimination. *Science*, 169(3950), 1042–1049. <https://doi.org/10.1126/SCIENCE.169.3950.1042>
- Brinkman, E. K., Chen, T., Amendola, M., & van Steensel, B. (2014). Easy quantitative assessment of genome editing by sequence trace decomposition. *Nucleic Acids Research*, 42(22). <https://doi.org/10.1093/NAR/GKU936>
- Briseño, C. G., Satpathy, A. T., Davidson, J. T., Ferris, S. T., Durai, V., Bagadia, P., O'Connor, K. W., Theisen, D. J., Murphy, T. L., & Murphy, K. M. (2018). Notch2-dependent DC2s mediate splenic germinal center responses. *Proceedings of the National Academy of Sciences of the United States of America*, 115(42), 10726–10731. https://doi.org/10.1073/PNAS.1809925115/SUPPL_FILE/PNAS.1809925115.SAPP.PDF
- Brown, C. C., Gudjonson, H., Pritykin, Y., Deep, D., Lavallée, V. P., Mendoza, A., Fromme, R., Mazutis, L., Ariyan, C., Leslie, C., Pe'er, D., & Rudensky, A. Y. (2019). Transcriptional Basis of Mouse and Human Dendritic Cell Heterogeneity. *Cell*, 179(4), 846–863.e24. <https://doi.org/10.1016/J.CELL.2019.09.035>

- BURNET, F. M. (1962). THE IMMUNOLOGICAL SIGNIFICANCE OF THE THYMUS. *Australasian Annals of Medicine*, 11(2), 79–91. <https://doi.org/10.1111/IMJ.1962.11.2.79>
- Busse, D., de La Rosa, M., Hobiger, K., Thurley, K., Flossdorf, M., Scheffold, A., & Höfer, T. (2010). Competing feedback loops shape IL-2 signaling between helper and regulatory T lymphocytes in cellular microenvironments. *Proceedings of the National Academy of Sciences of the United States of America*, 107(7), 3058. <https://doi.org/10.1073/PNAS.0812851107>
- Butcher, M. J., & Zhu, J. (2021). Recent advances in understanding the Th1/Th2 effector choice. *Faculty Reviews*, 10(30). <https://doi.org/10.12703/R/10-30>
- Cannons, J. L., Tangye, S. G., & Schwartzberg, P. L. (2011). SLAM Family Receptors and SAP Adaptors in Immunity. <Http://Dx.Doi.Org/10.1146/Annurev-Immunol-030409-101302>, 29, 665–705. <https://doi.org/10.1146/ANNUREV-IMMUNOL-030409-101302>
- Cannons, J. L., Wu, J. Z., Gomez-Rodriguez, J., Zhang, J., Dong, B., Liu, Y., Shaw, S., Siminovich, K. A., & Schwartzberg, P. L. (2010). Biochemical and Genetic Evidence for a SAP-PKC- θ Interaction Contributing to IL-4 Regulation. *The Journal of Immunology*, 185(5), 2819–2827. <https://doi.org/10.4049/JIMMUNOL.0902182>
- Cannons, J. L., Yu, L. J., Jankovic, D., Crotty, S., Horai, R., Kirby, M., Anderson, S., Cheever, A. W., Sher, A., & Schwartzberg, P. L. (2006). SAP regulates T cell-mediated help for humoral immunity by a mechanism distinct from cytokine regulation. *The Journal of Experimental Medicine*, 203(6), 1551. <https://doi.org/10.1084/JEM.20052097>
- Charles A Janeway, J., Travers, P., Walport, M., & Shlomchik, M. J. (2001). Immunobiology. *Immunobiology*, 14102, 1–10. <https://www.ncbi.nlm.nih.gov/books/NBK10757/>
- Chen, L., & Flies, D. B. (2013). Molecular mechanisms of T cell co-stimulation and co-inhibition. *Nature Reviews Immunology* 2013 13:4, 13(4), 227–242. <https://doi.org/10.1038/nri3405>
- Chen, W. J., Jin, W., Hardegen, N., Lei, K. J., Li, L., Marinos, N., McGrady, G., & Wahl, S. M. (2003). Conversion of peripheral CD4+CD25- naive T cells to CD4+CD25+ regulatory T cells by TGF-beta induction of transcription factor Foxp3. *The Journal of Experimental Medicine*, 198(12), 1875–1886. <https://doi.org/10.1084/JEM.20030152>
- Choi, J., & Crotty, S. (2021). Bcl6-Mediated Transcriptional Regulation of Follicular Helper T cells (TFH). *Trends in Immunology*, 42(4), 336–349. <https://doi.org/10.1016/J.IT.2021.02.002>
- Choi, Y. S., Gullicksrud, J. A., Xing, S., Zeng, Z., Shan, Q., Li, F., Love, P. E., Peng, W., Xue, H. H., & Crotty, S. (2015). LEF-1 and TCF-1 orchestrate TFH differentiation by regulating differentiation circuits upstream of the transcriptional repressor Bcl6. *Nature Immunology* 2015 16:9, 16(9), 980–990. <https://doi.org/10.1038/ni.3226>
- Christie, S. M., Fijen, C., & Rothenberg, E. (2022). V(D)J Recombination: Recent Insights in Formation of the Recombinase Complex and Recruitment of DNA Repair Machinery. *Frontiers in Cell and Developmental Biology*, 10, 850. <https://doi.org/10.3389/FCELL.2022.886718/BIBTEX>

- Chtanova, T., Tangye, S. G., Newton, R., Frank, N., Hodge, M. R., Rolph, M. S., & Mackay, C. R. (2004). T Follicular Helper Cells Express a Distinctive Transcriptional Profile, Reflecting Their Role as Non-Th1/Th2 Effector Cells That Provide Help for B Cells. *The Journal of Immunology*, *173*(1), 68–78. <https://doi.org/10.4049/JIMMUNOL.173.1.68>
- Chung, Y., Chang, S. H., Martinez, G. J., Yang, X. O., Nurieva, R., Kang, H. S., Ma, L., Watowich, S. S., Jetten, A. M., Tian, Q., & Dong, C. (2009). Critical regulation of early Th17 cell differentiation by interleukin-1 signaling. *Immunity*, *30*(4), 576–587. <https://doi.org/10.1016/J.IMMUNI.2009.02.007>
- Constant, S., Pfeiffer, C., Woodard, A., Pasqualini, T., & Bottomly, K. (1995). Extent of T cell receptor ligation can determine the functional differentiation of naive CD4+ T cells. *The Journal of Experimental Medicine*, *182*(5), 1591–1596. <https://doi.org/10.1084/JEM.182.5.1591>
- Cooper, M. D., & Alder, M. N. (2006). The evolution of adaptive immune systems. *Cell*, *124*(4), 815–822. <https://doi.org/10.1016/J.CELL.2006.02.001>
- Coquet, J. M., Kyparissoudis, K., Pellicci, D. G., Besra, G., Berzins, S. P., Smyth, M. J., & Godfrey, D. I. (2007). IL-21 Is Produced by NKT Cells and Modulates NKT Cell Activation and Cytokine Production. *The Journal of Immunology*, *178*(5), 2827–2834. <https://doi.org/10.4049/JIMMUNOL.178.5.2827>
- Cox, J., & Mann, M. (2008). MaxQuant enables high peptide identification rates, individualized p.p.b.-range mass accuracies and proteome-wide protein quantification. *Nature Biotechnology* *26*:12, *26*(12), 1367–1372. <https://doi.org/10.1038/nbt.1511>
- Crotty, S. (2011). Follicular Helper CD4 T Cells (TFH). <https://doi.org/10.1146/Annurev-Immunol-031210-101400>, *29*, 621–663. <https://doi.org/10.1146/ANNUREV-IMMUNOL-031210-101400>
- Crotty, S. (2019). T follicular helper cell biology: A decade of discovery and diseases. *Immunity*, *50*(5), 1132. <https://doi.org/10.1016/J.IMMUNI.2019.04.011>
- Davis, M. M., & Bjorkman, P. J. (1988). T-cell antigen receptor genes and T-cell recognition. *Nature*, *334*(6181), 395–402. <https://doi.org/10.1038/334395A0>
- Deenick, E. K., Chan, A., Ma, C. S., Gatto, D., Schwartzberg, P. L., Brink, R., & Tangye, S. G. (2010). Follicular helper T cell differentiation requires continuous antigen presentation that is independent of unique B cell signaling. *Immunity*, *33*(2), 241–253. <https://doi.org/10.1016/J.IMMUNI.2010.07.015>
- Demetz, S., Grey, H. M., & Sette, A. (1990). The minimal number of class II MHC-antigen complexes needed for T cell activation. *Science (New York, N.Y.)*, *249*(4972), 1028–1030. <https://doi.org/10.1126/SCIENCE.2118680>
- de Sousa Abreu, R., Penalva, L. O., Marcotte, E. M., & Vogel, C. (2009). Global signatures of protein and mRNA expression levels. *Molecular BioSystems*, *5*(12), 1512. <https://doi.org/10.1039/B908315D>

- Ditoro, D., Winstead, C., Pham, D., Witte, S., Andargachew, R., Singer, J. R., Wilson, C. G., Zindl, C. L., Luther, R. J., Silberger, D. J., Weaver, B., Kolawole, M., Martinez, R. J., Turner, H., Hatton, R. D., Moon, J., Way, S. S., Evavold, B. D., & Weaver, C. T. (2018). Differential IL-2 expression defines developmental fates of follicular versus nonfollicular helper T cells. *Science*, 361(6407). https://doi.org/10.1126/SCIENCE.AAO2933/SUPPL_FILE/AAO2933_DITORO_SM.PDF
- Dobin, A., Davis, C. A., Schlesinger, F., Drenkow, J., Zaleski, C., Jha, S., Batut, P., Chaisson, M., & Gingeras, T. R. (2013). STAR: ultrafast universal RNA-seq aligner. *Bioinformatics*, 29(1), 15–21. <https://doi.org/10.1093/BIOINFORMATICS/BTS635>
- Dodge, I. L., Carr, M. W., Cernadas, M., & Brenner, M. B. (2003). IL-6 Production by Pulmonary Dendritic Cells Impedes Th1 Immune Responses. *The Journal of Immunology*, 170(9), 4457–4464. <https://doi.org/10.4049/JIMMUNOL.170.9.4457>
- Doench, J. G., Fusi, N., Sullender, M., Hegde, M., Vaimberg, E. W., Donovan, K. F., Smith, I., Tothova, Z., Wilen, C., Orchard, R., Virgin, H. W., Listgarten, J., & Root, D. E. (2016). Optimized sgRNA design to maximize activity and minimize off-target effects of CRISPR-Cas9. *Nature Biotechnology*, 34(2), 184–191. <https://doi.org/10.1038/NBT.3437>
- Dölz, M., Marone, R., & Jeker, L. T. (2021). Plasmid- or Ribonucleoprotein-Mediated CRISPR/Cas Gene Editing in Primary Murine T Cells. *Methods in Molecular Biology (Clifton, N.J.)*, 2285, 255–264. https://doi.org/10.1007/978-1-0716-1311-5_20
- Dong, C. (2021). Cytokine Regulation and Function in T Cells. <https://doi.org/10.1146/Annurev-Immunol-061020-053702>, 39, 51–76. <https://doi.org/10.1146/ANNUREV-IMMUNOL-061020-053702>
- Dutko, F. J., & Oldstone, M. B. A. (1983). Genomic and biological variation among commonly used lymphocytic choriomeningitis virus strains. *The Journal of General Virology*, 64 (Pt 8)(8), 1689–1698. <https://doi.org/10.1099/0022-1317-64-8-1689>
- Eddahri, F., Denanglaire, S., Bureau, F., Spolski, R., Leonard, W. J., Leo, O., & Andris, F. (2009). Interleukin-6/STAT3 signaling regulates the ability of naive T cells to acquire B-cell help capacities. *Blood*, 113(11), 2426–2433. <https://doi.org/10.1182/BLOOD-2008-04-154682>
- Eisenbarth, S. C., Baumjohann, D., Craft, J., Fazilleau, N., Ma, C. S., Tangye, S. G., Vinuesa, C. G., & Linterman, M. A. (2021). CD4+ T cells that help B cells – a proposal for uniform nomenclature. *Trends in Immunology*, 42(8), 658. <https://doi.org/10.1016/J.IT.2021.06.003>
- Eto, D., Lao, C., DiToro, D., Barnett, B., Escobar, T. C., Kageyama, R., Yusuf, I., & Crotty, S. (2011). IL-21 and IL-6 Are Critical for Different Aspects of B Cell Immunity and Redundantly Induce Optimal Follicular Helper CD4 T Cell (T_{fh}) Differentiation. *PLOS ONE*, 6(3), e17739. <https://doi.org/10.1371/JOURNAL.PONE.0017739>
- Fazilleau, N., McHeyzer-Williams, L. J., Rosen, H., & McHeyzer-Williams, M. G. (2009). The function of follicular helper T cells is regulated by the strength of T cell antigen receptor binding. *Nature Immunology*, 10(4), 375–384. <https://doi.org/10.1038/NI.1704>

- Feng, H., Zhao, X., Xie, J., Bai, X., Fu, W., Chen, H., Tang, H., Wang, X., & Dong, C. (2022). Pathogen-associated T follicular helper cell plasticity is critical in anti-viral immunity. *Science China Life Sciences* 2022 65:6, 65(6), 1075–1090. <https://doi.org/10.1007/S11427-021-2055-X>
- Ferguson, S. E., Han, S., Kelsoe, G., & Thompson, C. B. (1996). CD28 is required for germinal center formation. *The Journal of Immunology*, 156(12).
- Fillatreau, S., & Gray, D. (2003). T Cell Accumulation in B Cell Follicles Is Regulated by Dendritic Cells and Is Independent of B Cell Activation. *Journal of Experimental Medicine*, 197(2), 195–206. <https://doi.org/10.1084/JEM.20021750>
- Förster, R., Mattis, A. E., Kremmer, E., Wolf, E., Brem, G., & Lipp, M. (1996). A Putative Chemokine Receptor, BLR1, Directs B Cell Migration to Defined Lymphoid Organs and Specific Anatomic Compartments of the Spleen. *Cell*, 87(6), 1037–1047. [https://doi.org/10.1016/S0092-8674\(00\)81798-5](https://doi.org/10.1016/S0092-8674(00)81798-5)
- Fukuta, M., Suzuki, K., Kojima, S., Yabe, Y., Suzuki, K., Iida, K., Yamada, H., Makino, S., Iwata, A., Tanaka, S., Iwamoto, T., Suto, A., Nakagomi, D., Wakashin, H., Maezawa, Y., Maezawa, Y., Takemoto, M., Asanuma, K., & Nakajima, H. (2021). Original research: Suppressor of cytokine signalling 3 (SOCS3) expressed in podocytes attenuates glomerulonephritis and suppresses autoantibody production in an imiquimod-induced lupus model. *Lupus Science & Medicine*, 8(1), 426. <https://doi.org/10.1136/LUPUS-2020-000426>
- Fulda, S., Gorman, A. M., Hori, O., & Samali, A. (2010). Cellular Stress Responses: Cell Survival and Cell Death. *International Journal of Cell Biology*, 2010. <https://doi.org/10.1155/2010/214074>
- Gabryšová, L., Alvarez-Martinez, M., Luisier, R., Cox, L. S., Sodenkamp, J., Hosking, C., Pérez-Mazliah, D., Whicher, C., Kannan, Y., Potempa, K., Wu, X., Bhaw, L., Wende, H., Sieweke, M. H., Elgar, G., Wilson, M., Briscoe, J., Metzis, V., Langhorne, J., ... O'Garra, A. (2018). c-Maf controls immune responses by regulating disease-specific gene networks and repressing IL-2 in CD4+ T cells. *Nature Immunology* 2018 19:5, 19(5), 497–507. <https://doi.org/10.1038/s41590-018-0083-5>
- Gao, X., Wang, H., Chen, Z., Zhou, P., & Yu, D. (2019). An optimized method to differentiate mouse follicular helper T cells in vitro. *Cellular & Molecular Immunology* 2019 17:7, 17(7), 779–781. <https://doi.org/10.1038/s41423-019-0329-7>
- Gasteiger, G., D'osualdo, A., Schubert, D. A., Weber, A., Bruscia, E. M., & Hartl, D. (2017). Cellular Innate Immunity: An Old Game with New Players. *Journal of Innate Immunity*, 9(2), 111–125. <https://doi.org/10.1159/000453397>
- Goenka, R., Barnett, L. G., Silver, J. S., O'Neill, P. J., Hunter, C. A., Cancro, M. P., & Laufer, T. M. (2011). Cutting Edge: Dendritic Cell-Restricted Antigen Presentation Initiates the Follicular Helper T Cell Program but Cannot Complete Ultimate Effector Differentiation. *The Journal of Immunology*, 187(3), 1091–1095. <https://doi.org/10.4049/JIMMUNOL.1100853>

- Grawunder, U., Zimmer, D., Fugmann, S., Schwarz, K., & Lieber, M. R. (1998). DNA ligase IV is essential for V(D)J recombination and DNA double-strand break repair in human precursor lymphocytes. *Molecular Cell*, 2(4), 477–484. [https://doi.org/10.1016/S1097-2765\(00\)80147-1](https://doi.org/10.1016/S1097-2765(00)80147-1)
- Guglielmo, C., Bin, S., Cantarelli, C., Hartzell, S., Angeletti, A., Donadei, C., Cumpelik, A., Anderson, L., Cody, E., Sage, P. T., la Manna, G., Fiaccadori, E., Heeger, P. S., & Cravedi, P. (2021). Erythropoietin reduces auto- And alloantibodies by inhibiting T follicular helper cell differentiation. *Journal of the American Society of Nephrology*, 32(10), 2542–2560. <https://doi.org/10.1681/ASN.2021010098/-/DCSUPPLEMENTAL>
- Harding, C. v., & Unanue, E. R. (1990). Quantitation of antigen-presenting cell MHC class II/peptide complexes necessary for T-cell stimulation. *Nature* 1990 346:6284, 346(6284), 574–576. <https://doi.org/10.1038/346574a0>
- Hardtke, S., Ohi, L., & Förster, R. (2005). Balanced expression of CXCR5 and CCR7 on follicular T helper cells determines their transient positioning to lymph node follicles and is essential for efficient B-cell help. *Blood*, 106(6), 1924–1931. <https://doi.org/10.1182/BLOOD-2004-11-4494>
- Harrington, L. E., Hatton, R. D., Mangan, P. R., Turner, H., Murphy, T. L., Murphy, K. M., & Weaver, C. T. (2005). Interleukin 17–producing CD4+ effector T cells develop via a lineage distinct from the T helper type 1 and 2 lineages. *Nature Immunology* 2005 6:11, 6(11), 1123–1132. <https://doi.org/10.1038/ni1254>
- Hatzi, K., Philip Nance, J., Kroenke, M. A., Bothwell, M., Haddad, E. K., Melnick, A., & Crotty, S. (2015). BCL6 orchestrates Tfh cell differentiation via multiple distinct mechanisms. *Journal of Experimental Medicine*, 212(4), 539–553. <https://doi.org/10.1084/JEM.20141380>
- Haynes, N. M., Allen, C. D. C., Lesley, R., Ansel, K. M., Killeen, N., & Cyster, J. G. (2007). Role of CXCR5 and CCR7 in Follicular Th Cell Positioning and Appearance of a Programmed Cell Death Gene-1High Germinal Center-Associated Subpopulation. *The Journal of Immunology*, 179(8), 5099–5108. <https://doi.org/10.4049/JIMMUNOL.179.8.5099>
- Heink, S., Yogev, N., Garbers, C., Herwerth, M., Aly, L., Gasperi, C., Husterer, V., Croxford, A. L., Möller-Hackbarth, K., Bartsch, H. S., Sotlar, K., Krebs, S., Regen, T., Blum, H., Hemmer, B., Misgeld, T., Wunderlich, T. F., Hidalgo, J., Oukka, M., ... Korn, T. (2017). Trans-presentation of interleukin-6 by dendritic cells is required for priming pathogenic TH17 cells. *Nature Immunology*, 18(1), 74. <https://doi.org/10.1038/NI.3632>
- He, W., Wang, H., Wei, Y., Jiang, Z., Tang, Y., Chen, Y., & Xu, H. (2021). GuidePro: A multi-source ensemble predictor for prioritizing sgRNAs in CRISPR/Cas9 protein knockouts. *Bioinformatics (Oxford, England)*, 37(1), 134–136. <https://doi.org/10.1093/BIOINFORMATICS/BTAA1068>
- Hirota, K., Turner, J. E., Villa, M., Duarte, J. H., Demengeot, J., Steinmetz, O. M., & Stockinger, B. (2013). Plasticity of TH17 cells in Peyer's patches is responsible for the induction of T cell-dependent IgA responses. *Nature Immunology* 2013 14:4, 14(4), 372–379. <https://doi.org/10.1038/ni.2552>

- Hogquist, K. A., Baldwin, T. A., & Jameson, S. C. (2005). Central tolerance: learning self-control in the thymus. *Nature Reviews Immunology* 2005 5:10, 5(10), 772–782. <https://doi.org/10.1038/nri1707>
- Hoshino, H., Lötvall, J., Skoogh, B. E., & Lindén, A. (1999). Neutrophil recruitment by interleukin-17 into rat airways in vivo. Role of tachykinins. *American Journal of Respiratory and Critical Care Medicine*, 159(5 Pt 1), 1423–1428. <https://doi.org/10.1164/AJRCCM.159.5.9806008>
- Huang, B., Phelan, J. D., Preite, S., Gomez-Rodriguez, J., Johansen, K. H., Shibata, H., Arthur L. Shaffer, I., Xu, Q., Jeffrey, B., Kirby, M., Anderson, S., Yang, Y., Gossa, S., McGavern, D. B., Staudt, L. M., & Schwartzberg, P. L. (2022). In vivo CRISPR screens reveal a HIF-1 α -mTOR-network regulates T follicular helper versus Th1 cells. *Nature Communications*, 13(1), 805. <https://doi.org/10.1038/S41467-022-28378-6>
- Hudson, P. J., & Kortt, A. A. (1999). High avidity scFv multimers; diabodies and triabodies. *Journal of Immunological Methods*, 231(1–2), 177–189. [https://doi.org/10.1016/S0022-1759\(99\)00157-X](https://doi.org/10.1016/S0022-1759(99)00157-X)
- Imbratta, C., Hussein, H., Andris, F., & Verdeil, G. (2020). c-MAF, a Swiss Army Knife for Tolerance in Lymphocytes. *Frontiers in Immunology*, 11, 206. <https://doi.org/10.3389/FIMMU.2020.00206>
- Jackson Laboratory. (2007). *Flow-cytometric analysis of 11 strains of mice*. <https://phenome.jax.org>
- Jang, S. G., Lee, J., Hong, S. M., Song, Y. S., Kim, M. J., Kwok, S. K., Cho, M. I., & Park, S. H. (2021). Niclosamide suppresses the expansion of follicular helper T cells and alleviates disease severity in two murine models of lupus via STAT3. *Journal of Translational Medicine*, 19(1), 86. <https://doi.org/10.1186/S12967-021-02760-2>
- Johnson, D. E., O’Keefe, R. A., & Grandis, J. R. (2018). Targeting the IL-6/JAK/STAT3 signalling axis in cancer. *Nature Reviews. Clinical Oncology*, 15(4), 234–248. <https://doi.org/10.1038/NRCLINONC.2018.8>
- Johnston, R. J., Choi, Y. S., Diamond, J. A., Yang, J. A., & Crotty, S. (2012a). STAT5 is a potent negative regulator of TFH cell differentiation. *Journal of Experimental Medicine*, 209(2), 243–250. <https://doi.org/10.1084/JEM.20111174>
- Johnston, R. J., Choi, Y. S., Diamond, J. A., Yang, J. A., & Crotty, S. (2012b). STAT5 is a potent negative regulator of TFH cell differentiation. *Journal of Experimental Medicine*, 209(2), 243–250. <https://doi.org/10.1084/JEM.20111174>
- Johnston, R. J., Poholek, A. C., DiToro, D., Yusuf, I., Eto, D., Barnett, B., Dent, A. L., Craft, J., & Crotty, S. (2009). Bcl6 and Blimp-1 are reciprocal and antagonistic regulators of T follicular helper cell differentiation. *Science (New York, N.Y.)*, 325(5943), 1006–1010. <https://doi.org/10.1126/SCIENCE.1175870>
- Kabashima, K., Honda, T., Ginhoux, F., & Egawa, G. (2018). The immunological anatomy of the skin. *Nature Reviews Immunology* 2018 19:1, 19(1), 19–30. <https://doi.org/10.1038/s41577-018-0084-5>

- Kaplan, M. H., Schindler, U., Smiley, S. T., & Grusby, M. J. (1996). Stat6 is required for mediating responses to IL-4 and for development of Th2 cells. *Immunity*, *4*(3), 313–319. [https://doi.org/10.1016/S1074-7613\(00\)80439-2](https://doi.org/10.1016/S1074-7613(00)80439-2)
- Kaplan, M. H., Sun, Y. L., Hoey, T., & Grusby, M. J. (1996). Impaired IL-12 responses and enhanced development of Th2 cells in Stat4-deficient mice. *Nature*, *382*(6587), 174–177. <https://doi.org/10.1038/382174A0>
- Karnowski, A., Chevrier, S., Belz, G. T., Mount, A., Emslie, D., D'Costa, K., Tarlinton, D. M., Kallies, A., & Corcoran, L. M. (2012). B and T cells collaborate in antiviral responses via IL-6, IL-21, and transcriptional activator and coactivator, Oct2 and OBF-1. *The Journal of Experimental Medicine*, *209*(11), 2049–2064. <https://doi.org/10.1084/JEM.20111504>
- Kehrl, J. H., Wakefield, L. M., Roberts, A. B., Jakowlew, S., Alvarez-Mon, M., Derynck, R., Sporn, M. B., & Fauci, A. S. (1986). Production of transforming growth factor beta by human T lymphocytes and its potential role in the regulation of T cell growth. *Journal of Experimental Medicine*, *163*(5), 1037–1050. <https://doi.org/10.1084/JEM.163.5.1037>
- Kim, C. H., Lim, H. W., Kim, J. R., Rott, L., Hillsamer, P., & Butcher, E. C. (2004). Unique gene expression program of human germinal center T helper cells. *Blood*, *104*(7), 1952–1960. <https://doi.org/10.1182/BLOOD-2004-03-1206>
- Kim, V., Lee, K., Tian, H., Jang, S. H., Diamond, B., & Kim, S. J. (2022). IL-17–producing follicular Th cells enhance plasma cell differentiation in lupus-prone mice. *JCI Insight*, *7*(11). <https://doi.org/10.1172/JCI.INSIGHT.157332>
- Kisielow, P., Blüthmann, H., Staerz, U. D., Steinmetz, M., & von Boehmer, H. (1988). Tolerance in T-cell-receptor transgenic mice involves deletion of nonmature CD4+8+ thymocytes. *Nature*, *333*(6175), 742–746. <https://doi.org/10.1038/333742A0>
- Klein, L., Kyewski, B., Allen, P. M., & Hogquist, K. A. (2014). Positive and negative selection of the T cell repertoire: what thymocytes see (and don't see). *Nature Reviews Immunology* *2014* *14*:6, *14*(6), 377–391. <https://doi.org/10.1038/nri3667>
- Kopf, M., Ruedl, C., Schmitz, N., Gallimore, A., Lefrang, K., Ecabert, B., Odermatt, B., & Bachmann, M. F. (1999). OX40-Deficient Mice Are Defective in Th Cell Proliferation but Are Competent in Generating B Cell and CTL Responses after Virus Infection. *Immunity*, *11*(6), 699–708. [https://doi.org/10.1016/S1074-7613\(00\)80144-2](https://doi.org/10.1016/S1074-7613(00)80144-2)
- Kornete, M., Marone, R., & Jeker, L. T. (2018). Highly Efficient and Versatile Plasmid-Based Gene Editing in Primary T Cells. *Journal of Immunology (Baltimore, Md. : 1950)*, *200*(7), 2489–2501. <https://doi.org/10.4049/JIMMUNOL.1701121>
- Korn, T., Bettelli, E., Gao, W., Awasthi, A., Jäger, A., Strom, T. B., Oukka, M., & Kuchroo, V. K. (2007). IL-21 initiates an alternative pathway to induce proinflammatory T(H)17 cells. *Nature*, *448*(7152), 484–487. <https://doi.org/10.1038/NATURE05970>

- Korn, T., Mitsdoerffer, M., Croxford, A. L., Awasthi, A., Dardalhon, V. A., Galileos, G., Vollmar, P., Sritesky, G. L., Kaplan, M. H., Waisman, A., Kuchroo, V. K., & Oukka, M. (2008). IL-6 controls Th17 immunity in vivo by inhibiting the conversion of conventional T cells into Foxp3⁺ regulatory T cells. *Proceedings of the National Academy of Sciences of the United States of America*, *105*(47), 18460–18465. <https://doi.org/10.1073/PNAS.0809850105>
- Krishnamoorthy, V., Kannanganat, S., Maienschein-Cline, M., Cook, S. L., Chen, J., Bahroos, N., Sievert, E., Corse, E., Chong, A., & Sciammas, R. (2017). The IRF4 gene regulatory module functions as a read-write integrator to dynamically coordinate T helper cell fate. *Immunity*, *47*(3), 481. <https://doi.org/10.1016/J.IMMUNI.2017.09.001>
- Krishnaswamy, J. K., Gowthaman, U., Zhang, B., Mattsson, J., Szeponik, L., Liu, D., Wu, R., White, T., Calabro, S., Xu, L., Collet, M. A., Yurieva, M., Alsén, S., Fogelstrand, P., Walter, A., Heath, W. R., Mueller, S. N., Yrlid, U., Williams, A., & Eisenbarth, S. C. (2017a). Migratory CD11b⁺ conventional dendritic cells induce T follicular helper cell-dependent antibody responses. *Science Immunology*, *2*(18). <https://doi.org/10.1126/SCIIMMUNOL.AAM9169>
- Krishnaswamy, J. K., Gowthaman, U., Zhang, B., Mattsson, J., Szeponik, L., Liu, D., Wu, R., White, T., Calabro, S., Xu, L., Collet, M. A., Yurieva, M., Alsén, S., Fogelstrand, P., Walter, A., Heath, W. R., Mueller, S. N., Yrlid, U., Williams, A., & Eisenbarth, S. C. (2017b). Migratory CD11b⁺ conventional dendritic cells induce T follicular helper cell-dependent antibody responses. *Science Immunology*, *2*(18). <https://doi.org/10.1126/SCIIMMUNOL.AAM9169>
- Kroenke, M. A., Eto, D., Locci, M., Cho, M., Davidson, T., Haddad, E. K., & Crotty, S. (2012). Bcl6 and Maf Cooperate To Instruct Human Follicular Helper CD4 T Cell Differentiation. *The Journal of Immunology*, *188*(8), 3734–3744. <https://doi.org/10.4049/JIMMUNOL.1103246>
- Krummel, M. F., Bartumeus, F., & Gérard, A. (2016). T-cell Migration, Search Strategies and Mechanisms. *Nature Reviews. Immunology*, *16*(3), 193. <https://doi.org/10.1038/NRI.2015.16>
- Kuen, D. S., Park, M., Ryu, H., Choi, G., Moon, Y. H., Kim, J. O., Kang, K. W., Kim, S. G., & Chung, Y. (2021). Critical regulation of follicular helper T cell differentiation and function by Gα13 signaling. *Proceedings of the National Academy of Sciences of the United States of America*, *118*(43). <https://doi.org/10.1073/PNAS.2108376118/-/DCSUPPLEMENTAL>
- Kwon, H., Thierry-Mieg, D., Thierry-Mieg, J., Kim, H. P., Oh, J., Tunyaplin, C., Carotta, S., Donovan, C. E., Goldman, M. L., Taylor, P., Ozato, K., Levy, D. E., Nutt, S. L., Calame, K., & Leonard, W. J. (2009). Analysis of Interleukin-21-Induced Prdm1 Gene Regulation Reveals Functional Cooperation of STAT3 and IRF4 Transcription Factors. *Immunity*, *31*(6), 941–952. <https://doi.org/10.1016/J.IMMUNI.2009.10.008>
- Kyewski, B., Derbinski, J., Gotter, J., & Klein, L. (2002). Promiscuous gene expression and central T-cell tolerance: More than meets the eye. *Trends in Immunology*, *23*(7), 364–371. [https://doi.org/10.1016/S1471-4906\(02\)02248-2](https://doi.org/10.1016/S1471-4906(02)02248-2)

- Laurence, A., Tato, C. M., Davidson, T. S., Kanno, Y., Chen, Z., Yao, Z., Blank, R. B. B., Meylan, F., Siegel, R., Hennighausen, L., Shevach, E. M., & O'Shea, J. J. J. (2007). Interleukin-2 Signaling via STAT5 Constrains T Helper 17 Cell Generation. *Immunity*, *26*(3), 371–381. <https://doi.org/10.1016/J.IMMUNI.2007.02.009>
- Lee, J. H., Hu, J. K., Georgeson, E., Nakao, C., Groschel, B., Dileepan, T., Jenkins, M. K., Seumois, G., Vijayanand, P., Schief, W. R., & Crotty, S. (2021). Modulating the quantity of HIV Env-specific CD4 T cell help promotes rare B cell responses in germinal centers. *Journal of Experimental Medicine*, *218*(2). <https://doi.org/10.1084/JEM.20201254/211636>
- Lee, P. P., Fitzpatrick, D. R., Beard, C., Jessup, H. K., Lehar, S., Makar, K. W., Pérez-Melgosa, M., Sweetser, M. T., Schlissel, M. S., Nguyen, S., Cherry, S. R., Tsai, J. H., Tucker, S. M., Weaver, W. M., Kelso, A., Jaenisch, R., & Wilson, C. B. (2001). A critical role for Dnmt1 and DNA methylation in T cell development, function, and survival. *Immunity*, *15*(5), 763–774. [https://doi.org/10.1016/S1074-7613\(01\)00227-8](https://doi.org/10.1016/S1074-7613(01)00227-8)
- Leonard, W. J., & Wan, C. K. (2016). IL-21 Signaling in Immunity. *F1000Research*, *5*. <https://doi.org/10.12688/F1000RESEARCH.7634.1>
- León, B., Bradley, J. E., Lund, F. E., Randall, T. D., & Ballesteros-Tato, A. (2014a). FoxP3+ regulatory T cells promote influenza-specific Tfh responses by controlling IL-2 availability. *Nature Communications* *2014 5:1*, *5*(1), 1–10. <https://doi.org/10.1038/ncomms4495>
- León, B., Bradley, J. E., Lund, F. E., Randall, T. D., & Ballesteros-Tato, A. (2014b). FoxP3+ regulatory T cells promote influenza-specific Tfh responses by controlling IL-2 availability. *Nature Communications*, *5*. <https://doi.org/10.1038/NCOMMS4495>
- Liao, Y., Smyth, G. K., & Shi, W. (2014). featureCounts: an efficient general purpose program for assigning sequence reads to genomic features. *Bioinformatics (Oxford, England)*, *30*(7), 923–930. <https://doi.org/10.1093/BIOINFORMATICS/BTT656>
- Liberzon, A., Birger, C., Thorvaldsdóttir, H., Ghandi, M., Mesirov, J. P., & Tamayo, P. (2015). The Molecular Signatures Database (MSigDB) hallmark gene set collection. *Cell Systems*, *1*(6), 417. <https://doi.org/10.1016/J.CELS.2015.12.004>
- Li, C., Liu, P., Yao, H., Zhu, H., Zhang, S., Meng, F., Li, S., Li, G., Peng, Y., Gu, J., Zhu, L., Jiang, Y., & Dai, A. (2022). Regulatory B cells protect against chronic hypoxia-induced pulmonary hypertension by modulating the Tfh/Tfr immune balance. *Immunology*. <https://doi.org/10.1111/IMM.13589>
- Li, J., Jin, J., Li, S., Zhong, Y., Jin, Y., Zhang, X., Xia, B., Zhu, Y., Guo, R., Sun, X., Guo, J., Hu, F., Xiao, W., Huang, F., Ye, H., Li, R., Zhou, Y., Xiang, X., Yao, H., ... Li, Z. (2022). Tonsillar Microbiome-Derived Lantibiotics Induce Structural Changes of IL-6 and IL-21 Receptors and Modulate Host Immunity. *Advanced Science*, *9*(30). <https://doi.org/10.1002/ADVS.202202706>
- Li, J., Lu, E., Yi, T., & Cyster, J. G. (2016). EB12 augments Tfh cell fate by promoting interaction with IL-2-queenching dendritic cells. *Nature*, *533*(7601), 110–114. <https://doi.org/10.1038/NATURE17947>

- Linterman, M. A., Denton, A. E., Divekar, D. P., Zvetkova, I., Kane, L., Ferreira, C., Veldhoen, M., Clare, S., Dougan, G., Espéli, M., & Smith, K. G. C. (2014). CD28 expression is required after T cell priming for helper T cell responses and protective immunity to infection. *ELife*, 3(October2014), 1–21. <https://doi.org/10.7554/ELIFE.03180>
- Linterman, M. A., Rigby, R. J., Wong, R., Silva, D., Withers, D., Anderson, G., Verma, N. K., Brink, R., Hutloff, A., Goodnow, C. C., & Vinuesa, C. G. (2009). Roquin Differentiates the Specialized Functions of Duplicated T Cell Costimulatory Receptor Genes Cd28 and Icos. *Immunity*, 30(2), 228–241. <https://doi.org/10.1016/J.IMMUNI.2008.12.015>
- Lin, X., Twelkmeyer, T., Zhu, D., Zhang, L., Zhao, Y., Zhang, C., Iwakura, Y., Meng, G., Hua, Z., Yan, B., Liu, W. J., Luo, Z., Gong, S., Chen, H., Li, S., Hou, B., & Tang, H. (2021). Homeostatic regulation of T follicular helper and antibody response to particle antigens by IL-1Ra of medullary sinus macrophage origin. *Proceedings of the National Academy of Sciences of the United States of America*, 118(17), e2019798118. https://doi.org/10.1073/PNAS.2019798118/SUPPL_FILE/PNAS.2019798118.SAPP.PDF
- Liu, X., Chen, X., Zhong, B., Wang, A., Wang, X., Chu, F., Nurieva, R. I., Yan, X., Chen, P., van der Flier, L. G., Nakatsukasa, H., Neelapu, S. S., Chen, W., Clevers, H., Tian, Q., Qi, H., Wei, L., & Dong, C. (2014). Transcription factor achaete-scute homologue 2 initiates follicular T-helper-cell development. *Nature* 2014 507:7493, 507(7493), 513–518. <https://doi.org/10.1038/nature12910>
- Locci, M., Wu, J. E., Arumemi, F., Mikulski, Z., Dahlberg, C., Miller, A. T., & Crotty, S. (2016). Activin A programs the differentiation of human TFH cells. *Nature Immunology* 2016 17:8, 17(8), 976–984. <https://doi.org/10.1038/ni.3494>
- Love, M. I., Huber, W., & Anders, S. (2014). Moderated estimation of fold change and dispersion for RNA-seq data with DESeq2. *Genome Biology*, 15(12). <https://doi.org/10.1186/S13059-014-0550-8>
- Lu, K. T., Kanno, Y., Cannons, J. L., Handon, R., Bible, P., Elkahloun, A. G., Anderson, S. M., Wei, L., Sun, H., O’Shea, J. J., & Schwartzberg, P. L. (2011). Functional and Epigenetic Studies Reveal Multistep Differentiation and Plasticity of In Vitro-Generated and In Vivo-Derived Follicular T Helper Cells. *Immunity*, 35(4), 622–632. <https://doi.org/10.1016/J.IMMUNI.2011.07.015>
- Ma, C. S., Suryani, S., Avery, D. T., Chan, A., Nanan, R., Santner-Nanan, B., Deenick, E. K., & Tangye, S. G. (2009). Early commitment of naïve human CD4+ T cells to the T follicular helper (TFH) cell lineage is induced by IL-12. *Immunology and Cell Biology*, 87(8), 590–600. <https://doi.org/10.1038/ICB.2009.64>
- Marshall, H. D., Ray, J. P., Laidlaw, B. J., Zhang, N., Gawande, D., Staron, M. M., Craft, J., & Kaech, S. M. (2015). The transforming growth factor beta signaling pathway is critical for the formation of CD4 T follicular helper cells and isotype-switched antibody responses in the lung mucosa. *ELife*, 2015(4). <https://doi.org/10.7554/ELIFE.04851>

- McCarron, M. J., & Marie, J. C. (2014). TGF- β prevents T follicular helper cell accumulation and B cell autoreactivity. *The Journal of Clinical Investigation*, *124*(10), 4375–4386. <https://doi.org/10.1172/JCI76179>
- McGeachy, M. J., Chen, Y., Tato, C. M., Laurence, A., Joyce-Shaikh, B., Blumenschein, W. M., McClanahan, T. K., O'Shea, J. J., & Cua, D. J. (2009). The interleukin 23 receptor is essential for the terminal differentiation of interleukin 17-producing effector T helper cells in vivo. *Nature Immunology*, *10*(3), 314–324. <https://doi.org/10.1038/NI.1698>
- McKarns, S. C., Schwartz, R. H., & Kaminski, N. E. (2004). Smad3 Is Essential for TGF- β 1 to Suppress IL-2 Production and TCR-Induced Proliferation, but Not IL-2-Induced Proliferation. *The Journal of Immunology*, *172*(7), 4275–4284. <https://doi.org/10.4049/JIMMUNOL.172.7.4275>
- Medzhitov, R. (2010). Inflammation 2010: New Adventures of an Old Flame. *Cell*, *140*(6), 771–776. <https://doi.org/10.1016/J.CELL.2010.03.006>
- Medzhitov, R., & Janeway, C. A. (1997). Innate immunity: the virtues of a nonclonal system of recognition. *Cell*, *91*(3), 295–298. [https://doi.org/10.1016/S0092-8674\(00\)80412-2](https://doi.org/10.1016/S0092-8674(00)80412-2)
- Michlits, G., Jude, J., Hinterndorfer, M., de Almeida, M., Vainorius, G., Hubmann, M., Neumann, T., Schleiffer, A., Burkard, T. R., Fellner, M., Gijbsbertsen, M., Traunbauer, A., Zuber, J., & Elling, U. (2020). Multilayered VBC score predicts sgRNAs that efficiently generate loss-of-function alleles. *Nature Methods*, *17*(7), 708–716. <https://doi.org/10.1038/S41592-020-0850-8>
- Mitsdoerffer, M., Lee, Y., Jäger, A., Kim, H. J., Korn, T., Kolls, J. K., Cantor, H., Bettellie, E., & Kuchroo, V. K. (2010). Proinflammatory T helper type 17 cells are effective B-cell helpers. *Proceedings of the National Academy of Sciences of the United States of America*, *107*(32), 14292–14297. https://doi.org/10.1073/PNAS.1009234107/SUPPL_FILE/PNAS.201009234SI.PDF
- Mootha, V. K., Lindgren, C. M., Eriksson, K. F., Subramanian, A., Sihag, S., Lehar, J., Puigserver, P., Carlsson, E., Ridderstråle, M., Laurila, E., Houstis, N., Daly, M. J., Patterson, N., Mesirov, J. P., Golub, T. R., Tamayo, P., Spiegelman, B., Lander, E. S., Hirschhorn, J. N., ... Groop, L. C. (2003). PGC-1 α -responsive genes involved in oxidative phosphorylation are coordinately down-regulated in human diabetes. *Nature Genetics* *2003* *34*:3, *34*(3), 267–273. <https://doi.org/10.1038/ng1180>
- Mosmann, T. R., Cherwinski, H., Bond, M. W., Giedlin, M. A., & Coffman, R. L. (1986). Two types of murine helper T cell clone. I. Definition according to profiles of lymphokine activities and secreted proteins. *The Journal of Immunology*, *136*(7).
- Munger, J. S., & Sheppard, D. (2011). Cross Talk among TGF- β Signaling Pathways, Integrins, and the Extracellular Matrix. *Cold Spring Harbor Perspectives in Biology*, *3*(11), 5017–5018. <https://doi.org/10.1101/CSHPERSPECT.A005017>
- Nakawesi, J., This, S., Hütter, J., Boucard-Jourdin, M., Barateau, V., Muleta, K. G., Gooday, L. J., Thomsen, K. F., López, A. G., Ulmert, I., Poncet, D., Malissen, B., Greenberg, H., Thauinat, O., Defrance, T., Paidassi, H., & Lahl, K. (2020). $\alpha\beta 8$ integrin-expression by BATF3-dependent

- dendritic cells facilitates early IgA responses to Rotavirus. *Mucosal Immunology* 2020 14:1, 14(1), 53–67. <https://doi.org/10.1038/s41385-020-0276-8>
- Nakayamada, S., Kanno, Y., Takahashi, H., Jankovic, D., Lu, K. T., Johnson, T. A., Sun, H. wei, Vahedi, G., Hakim, O., Handon, R., Schwartzberg, P. L., Hager, G. L., & O'Shea, J. J. (2011). Early Th1 cell differentiation is marked by a Tfh cell-like transition. *Immunity*, 35(6), 919–931. <https://doi.org/10.1016/J.IMMUNI.2011.11.012>
- Nakayamada, S., Takahashi, H., Kanno, Y., & O'Shea, J. J. (2012). Helper T cell diversity and plasticity. *Current Opinion in Immunology*, 24(3), 297–302. <https://doi.org/10.1016/J.COI.2012.01.014>
- Nemazee, D. (2017). Mechanisms of central tolerance for B cells. *Nature Reviews Immunology* 2017 17:5, 17(5), 281–294. <https://doi.org/10.1038/nri.2017.19>
- Nguyen, D. N., Roth, T. L., Li, P. J., Chen, P. A., Apathy, R., Mamedov, M. R., Vo, L. T., Tobin, V. R., Goodman, D., Shifrut, E., Bluestone, J. A., Puck, J. M., Szoka, F. C., & Marson, A. (2020). Polymer-stabilized Cas9 nanoparticles and modified repair templates increase genome editing efficiency. *Nature Biotechnology*, 38(1), 44–49. <https://doi.org/10.1038/S41587-019-0325-6>
- Nian, Y., Xiong, Z., Zhan, P., Wang, Z., Xu, Y., Wei, J., Zhao, J., & Fu, Y. (2021). IL-21 Receptor Blockade Shifts the Follicular T Cell Balance and Reduces De Novo Donor-Specific Antibody Generation. *Frontiers in Immunology*, 12, 1. <https://doi.org/10.3389/FIMMU.2021.661580>
- Nikolich-Žugich, J., Slifka, M. K., & Messaoudi, I. (2004). The many important facets of T-cell repertoire diversity. *Nature Reviews Immunology* 2004 4:2, 4(2), 123–132. <https://doi.org/10.1038/nri1292>
- Niño, J. L. G., Pajeon, S. v., Tay, S. S., Colakoglu, F., Kempe, D., Hywood, J., Mazalo, J. K., Cremasco, J., Govendir, M. A., Dagley, L. F., Hsu, K., Rizzetto, S., Zieba, J., Rice, G., Prior, V., O'Neill, G., Williams, R. J., Nisbet, D. R., Kramer, B., ... Biro, M. (2020). Cytotoxic T cells swarm by homotypic chemokine signalling. *ELife*, 9, 1–71. <https://doi.org/10.7554/ELIFE.56554>
- Niogret, J., Berger, H., Rebe, C., Mary, R., Ballot, E., Truntzer, C., Thibaudin, M., Derangère, V., Hibos, C., Hampe, L., Rageot, D., Accogli, T., Joubert, P., Routy, B., Harker, J., Vegran, F., Ghiringhelli, F., & Chalmin, F. (2021). Original research: Follicular helper-T cells restore CD8+-dependent antitumor immunity and anti-PD-L1/PD-1 efficacy. *Journal for Immunotherapy of Cancer*, 9(6), 2157. <https://doi.org/10.1136/JITC-2020-002157>
- Nurieva, R. I., Chung, Y., Hwang, D., Yang, X. O., Kang, H. S., Ma, L., Wang, Y. hong, Watowich, S. S., Jetten, A. M., Tian, Q., & Dong, C. (2008). Generation of follicular helper T cells is mediated by IL-21 but independent of TH1, TH2 or TH17 lineages. *Immunity*, 29(1), 138. <https://doi.org/10.1016/J.IMMUNI.2008.05.009>
- Nurieva, R. I., Chung, Y., Martinez, G. J., Yang, X. O., Tanaka, S., Matskevitch, T. D., Wang, Y. H., & Dong, C. (2009). Bcl6 mediates the development of T follicular helper cells. *Science*, 325(5943), 1001–1005. https://doi.org/10.1126/SCIENCE.1176676/SUPPL_FILE/NU-RIEVA_SOM.PDF

- Nurieva, R., Yang, X. O., Martinez, G., Zhang, Y., Panopoulos, A. D., Ma, L., Schluns, K., Tian, Q., Watowich, S. S., Jetten, A. M., & Dong, C. (2007). Essential autocrine regulation by IL-21 in the generation of inflammatory T cells. *Nature*, *448*(7152), 480–483. <https://doi.org/10.1038/NATURE05969>
- Oestreich, K. J., Huang, A. C., & Weinmann, A. S. (2011). The lineage-defining factors T-bet and Bcl-6 collaborate to regulate Th1 gene expression patterns. *Journal of Experimental Medicine*, *208*(5), 1001–1013. <https://doi.org/10.1084/JEM.20102144>
- Okada, T., Ngo, V. N., Ekland, E. H., Förster, R., Lipp, M., Littman, D. R., & Cyster, J. G. (2002). Chemokine requirements for b cell entry to lymph nodes and Peyer's patches. *Journal of Experimental Medicine*, *196*(1), 65–75. <https://doi.org/10.1084/JEM.20020201/VIDEO-2>
- O'Shea, J., & Paul, W. E. (2010). Mechanisms underlying lineage commitment and plasticity of helper CD4 + T cells. *Science*, *327*(5969), 1098–1102. https://doi.org/10.1126/SCIENCE.1178334/ASSET/6D2E92E2-30FB-4D92-8D44-C1A0FEFF75E7/ASSETS/GRAPHIC/327_1098_F2.JPEG
- Pabst, O., & Slack, E. (2019). IgA and the intestinal microbiota: the importance of being specific. *Mucosal Immunology 2019 13:1*, *13*(1), 12–21. <https://doi.org/10.1038/s41385-019-0227-4>
- Paludan, S. R., Pradeu, T., Masters, S. L., & Mogensen, T. H. (2020). Constitutive immune mechanisms: mediators of host defence and immune regulation. *Nature Reviews Immunology 2020 21:3*, *21*(3), 137–150. <https://doi.org/10.1038/s41577-020-0391-5>
- Pandiyani, P., Zheng, L., Ishihara, S., Reed, J., & Lenardo, M. J. (2007). CD4+CD25+Foxp3+ regulatory T cells induce cytokine deprivation-mediated apoptosis of effector CD4+ T cells. *Nature Immunology 2007 8:12*, *8*(12), 1353–1362. <https://doi.org/10.1038/ni1536>
- Papillion, A., Powell, M. D., Chisolm, D. A., Bachus, H., Fuller, M. J., Weinmann, A. S., Villarino, A., O'Shea, J. J., León, B., Oestreich, K. J., & Ballesteros-Tato, A. (2019). Inhibition of IL-2 responsiveness by IL-6 is required for the generation of GC-TFH cells. *Science Immunology*, *4*(39). <https://doi.org/10.1126/SCIIMMUNOL.AAW7636>
- Park, H., Li, Z., Yang, X. O., Chang, S. H., Nurieva, R., Wang, Y. H., Wang, Y., Hood, L., Zhu, Z., Tian, Q., & Dong, C. (2005). A distinct lineage of CD4 T cells regulates tissue inflammation by producing interleukin 17. *Nature Immunology 2005 6:11*, *6*(11), 1133–1141. <https://doi.org/10.1038/ni1261>
- Peters, A., Pitcher, L. A., Sullivan, J. M., Mitsdoerffer, M., Acton, S. E., Franz, B., Wucherpfennig, K., Turley, S., Carroll, M. C., Sobel, R. A., Bettelli, E., & Kuchroo, V. K. (2011). Th17 Cells Induce Ectopic Lymphoid Follicles in Central Nervous System Tissue Inflammation. *Immunity*, *35*(6), 986–996. <https://doi.org/10.1016/J.IMMUNI.2011.10.015>
- Philip, M., & Schietinger, A. (2021). CD8+ T cell differentiation and dysfunction in cancer. *Nature Reviews Immunology 2021 22:4*, *22*(4), 209–223. <https://doi.org/10.1038/s41577-021-00574-3>

- Price, A. E., Reinhardt, R. L., Liang, H. E., & Locksley, R. M. (2012). Marking and Quantifying IL-17A-Producing Cells In Vivo. *PLoS ONE*, 7(6). <https://doi.org/10.1371/JOURNAL.PONE.0039750>
- Qi, H. (2016). T follicular helper cells in space-time. *Nature Reviews Immunology* 2016 16:10, 16(10), 612–625. <https://doi.org/10.1038/nri.2016.94>
- Qi, H., Cannons, J. L., Klauschen, F., Schwartzberg, P. L., & Germain, R. N. (2008). SAP-controlled T-B cell interactions underlie germinal centre formation. *Nature*, 455(7214), 764–769. <https://doi.org/10.1038/NATURE07345>
- Rasheed, A. U., Rahn, H. P., Sallusto, F., Lipp, M., & Müller, G. (2006). Follicular B helper T cell activity is confined to CXCR5hiICOShi CD4 T cells and is independent of CD57 expression. *European Journal of Immunology*, 36(7), 1892–1903. <https://doi.org/10.1002/EJL.200636136>
- R Core Team. (2017). *R: A language and environment for statistical computing*. R Foundation for Statistical Computing.
- Reinhardt, R. L., Liang, H. E., & Locksley, R. M. (2009). Cytokine-secreting follicular T cells shape the antibody repertoire. *Nature Immunology* 2009 10:4, 10(4), 385–393. <https://doi.org/10.1038/ni.1715>
- Rogers, P. R., & Croft, M. (2000). CD28, Ox-40, LFA-1, and CD4 Modulation of Th1/Th2 Differentiation Is Directly Dependent on the Dose of Antigen. *The Journal of Immunology*, 164(6), 2955–2963. <https://doi.org/10.4049/JIMMUNOL.164.6.2955>
- Russell, J. H., & Ley, T. J. (2002). Lymphocyte-mediated cytotoxicity. *Annual Review of Immunology*, 20, 323–370. <https://doi.org/10.1146/ANNUREV.IMMUNOL.20.100201.131730>
- Sabatos, C. A., Doh, J., Chakravarti, S., Friedman, R. S., Pandurangi, P. G., Tooley, A. J., & Krummel, M. F. (2008). A synaptic basis for paracrine interleukin-2 signaling during homotypic T cell interaction. *Immunity*, 29(2), 238–248. <https://doi.org/10.1016/J.IMMUNI.2008.05.017>
- Sage, P. T., Ron-Harel, N., Juneja, V. R., Sen, D. R., Maleri, S., Sungnak, W., Kuchroo, V. K., Haining, W. N., Chevrier, N., Haigis, M., & Sharpe, A. H. (2016). Suppression by TFR cells leads to durable and selective inhibition of B cell effector functions. *Nature Immunology*, 17(12), 1436. <https://doi.org/10.1038/NI.3578>
- Sakaguchi, S., Fukuma, K., Kuribayashi, K., & Masuda, T. (1985). Organ-specific autoimmune diseases induced in mice by elimination of T cell subset. I. Evidence for the active participation of T cells in natural self-tolerance; deficit of a T cell subset as a possible cause of autoimmune disease. *Journal of Experimental Medicine*, 161(1), 72–87. <https://doi.org/10.1084/JEM.161.1.72>
- Sakaguchi, S., Mikami, N., Wing, J. B., Tanaka, A., Ichiyama, K., & Ohkura, N. (2020). Regulatory T Cells and Human Disease. <https://doi.org/10.1146/Annurev-Immunol-042718-041717>, 38, 541–566. <https://doi.org/10.1146/ANNUREV-IMMUNOL-042718-041717>

- Sallusto, F. (2016). Heterogeneity of Human CD4⁺ T Cells Against Microbes. <https://doi.org/10.1146/Annurev-Immunol-032414-112056>, *34*, 317–334. <https://doi.org/10.1146/ANNUREV-IMMUNOL-032414-112056>
- Sakurai, S., Furuhashi, K., Horiguchi, R., Nihashi, F., Yasui, H., Karayama, M., Suzuki, Y., Hozumi, H., Enomoto, N., Fujisawa, T., Nakamura, Y., Inui, N., & Suda, T. (2021). Conventional type 2 lung dendritic cells are potent inducers of follicular helper T cells in the asthmatic lung. *Allergology International*, *70*(3), 351–359. <https://doi.org/10.1016/J.ALIT.2021.01.008>
- Saravia, J., Chapman, N. M., & Chi, H. (2019a). Helper T cell differentiation. *Cellular & Molecular Immunology* *2019 16:7*, *16*(7), 634–643. <https://doi.org/10.1038/s41423-019-0220-6>
- Saravia, J., Chapman, N. M., & Chi, H. (2019b). Helper T cell differentiation. *Cellular & Molecular Immunology* *2019 16:7*, *16*(7), 634–643. <https://doi.org/10.1038/s41423-019-0220-6>
- Schmitt, N., Bustamante, J., Bourdery, L., Bentebibel, S. E., Boisson-Dupuis, S., Hamlin, F., Tran, M. v., Blankenship, D., Pascual, V., Savino, D. A., Banchereau, J., Casanova, J. L., & Ueno, H. (2013). IL-12 receptor β 1 deficiency alters in vivo T follicular helper cell response in humans. *Blood*, *121*(17), 3375. <https://doi.org/10.1182/BLOOD-2012-08-448902>
- Schmitt, N., Liu, Y., Bentebibel, S. E., Munagala, I., Bourdery, L., Venuprasad, K., Banchereau, J., & Ueno, H. (2014a). The cytokine TGF- β co-opts signaling via STAT3-STAT4 to promote the differentiation of human TFH cells. *Nature Immunology*, *15*(9), 856–865. <https://doi.org/10.1038/NI.2947>
- Schmitt, N., Liu, Y., Bentebibel, S. E., Munagala, I., Bourdery, L., Venuprasad, K., Banchereau, J., & Ueno, H. (2014b). The cytokine TGF- β co-opts signaling via STAT3-STAT4 to promote the differentiation of human TFH cells. *Nature Immunology* *2014 15:9*, *15*(9), 856–865. <https://doi.org/10.1038/ni.2947>
- Schmitt, N., Morita, R., Bourdery, L., Bentebibel, S. E., Zurawski, S. M., Banchereau, J., & Ueno, H. (2009). Human Dendritic Cells Induce the Differentiation of Interleukin-21-Producing T Follicular Helper-like Cells through Interleukin-12. *Immunity*, *31*(1), 158–169. <https://doi.org/10.1016/J.IMMUNI.2009.04.016>
- Seder, R. A., Paul, W. E., Davis, M. M., & Fazekas de St. Groth, B. (1992). The presence of interleukin 4 during in vitro priming determines the lymphokine-producing potential of CD4⁺ T cells from T cell receptor transgenic mice. *Journal of Experimental Medicine*, *176*(4), 1091–1098. <https://doi.org/10.1084/JEM.176.4.1091>
- Seki, A., & Rutz, S. (2018). Optimized RNP transfection for highly efficient CRISPR/Cas9-mediated gene knockout in primary T cells. *The Journal of Experimental Medicine*, *215*(3), 985–997. <https://doi.org/10.1084/JEM.20171626>
- Seo, Y. B., Im, S. J., Namkoong, H., Kim, S. W., Choi, Y. W., Kang, M. C., Lim, H. S., Jin, H. T., Yang, S. H., Cho, M. I., Kim, Y.-M., Lee, S.-W., Choi, Y. K., Surh, C. D., & Sung, Y. C. (2014). Crucial Roles of Interleukin-7 in the Development of T Follicular Helper Cells and in the Induction of Humoral Immunity. *Journal of Virology*, *88*(16), 8998–9009.

- <https://doi.org/10.1128/JVI.00534-14/ASSET/F2FD18AB-B7E2-45C4-ADDF-8A0631962928/ASSETS/GRAPHIC/ZJV9990993480008.JPEG>
- Sette, A., & Crotty, S. (2021). Adaptive immunity to SARS-CoV-2 and COVID-19. *Cell*, *184*(4), 861–880. <https://doi.org/10.1016/J.CELL.2021.01.007>
- Shevryev, D., & Tereshchenko, V. (2020). Treg Heterogeneity, Function, and Homeostasis. *Frontiers in Immunology*, *10*, 3100. <https://doi.org/10.3389/FIMMU.2019.03100/BIBTEX>
- Shi, J., Hou, S., Fang, Q., Liu, X., Liu, X., & Qi, H. (2018). PD-1 Controls Follicular T Helper Cell Positioning and Function. *Immunity*, *49*(2), 264. <https://doi.org/10.1016/J.IMMUNI.2018.06.012>
- Smith, C. M., Wilson, N. S., Waithman, J., Villadangos, J. A., Carbone, F. R., Heath, W. R., & Belz, G. T. (2004). Cognate CD4+ T cell licensing of dendritic cells in CD8+ T cell immunity. *Nature Immunology* *2004* *5*:11, *5*(11), 1143–1148. <https://doi.org/10.1038/ni1129>
- Stuart, T., Butler, A., Hoffman, P., Hafemeister, C., Papalexi, E., Mauck, W. M., Hao, Y., Stoeckius, M., Smibert, P., & Satija, R. (2019). Comprehensive Integration of Single-Cell Data. *Cell*, *177*(7), 1888-1902.e21. <https://doi.org/10.1016/J.CELL.2019.05.031>
- Subramanian, A., Tamayo, P., Mootha, V. K., Mukherjee, S., Ebert, B. L., Gillette, M. A., Paulovich, A., Pomeroy, S. L., Golub, T. R., Lander, E. S., & Mesirov, J. P. (2005). Gene set enrichment analysis: A knowledge-based approach for interpreting genome-wide expression profiles. *Proceedings of the National Academy of Sciences of the United States of America*, *102*(43), 15545–15550. https://doi.org/10.1073/PNAS.0506580102/SUPPL_FILE/06580FIG7.JPG
- Suto, A., Kashiwakuma, D., Kagami, S. I., Hirose, K., Watanabe, N., Yokote, K., Saito, Y., Nakayama, T., Grusby, M. J., Iwamoto, I., & Nakajima, H. (2008). Development and characterization of IL-21–producing CD4+ T cells. *The Journal of Experimental Medicine*, *205*(6), 1369. <https://doi.org/10.1084/JEM.20072057>
- Suzuki, K., Maruya, M., Kawamoto, S., Sitnik, K., Kitamura, H., Agace, W. W., & Fagarasan, S. (2010). The Sensing of Environmental Stimuli by Follicular Dendritic Cells Promotes Immunoglobulin A Generation in the Gut. *Immunity*, *33*(1), 71–83. <https://doi.org/10.1016/J.IMMUNI.2010.07.003>
- Toellner, K. M., Luther, S. A., Sze, D. M. Y., Choy, R. K. W., Taylor, D. R., MacLennan, I. C. M., & Acha-Orbea, H. (1998). T Helper 1 (Th1) and Th2 Characteristics Start to Develop During T Cell Priming and Are Associated with an Immediate Ability to Induce Immunoglobulin Class Switching. *Journal of Experimental Medicine*, *187*(8), 1193–1204. <https://doi.org/10.1084/JEM.187.8.1193>
- Utzschneider, D. T., Legat, A., Fuertes Marraco, S. A., Carrié, L., Luescher, I., Speiser, D. E., & Zehn, D. (2013). T cells maintain an exhausted phenotype after antigen withdrawal and population reexpansion. *Nature Immunology*, *14*(6), 603–610. <https://doi.org/10.1038/NI.2606>

- Valitutti, S., Miller, S., Cella, M., Padovan, E., & Lanzavecchia, A. (1995). Serial triggering of many T-cell receptors by a few peptide–MHC complexes. *Nature* 1995 375:6527, 375(6527), 148–151. <https://doi.org/10.1038/375148a0>
- van Panhuys, N., Tang, S. C., Prout, M., Camberis, M., Scarlett, D., Roberts, J., Hu-Li, J., Paul, W. E., & le Gros, G. (2008). In vivo studies fail to reveal a role for IL-4 or STAT6 signaling in Th2 lymphocyte differentiation. *Proceedings of the National Academy of Sciences of the United States of America*, 105(34), 12423–12428. <https://doi.org/10.1073/PNAS.0806372105>
- Veldhoen, M., Hocking, R. J., Atkins, C. J., Locksley, R. M., & Stockinger, B. (2006). TGFbeta in the context of an inflammatory cytokine milieu supports de novo differentiation of IL-17-producing T cells. *Immunity*, 24(2), 179–189. <https://doi.org/10.1016/J.IMMUNI.2006.01.001>
- Vinuesa, C. G., Linterman, M. A., Yu, D., & Maclennan, I. C. M. (2016). Follicular Helper T Cells. <https://doi.org/10.1146/Annurev-Immunol-041015-055605>, 34, 335–368. <https://doi.org/10.1146/ANNUREV-IMMUNOL-041015-055605>
- Viola, A., & Lanzavecchia, A. (1996). T Cell Activation Determined by T Cell Receptor Number and Tunable Thresholds. *Science*, 273(5271), 104–106. <https://doi.org/10.1126/SCIENCE.273.5271.104>
- Vogel, C., & Marcotte, E. M. (2012). Insights into the regulation of protein abundance from proteomic and transcriptomic analyses. *Nature Reviews Genetics* 2012 13:4, 13(4), 227–232. <https://doi.org/10.1038/nrg3185>
- Vogelzang, A., McGuire, H. M., Yu, D., Sprent, J., Mackay, C. R., & King, C. (2008). A Fundamental Role for Interleukin-21 in the Generation of T Follicular Helper Cells. *Immunity*, 29(1), 127–137. <https://doi.org/10.1016/J.IMMUNI.2008.06.001>
- Walker, J. A., & McKenzie, A. N. J. (2017). TH2 cell development and function. *Nature Reviews Immunology* 2017 18:2, 18(2), 121–133. <https://doi.org/10.1038/nri.2017.118>
- Wang, H., Li, X., Kajikawa, T., Shin, J., Lim, J. H., Kourtzelis, I., Nagai, K., Korostoff, J. M., Grossklaus, S., Naumann, R., Chavakis, T., & Hajishengallis, G. (2021). Stromal cell–derived DEL-1 inhibits Tfh cell activation and inflammatory arthritis. *The Journal of Clinical Investigation*, 131(19). <https://doi.org/10.1172/JCI150578>
- Wang, X., Li, Z., Naganuma, A., & Ye, B. H. (2002). Negative autoregulation of BCL-6 is bypassed by genetic alterations in diffuse large B cell lymphomas. *Proceedings of the National Academy of Sciences of the United States of America*, 99(23), 15018–15023. <https://doi.org/10.1073/PNAS.232581199/ASSET/904BC24E-04AE-414D-AA1E-FE74A58776D6/ASSETS/GRAPHIC/PQ2325811006.JPEG>
- Wan, S., Ni, L., Zhao, X., Liu, X., Xu, W., Jin, W., Wang, X., & Dong, C. (2021). Costimulation molecules differentially regulate the ERK-Zfp831 axis to shape T follicular helper cell differentiation. *Immunity*, 54(12), 2740–2755.e6. <https://doi.org/10.1016/J.IMMUNI.2021.09.018>

- Wei, L., Laurence, A., Elias, K. M., & O'Shea, J. J. (2007). IL-21 is produced by Th17 cells and drives IL-17 production in a STAT3-dependent manner. *The Journal of Biological Chemistry*, 282(48), 34605–34610. <https://doi.org/10.1074/JBC.M705100200>
- Wende, H., Lechner, S. G., Cheret, C., Bourane, S., Kolanczyk, M. E., Pattyn, A., Reuter, K., Munnier, F. L., Carroll, P., Lewin, G. R., & Birchmeier, C. (2012). The transcription factor c-Maf controls touch receptor development and function. *Science (New York, N.Y.)*, 335(6074), 1373–1376. <https://doi.org/10.1126/SCIENCE.1214314>
- Wickham, H. (2016). *ggplot2*. <https://doi.org/10.1007/978-3-319-24277-4>
- Wickham, H., Averick, M., Bryan, J., Chang, W., D'Almeida, L., Mcgowan, A., François, R., Grolemund, G., Hayes, A., Henry, L., Hester, J., Kuhn, M., Lin Pedersen, T., Miller, E., Bache, S. M., Müller, K., Ooms, J., Robinson, D., Seidel, D. P., ... Yutani, H. (2019). Welcome to the Tidyverse. *Journal of Open Source Software*, 4(43), 1686. <https://doi.org/10.21105/JOSS.01686>
- Wing, K., Onishi, Y., Prieto-Martin, P., Yamaguchi, T., Miyara, M., Fehervari, Z., Nomura, T., & Sakaguchi, S. (2008). CTLA-4 control over Foxp3+ regulatory T cell function. *Science (New York, N.Y.)*, 322(5899), 271–275. <https://doi.org/10.1126/SCIENCE.1160062>
- Winter, S. V., Meier, F., Wichmann, C., Cox, J., Mann, M., & Meissner, F. (2018). EASI-tag enables accurate multiplexed and interference-free MS2-based proteome quantification. *Nature Methods* 2018 15:7, 15(7), 527–530. <https://doi.org/10.1038/s41592-018-0037-8>
- Wu, H., Deng, Y., Long, D., Yang, M., Li, Q., Feng, Y., Chen, Y., Qiu, H., Huang, X., He, Z., Hu, L., Yin, H., Li, G., Guo, Y., Du, W., Zhao, M., Lu, L., & Lu, Q. (2022). The IL-21-TET2-AIM2-c-MAF pathway drives the T follicular helper cell response in lupus-like disease. *Clinical and Translational Medicine*, 12(3). <https://doi.org/10.1002/CTM2.781>
- Wurster, A. L., Rodgers, V. L., Satoskar, A. R., Whitters, M. J., Young, D. A., Collins, M., & Grusby, M. J. (2002). Interleukin 21 Is a T Helper (Th) Cell 2 Cytokine that Specifically Inhibits the Differentiation of Naive Th Cells into Interferon γ -producing Th1 Cells. *Journal of Experimental Medicine*, 196(7), 969–977. <https://doi.org/10.1084/JEM.20020620>
- Xu, D., & Lu, W. (2020). Defensins: A Double-Edged Sword in Host Immunity. *Frontiers in Immunology*, 11. <https://doi.org/10.3389/FIMMU.2020.00764>
- Xu, J., Yang, Y., Qiu, G., Lal, G., Wu, Z., Levy, D. E., Ochando, J. C., Bromberg, J. S., & Ding, Y. (2009). c-Maf Regulates IL-10 Expression during Th17 Polarization. *Journal of Immunology (Baltimore, Md. : 1950)*, 182(10), 6226. <https://doi.org/10.4049/JIMMUNOL.0900123>
- Yu, D., Rao, S., Tsai, L. M., Lee, S. K., He, Y., Sutcliffe, E. L., Srivastava, M., Linterman, M., Zheng, L., Simpson, N., Ellyard, J. I., Parish, I. A., Ma, C. S., Li, Q. J., Parish, C. R., Mackay, C. R., & Vinuesa, C. G. (2009). The transcriptional repressor Bcl-6 directs T follicular helper cell lineage commitment. *Immunity*, 31(3), 457–468. <https://doi.org/10.1016/J.IMMUNI.2009.07.002>
- Zhang, N., & Bevan, M. J. (2011). CD8+ T Cells: Foot Soldiers of the Immune System. *Immunity*, 35(2), 161. <https://doi.org/10.1016/J.IMMUNI.2011.07.010>

- Zhang, X., Smits, A. H., van Tilburg, G. B. A., Ovaa, H., Huber, W., & Vermeulen, M. (2018). Proteome-wide identification of ubiquitin interactions using UblA-MS. *Nature Protocols* 2018 13:3, 13(3), 530–550. <https://doi.org/10.1038/nprot.2017.147>
- Zheng, J., Meyerholz, D., Wong, L. Y. R., Gelb, M., Murakami, M., & Perlman, S. (2021). Coronavirus-specific antibody production in middle-aged mice requires phospholipase A2G2D. *The Journal of Clinical Investigation*, 131(11). <https://doi.org/10.1172/JCI147201>
- Zhou, L., Ivanov, I. I., Spolski, R., Min, R., Shenderov, K., Egawa, T., Levy, D. E., Leonard, W. J., & Littman, D. R. (2007). IL-6 programs T(H)-17 cell differentiation by promoting sequential engagement of the IL-21 and IL-23 pathways. *Nature Immunology*, 8(9), 967–974. <https://doi.org/10.1038/NI1488>
- Zhu, J. (2018). T Helper Cell Differentiation, Heterogeneity, and Plasticity. *Cold Spring Harbor Perspectives in Biology*, 10(10), a030338. <https://doi.org/10.1101/CSHPERSPECT.A030338>
- Zhu, J., Guo, L., Watson, C. J., Hu-Li, J., & Paul, W. E. (2001). Stat6 Is Necessary and Sufficient for IL-4's Role in Th2 Differentiation and Cell Expansion. *The Journal of Immunology*, 166(12), 7276–7281. <https://doi.org/10.4049/JIMMUNOL.166.12.7276>
- Zielinski, C. E., Mele, F., Aschenbrenner, D., Jarrossay, D., Ronchi, F., Gattorno, M., Monticelli, S., Lanzavecchia, A., & Sallusto, F. (2012). Pathogen-induced human TH17 cells produce IFN- γ or IL-10 and are regulated by IL-1 β . *Nature*, 484(7395), 514–518. <https://doi.org/10.1038/NATURE10957>

Acknowledgements

I would like to express my sincere gratitude to all the people who supported me throughout this lengthy journey. Without you, this thesis would not have been possible.

First of all, I would like to thank my supervisor Prof. Dr. Dirk Baumjohann for his continued support, mentorship, and providing me with the means and freedom to explore this fantastic field.

I express gratitude to Prof. Dr. Anne Krug, Prof. Dr. Vigo Heissmeyer and Dr. Anneli Peters as members of my thesis advisory committee for their suggestions and experimental input.

I would like to thank all present and former members of the Baumjohann lab, both in Munich and in Bonn for the wonderful working atmosphere. In particular, I would like to thank Luisa Bach for helping me to redo a multitude of experiment with more replicates. I also thank Nicolás Gutiérrez-Melo for his aid in the analysis of the single-cell RNA-sequencing data. I greatly appreciate our lab technicians Frank Dahlström and Jennifer-Christin Becker for help with breeding and genotyping of the required mice.

I would like to acknowledge all my collaborators that strongly contributed to this research work:

Marko Hasiuk and Prof. Dr. Lukas Jeker for their expertise and performing the CRISPR/Cas9 screening.

Dr. Carlson Tsui, Lifen Wen, and Prof. Dr. Axel Kallies for kindly providing the LCMV infection data.

Tarek Elmzahi and Prof. Dr. Marc Beyer for their support in both performing and analyzing the single-cell RNA-sequencing.

Sarah Reschke, Dr. Stefan Krebs, and Prof. Dr. Helmut Blum for performing the RNA-sequencing in Munich, and the NGS Core facility at the UKB for performing the RNA-sequencing in Bonn.

Jingyuan Cheng and Prof. Dr. Felix Meissner for performing proteomics measurements on our samples.

Dr. Sylvia Heink, Prof. Dr. Thomas Korn, Dr. Caspar Ohnmacht, and Dr. Christian Neumann for kindly providing some of the mouse models used in this work.

Additionally, I would like to thank the staff of the Flow Cytometry Core Facility at the BMC in Munich and the UKB in Bonn, as well as the Core Facility Animal Models at the BMC in Munich and the HET in Bonn.

Lastly, my deepest gratefulness goes out to my family and my dearest friends for always believing in me and endlessly supporting me.

Affidavit



Affidavit

Chang, Yinshui

Surname, first name

Brombeerweg 4

Street

53127, Bonn, Germany

Zip code, town, country

I hereby declare, that the submitted thesis entitled:

TGFβ differentially specifies T follicular helper versus Th17 cell fates of murine CD4⁺ T cells.....

is my own work. I have only used the sources indicated and have not made unauthorised use of services of a third party. Where the work of others has been quoted or reproduced, the source is always given.

I further declare that the dissertation presented here has not been submitted in the same or similar form to any other institution for the purpose of obtaining an academic degree.

Bonn, 26.10.2023

place, date

Yinshui Chang

Signature doctoral candidate

Confirmation of congruency



Confirmation of congruency between printed and electronic version of the doctoral thesis

Chang, Yinshui

Surname, first name

Brombeerweg 4

Street

53127, Bonn, Germany

Zip code, town, country

I hereby declare, that the submitted thesis entitled:

TGFβ differentially specifies T follicular helper versus Th17 cell fates of murine CD4⁺ T cells.....

is congruent with the printed version both in content and format.

Bonn, 26.10.2023

place, date

Yinshui Chang

Signature doctoral candidate

List of publications

Guidelines for the use of flow cytometry and cell sorting in immunological studies (third edition)

Andrea Cossarizza, Hyun-Dong Chang, Andreas Radbruch, ..., Dirk Baumjohann, ..., **Yinshui Chang**, ...

Eur J Immunol. 2021 Dec;51(12):2708-3145. doi: 10.1002/eji.202170126.

Functional analysis of peripheral and intratumoral neoantigen-specific TCRs identified in a patient with melanoma

Eva Bräunlein, Gaia Lupoli, Franziska Fuchsl, Esam T Abualrous, Niklas de Andrade Krätzig, Dario Gosmann, Lukas Wietbrock, Sebastian Lange, Thomas Engleitner, Huan Lan, Stefan Audehm, Manuel Effenberger, Melanie Boxberg, Katja Steiger, **Yinshui Chang**, Kai Yu, Cigdem Atay, Florian Bassermann, Wilko Weichert, Dirk H Busch, Roland Rad, Christian Freund, Iris Antes, Angela M Krackhardt

J Immunother Cancer. 2021 Sep;9(9):e002754. doi: 10.1136/jitc-2021-002754.

T cell-expressed microRNAs critically regulate germinal center T follicular helper cell function and maintenance in acute viral infection in mice

Julia Zeitrüg, Frank Dahlström, **Yinshui Chang**, Dominik Alterauge, Daniel Richter, Julia Niemietz, Dirk Baumjohann

Eur J Immunol. 2021 Feb;51(2):408-413. doi: 10.1002/eji.202048867.

Fingolimod Profoundly Reduces Frequencies and Alters Subset Composition of Circulating T Follicular Helper Cells in Multiple Sclerosis Patients

Johanna E Huber, **Yinshui Chang**, Ingrid Meinl, Tania Kümpfel, Edgar Meinl, Dirk Baumjohann

J Immunol. 2020 Mar 1;204(5):1101-1110. doi: 10.4049/jimmunol.1900955.